Bedeutung des p53-Signalwegs für Apoptoseaktivierung und Zellzyklusarrestregulation durch das $p14^{ARF}$ Tumorsuppressorgen

D i s s e r t a t i o n

zur Erlangung des akademischen Grades

d o c t o r r e r u m n a t u r a l i u m

(Dr. rer. nat.)

im Fach Biologie

eingereicht an der

Mathematisch-Naturwissenschaftlichen Fakultät I

der Humboldt-Universität zu Berlin

von

Diplom-Biologe Tim Overkamp

Präsident der Humboldt-Universität zu Berlin

Prof. Dr. Jan-Hendrik Olbertz

Dekan der Mathematisch-Naturwissenschaftlichen Fakultät I

Prof. Dr. Andreas Herrmann

Gutachter: 1. Prof. Dr. Harald Saumweber

2. Prof. Dr. Peter Daniel

3. PD Dr. Jürgen Eberle

Arbeit eingereicht am: 31. Januar 2012

Tag der mündlichen Prüfung: 11. Oktober 2012

Abstract

BH3-only proteins, a pro-apoptotic subgroup of the Bcl-2 family of proteins, are central mediators of apoptosis signals by regulating the intrinsic apoptosis pathway. We have recently shown, that apoptosis triggered by the $p14^{ARF}$ tumour suppressor protein is mediated by the p53-dependent activation of the BH3-only protein Puma/Bbc3. Nevertheless, expression of $p14^{ARF}$ in p53-family deficient cells is capable of inducing both cell cycle arrest and apoptosis, but the signalling pathways initiated remain elusive. Here, we report that the BH3-only protein Bmf (Bcl-2 modifying factor) is involved in cell death in p53-deficient cells triggered by $p14^{ARF}$. Expression of $p14^{ARF}$ leads to the induction of the PERK kinase, subsequent phosphorylation of eIF2α and activation of transcription factors ATF4 and CHOP. This signalling cascade is usually part of the 'unfolded protein response' (UPR), which is activated upon ER stress to reduce the amount of misfolded proteins by reduction of global protein translation initiation and upregulation of chaperones. Of note, $p14^{ARF}$ does not induce ER stress but activates the PERK – CHOP pathway. ATF4 and CHOP transcription factors directly bind to the promotor region of *bmf* and induce its transcription. These data suggest that the PERK – eIF2α – ATF4 – CHOP signalling pathway may play a substantial role in mediating $p14^{ARF}$-triggered apoptosis. This pathway could play the role of a 'fail-safe' mechanism that allows cells, even after loss of p53, to undergo apoptosis induced by upregulation of $p14^{ARF}$ by oncogenes.

Keywords:

apoptosis, BH3-only, Bcl-2 modifying factor (Bmf), $p14^{ARF}$, p53, unfolded protein response (UPR), endoplasmic reticulum (ER)

Zusammenfassung

BH3-only Proteine, eine pro-apoptotische Untergruppe der Bcl-2 Proteinfamilie, sind zentrale Mediatoren von apoptotischen Signalen durch die Regulierung intrinsischer Apoptose-signalwege. Unsere Arbeitsgruppe hat vor kurzem gezeigt, dass Apoptose, die durch den $p14^{ARF}$ Tumorsuppressor induziert wird über die p53-abhängige Aktivierung des BH3-only Proteins Puma/Bbc3 vermittelt wird. Interessanterweise induziert $p14^{ARF}$ aber auch in p53 defizienten Zellen Zellzyklusarrest und Apoptose. Die dahinterliegenden Signalwege sind jedoch nicht bekannt. In dieser Arbeit berichten wir, dass das BH3-only Protein Bmf (Bcl-2 modifying factor) beim $p14^{ARF}$-induzierten Zelltod in p53 defizienten Zellen eine wichtige Rolle spielt. Expression von $p14^{ARF}$ führt zu einer Induktion der PERK Kinase, daran anschließender Phosphorylierung von eIF2α sowie Aktivierung der stromabwärts liegenden Transkriptionsfaktoren ATF4 und CHOP. Diese Signalkaskade ist normalerweise Teil einer zellulären Antwort auf fehl- oder ungefaltete Proteine im Endoplasmatischen Retikulum (ER), der sogenannten 'unfolded protein response' (UPR), die zum einen durch verminderte Translationsinitiation und Hochregulierung von Chaperonen die Menge der fehlgefalteten Proteine reduzieren soll. Allerdings induziert $p14^{ARF}$ keinen ER Stress, sondern den PERK–CHOP Signalweg. Die Transkriptionsfaktoren ATF4 und CHOP binden direkt in der Promotorregion von *bmf* und sind für dessen transkriptionelle Regulation verantwortlich. Unsere Daten zeigen, dass der PERK–eIF2α–ATF4–CHOP Signalweg eine wesentliche Rolle bei der Induktion von Apoptose durch $p14^{ARF}$ spielt. Dieser Weg könnte ein Sicherungsmechanismus sein, der es den Zellen auch nach Verlust von p53 erlaubt Apoptose einzuleiten, nachdem $p14^{ARF}$ durch Onkogene hochreguliert wurde.

Stichwörter:

Apoptose, BH3-only, Bcl-2 modifying factor (Bmf), $p14^{ARF}$, p53, unfolded protein response (UPR), Endoplasmatisches Retikulum (ER)

Table of Contents

1. Introduction

The concept of a natural instead of a pathological form of cell death was described as early as 1842 by Carl Vogt in studies about the development of the midwife toad *Alytes obstetricans* (Vogt, 1842), only three years after Schwann and Schleiden's cell theory in 1839 (Schwann, 1839). More than a century later, the term apoptosis (from greek από [apo; from] and πτωσις [ptosis; falling, a fall]; like leaves or petals falling from a plant) had been coined in order to describe morphological processes leading to controlled cellular self-destruction and was first introduced in a publication by Kerr, Wyllie and Currie (Kerr *et al.*, 1972).

Apoptosis, or Type I cell death, can be described as an active and evolutionary defined process which plays an important role in the development of multicellular organisms and in the regulation and maintenance of the cell homeostasis in tissues upon physiological and pathological conditions. One type of apoptosis designated as 'anoikis' (from greek άν [an; without], οίκ [oik; house], and ις [is; extracted from apoptosis]; the state of being without a home) is induced by detachment or inadequate and inappropriate cell-matrix interactions (Frisch and Francis, 1994). Apoptosis is the most frequent form of programmed cell death, followed by autophagy/autophagocytosis (from greek αυτό [auto; self] and φαγία [phagia; to eat), or Type II cell death, where the cell's own components are catabolic degraded through its lysosomal machinery. Autophagy was initially described as a cellular response to starvation by Christian de Duve in 1963 (de Duve, 1963). Next to these types of programmed cell death, other, non-apoptotic types, e.g. caspase-independent programmed cell death, are also of biological significance (Leist and Jäättelä, 2001).

Programmed cell death mechanisms differ from necrosis (from greek νεκρός [necros; death, dead]), or Type III cell death, which is an accidental and unordered cell death where the release of cellular contents causes an inflammatory response. In contrast, apoptosis leads to shrinkage and fragmentation of the nucleus, condensation of chromatin and blebbing of the cell membrane due to breakdown of the cytoskeleton. These constricted particles, so called apoptotic bodies, are eventually taken up by phagocytes and the components are recycled.

Autophagy and apoptotic processes are involved in development, starting in ontogenesis, when gastrulation of the early embryo is made possible by programmed death of cells within the blastula, later on during digit formation when web cells die off and disappear (Zuzarte-Luís and Hurlé, 2002) and throughout the life of the organism. In the immune system, apoptosis is responsible for negative selection of autoreactive B- and T-cells as well as for removing virus-infected cells. In the human body about 100,000 cells are produced every

second by mitosis and meiosis and a similar number die by apoptosis (Vaux and Korsmeyer, 1999). This homeostasis between the regulation of cell cycle and apoptosis is achieved by a tight regulation of pro- and anti-apoptotic proteins (Krammer *et al.*, 1994; Daniel, 2000). One of the key regulators is the tumour suppressor p53, also termed "guardian of the genome" (Lane, 1992). This protein was identified in 1979 and is known to be activated upon different types of stress, e.g. DNA damage, oxidative shock and deregulated oncogene expression (Finlay *et al.*, 1989; Han *et al.*, 2008). Oncogenic stress activates the INK4b-ARF-INK4a locus that gives raise to proteins that on the one hand arrest the cell in the cell cycle and on the other hand induce p53. Disruption of cell cycle pathways and programmed cell death deregulation participates in the pathogenesis of several diseases. Uninhibited cell proliferation leads to cancer or auto-immune diseases, while upregulation of apoptosis leads to neurodegenerative diseases such as Creutzfeldt Jakob, Alzheimer's and Parkinson's disease (Yuan and Yankner, 2000; Rathmell and Thompson, 2002; Daniel in Ganten and Ruckpaul, 2007).

1.1 Apoptosis pathways

Apoptosis is executed by a network of genetically encoded components. It can be triggered by various stimuli from outside or inside the cell, leading to the activation of the extrinsic or death receptor pathway and the intrinsic or mitochondrial pathway. Every cellular organelle or subcellular component, e.g. the endoplasmic reticulum (ER) or the nucleolus, can sense stressful and pathogenic alterations and initiate local or global responses leading to adaptation or, once a critical threshold of damage has been reached, cell death (Ferri and Kroemer, 2001). The activation of cell death is mediated by cysteine-dependent aspartate-specific proteases (caspases). These are synthesised as inactive zymogenes (procaspases) and are located in the cytosol and the nucleus. Activation of the so called caspase cascade requires the prior cleavage of upstream caspases called initiator caspases, such as caspase-8 and -9, that are autocatalytically cleaved and activated through recruitment by adaptor proteins that share death-effector domains (DED) or caspase activation and recruitment domains (CARD) with these initiator caspases (Nicholson, 1999). Downstream effector (or executioner) caspases-3, -6, and -7 will then cleave multiple structural and repair proteins within the cell to trigger apoptosis (Slee *et al.*, 2001).

Caspases-12 (murine) and -4 (human) have been proposed to function as initiator caspases that are activated by the endoplasmic reticulum (ER). The human *caspase-12* gene has aquired several nonsense mutations, leading to a premature translational stop or a loss-of function mutation (Rocher *et al.*, 1997; Fischer *et al.*, 2002). Human caspase-4 is partially localised to the ER and is selectively activated in response to ER stress (Hitomi *et al.*, 2004b), although events upstream of its activation remain poorly defined (Heath-Engel *et al.*, 2008). Nevertheless, compared to the murine system, other factors than caspases seem to play a role in the human system linking the ER to induction of apoptosis (Hitomi *et al.*, 2004a).

1.1.1 Death receptor pathway

The death receptor pathway is mediated by transmembrane receptors, a subfamily of the TNF-R family (tumour necrosis factor-receptor), located in the plasma membrane. Trimerisation of these death receptors by death ligands, e.g. TNFα or TRAIL (TNF-related apoptosis inducing ligand), leads to recrution of adaptor proteins, e.g. FADD (fas associated protein with death domain), TRADD (TNF-R type 1-associated death domain protein), RIP (receptor interacting protein 1) or RAIDD (RIP-associated ICH-1/Ced3 homologous protein with a death domain) via their death domains (DD) and formation of the death-inducing signalling complex (DISC) (Banner *et al.*, 1993; Boldin *et al.*, 1995). Here, procaspase-8 binds via its death effector domain (DED) and is cleaved into its active form that subsequently activates downstream effector caspases -3, -6, and -7. Activation of caspase-8 is also achieved by a membrane independent, cytosolic complex induced by activation of TNF-R1. This so called 'complex II' consists of pro-caspase-8, FADD, TRADD and RIP1-kinase and is able to induce self-processing of caspase-8 and NF-κB (Micheau and Tschopp, 2003).

Cytosol localised FLIP (FADD-like interleukin-1β converting enzyme (FLICE) inhibitory protein) proteins carry two tandem DEDs which can bind FADD and procaspase-8 thereby forming a proteolytically inactive heterodimer, inhibiting activation of caspase-8 (Krueger *et al.*, 2001; Golks *et al.*, 2005).

1.1.2 Mitochondrial pathway

The mitochondria-initiated apoptotic pathway is tightly regulated by Bcl-2 family proteins that mediate diverse cellular stress signals, e.g. DNA damage, hypoxia, endoplasmatic reticulum (ER) or nutritive stress (Daniel *et al.*, 2003). Pro-apoptotic members Bax (Bcl-2

associated X protein) and Bak (Bcl-2 antagonist/killer) are activated by a variety of these apoptotic stimuli, leading to oligomerisation and insertion into the mitochondrial outer membrane. This leads to a loss of mitochondrial membrane potential ($\Delta\Psi_m$) and release of cytochrome *c* and other apoptotic factors that are normally sequestered in the mitochondrial intermembrane space. Cytochrome *c* and d(ATP) bind to cytosolic apoptotic protease activating factor 1 (Apaf-1), also recruiting procaspase-9 which together build the mitochondrial apoptosome (Perkins *et al.*, 1998). Here, procaspase-9 is activated and functions as initiator caspase upon which the caspase cascade is started.

The death receptor and the mitochondrial pathway are connected by caspase-8 and the BH3-

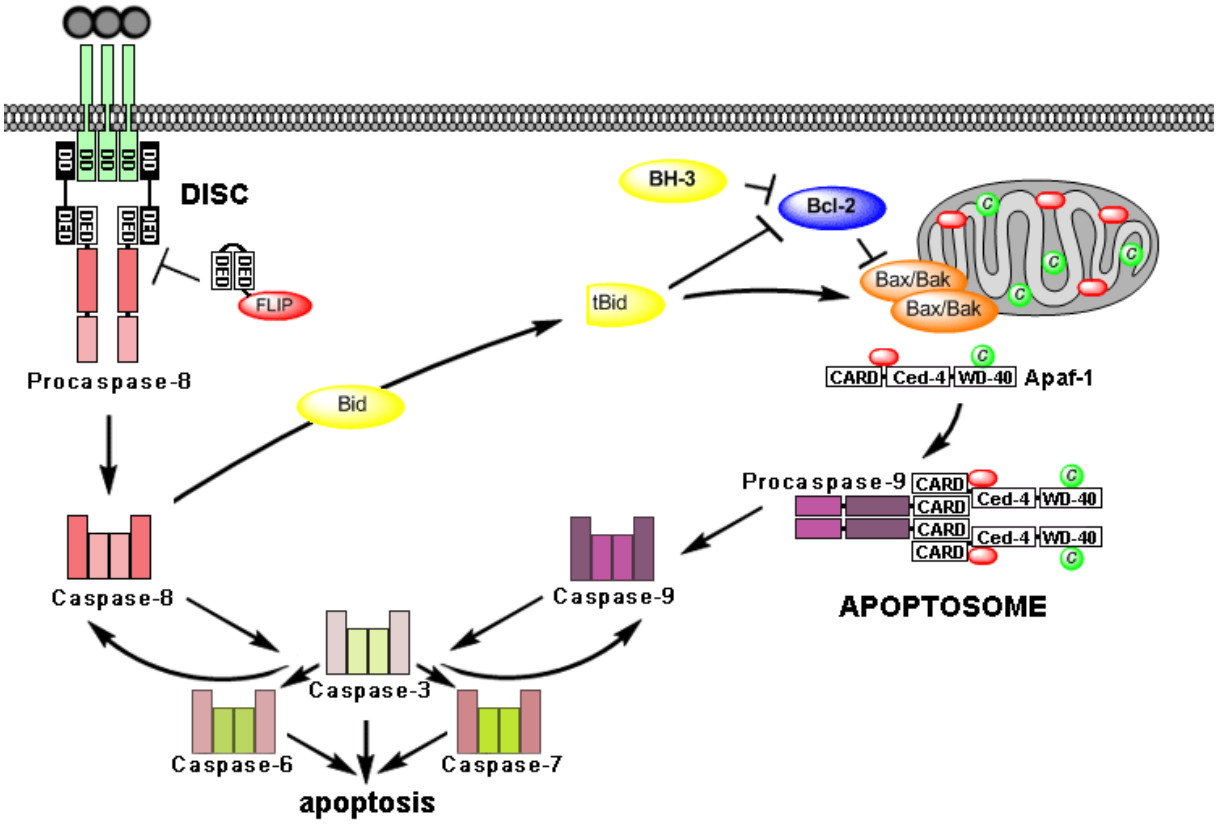

Figure 1. Extrinsic or death receptor pathway (left) and intrinsic or mitochondrial pathway (right). The extrinsic pathway is induced by binding of death ligands and assembly of the death-inducing signalling complex (DISC) that leads to cleavage of procaspase-8 to active caspase-8. This initiator caspase then activates effector caspases -3, -6, -7 and thereby eventually apoptosis. FLIP inhibits caspase-8 activation at the DISC by forming proteolytically inactive heterodimer with procaspase-8. The intrinsic pathway is activated by stress signals that are relayed by BH3-only proteins, which inactivate anti-apoptotic Bcl-2 family proteins, thereby releasing Bax and Bak. Activation of the mitochondria leads to the release of cytochrome *c* (depicted in green), (d)ATP (depicted in red) and several pro-apoptotic factors. Cytochrome *c* and d(ATP) bind to cytosolic Apaf-1, also recruiting procaspase-9 which together build the mitochondrial apoptosome. Procaspase-9 is cleaved autocatalytically and the caspase cascade is activated. Both pathways are connected by the BH3-only protein Bid, which is cleaved by caspase-8 into a truncated form (tBid) that can activate the mitochondrial pathway. Abbreviations: death domain (DD), death-effector domain (DED), caspase recruitment domain (CARD), *Caenorhabditis elegans* homology domain (Ced-4), repeating sequence at C-terminus (WD-40).

only protein Bid (BH3 interacting domain death agonist). Bid is cleaved into its active truncated form tBid by caspase-8. tBid then activates the mitochondrial pathway. After formation of the apoptosome, active caspase-9 cleaves and activates caspase-3 that subsequently, in a feedback amplification loop, activates caspase-8 (Crompton, 2000). In so called "type I cells" processed caspase-8 directly activates effector caspases, while in "type II cells" caspase-8 first needs to activate the mitochondria via tBid to induce the apoptosome which then activates effector caspases through caspase-9 (Scaffidi *et al.*, 1998).

1.1.3 Endoplasmic reticulum pathways

The endoplasmic reticulum (ER) is the place for synthesis and folding of secreted and membranous protein and lipid biosynthesis. It is the major organelle involved in intracellular calcium ion (Ca^{2+}) homeostasis and signalling. ER and mitochondria cooperate in cell death induction by Ca^{2+} signalling, which, released from the ER, can trigger cytochrome *c* release from mitochondria (Rong and Distelhorst, 2008).

Perturbances in ER homeostasis, protein folding and ER calcium concentrations will also result in a cytoprotective response called the unfolded protein response (UPR). UPR is mediated by three ER transmembrane proteins: protein kinase RNA-dependent-like ER kinase (PERK), activation transcription factor 6 (ATF6) and inositol requiring ER-to-nucleus signal kinase 1 (IRE1):

PERK is activated by dimer formation and is then autophosphorylated (Zhou *et al.*, 2006). It will phosphorylate the eucaryotic translation initiation factor 2 α (eIF2α), which together with eIF2β and eIF2γ is part of the heterotrimer eIF2. Under normal conditions eIF2 mediates binding of $tRNA^{met}$ to the 40 S subunit of the ribosome in a GTP-dependent manner to form the 43 S preinitiation complex. Phosphorylation of eIF2α results in sequestration of eIF2B, the GDP/GTP exchange factor, thereby inhibiting formation of the 43 S complex and stopping global cap-dependent translation. The 'cap' is a specifically altered nucleotide, i.e. 7-methylguanylate (m^7G), on the 5' end of most nuclear mRNAs. Certain mRNAs carrying regulatory sequences in their 5' untranslated regions, e.g. the internal ribosomal entry site (IRES), can bypass the eIF2α-dependent translational block (Schröder and Kaufman, 2005). Activation transcription factor 4 (ATF4) contains two upstream open reading frames (uORFs) in front of the ORF that codes for the protein itself, which facilitate ribosome scanning and reinitiation at the next uORF, an inhibitory element, that blocks ATF4 expression under

normal conditions. Phosphorylation of eIF2α delays reinitiation and initiates at the ATF4-coding region (Vattem and Wek, 2004). ATF4 is a transcription factor, which belongs to the CREB/ATF family of bZIP (basic leucine zipper domain) proteins (Rutkowski and Kaufman, 2003). Targets of ATF4 include genes involved in amino-acid metabolism, resistance to oxidative stress and the pro-apoptotic transcription factor C/EBP (CCAAT/enhancer-binding protein) homologous protein (CHOP) also known as C/EBPζ (Ma *et al.*, 2002).

C/EBPζ (CHOP) is also a target of ATF6, a second transducer, which is cleaved at the Golgi apparatus by site 1 and site 2 (S1/S2) proteases into its active form that moves to the nucleus and induces the activation of genes with an ER stress response element (ERSE) in their promoter (Schröder and Kaufman, 2005). Other targets of ATF6 include BiP and X box binding-protein 1 (XBP1) which is important in IRE1 signalling.

On activation, transducer number three, IRE1 will remove a 26-nucleotide intron from the XBP1 mRNA and the frameshift splice variant (sXBP1) encodes a stable, active transcription factor (Yoshida *et al.*, 2001) which targets different ER chaperones and some members of the HSP40 family. Via binding to the TNF-receptor-associated factor 2 (TRAF2), the IRE1-TRAF2 complex can recruit the apoptosis-signal-regulating kinase 1 (ASK1), which is a mitogen-activated protein 3-kinase (MAP3K) that has been shown to relay various stress signals to the downstream MAPK c-Jun N-terminal kinase (JNK) (Nishitoh *et al.*, 1998).

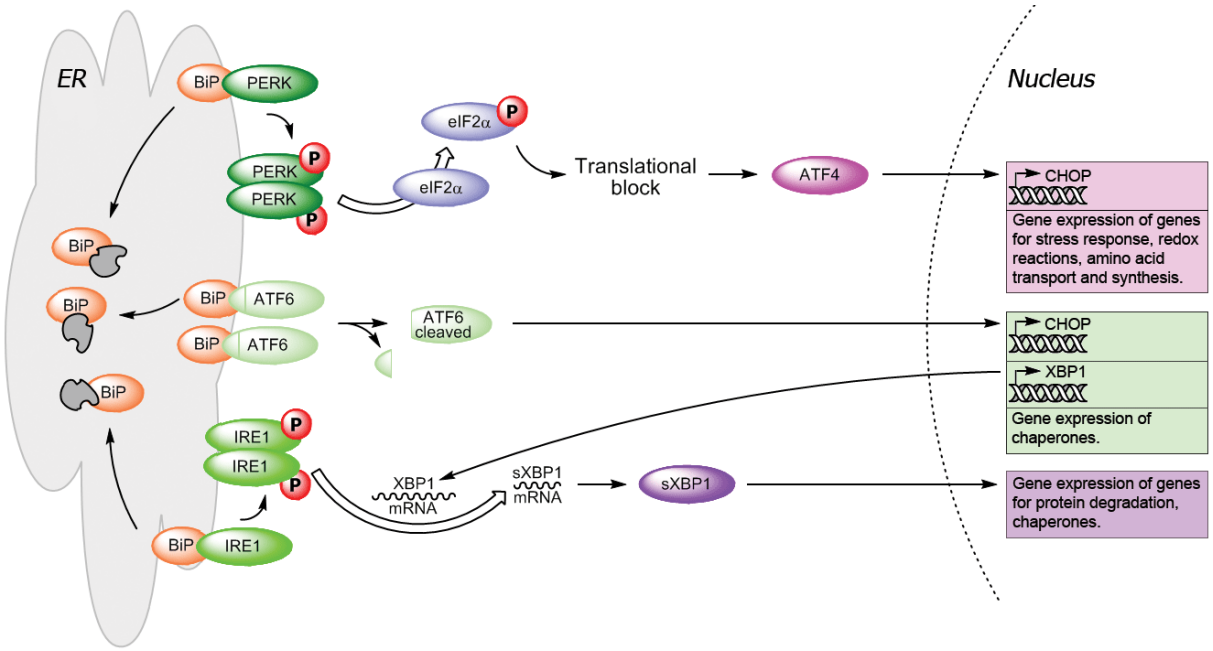

Figure 2. Unfolded protein response (UPR) pathway. Release of transducer proteins PERK, ATF6 and IRE1 by BiP upon aggregation of unfolded proteins (depicted in grey) within the ER leads to the activation of transcription factors and gene expression of genes for stress response, protein degradation and chaperones. Prolonged UPR eventually leads to apoptosis (modified after Szegezdi *et al.*, 2009).

Activation of JNK is known to influence the cell death machinery through the regulation of Bcl-2 family proteins, e.g. by phosphorylating Bcl-2 its anti-apoptotic activity is suppressed while phosphorylating Bim enhances its pro-apoptotic potential (Davis, 2000).
Under physiological conditions all transducer proteins are bound to BiP (immunoglobulin heavy chain binding protein; also known as GRP78, glucose-regulated protein 78 kDa) and are released when unfolded proteins accumulate within the ER lumen because of a higher affinity of BiP to misfolded proteins. BiP is an abundant protein under all growth conditions, but its synthesis is markedly induced under conditions that lead to the accumulation of unfolded polypeptides in the ER (Kozutsumi *et al.*, 1988).

Phosphorylation of eIF2α is a critical convergence point of the integrated stress response (ISR), which supports eukaryotic cellular adaptation to diverse environmental and engogenous stress signals, including ER stress, amino acid deprivation, infection with double-stranded RNA viruses, osmotic stress, UV light exposure, heme deficiency, and oxidative stress (Lu *et al.*, 2001; Deng *et al.*, 2002; Ron, 2002; Zhang *et al.*, 2002). Next to arrest of global cap-dependent translation, numerous stress-triggered cytoprotective genes are induced. Also, short half life proteins, e.g. cyclin D1, a regulator of G_1 to S-phase cell cycle transition and an important cofactor for several transcription factors in numerous cell types, as well as anti-apoptotic proteins disappear by degradation in the proteasome (Brewer *et al.*, 1999; Scheuner *et al.*, 2006), thereby giving the cell time to react to stressful conditions and/or enabling it to undergo apoptosis.

Accumulation of small aggregates from unfolded or misfolded proteins are thought to be highly toxic, as they impair the ubiquitin proteasome pathway (Bence *et al.*, 2001). Malfunctions of the ER stress responses caused by aging, genetic mutations, or environmental factors can result in various diseases such as diabetes, inflammation, and neurodegenerative disorders including Alzheimer's and Parkinson's disease (Yoshida, 2007).
Patients with multiple myeloma, a haematological cancer that results from the malignant transformation of plasma cells, show high expression levels of XBP1. Because plasma-cell development and survival depend on an intact UPR, this signalling pathway is also an intriguing target for novel treatments of myeloma.

1.2 Bcl-2 family of proteins

One of the first proteins identified to be involved in apoptosis was the second B-cell lymphoma gene (*bcl-2*; described by Vaux *et al.*, 1988). Initially characterised as a proto-oncogene, overexpression of *bcl-2* was found to increase the survival of haematopoietic cells by reducing the sensitivity to apoptosis (Tsujimoto and Croce, 1986). Today more than 20 human proteins of the Bcl-2 family are known, that are able to regulate the permeability of intracellular membranes to ions and proteins (Sharpe *et al.*, 2004).

The Bcl-2 family can be divided into the anti-apoptotic subfamily and the pro-apoptotic subfamily, which can be subdivided into the Bax and BH3-only subfamilies (Figure 3). These proteins contain highly conserved domains, referred to as BH (Bcl-2 homology) domains (BH1-4), which are important for complex formation. In response to death signals, such as cytotoxic agents or radiation, the BH3-only proteins antagonises the function of the antiapoptotic proteins. The BH3 domains of these proapoptotic molecules form an amphipathic α-helical fold when bound to a groove lined by the BH1, BH2, and BH3 domains of antiapoptotic proteins, a step thought to be important for apoptosis induction (Czabotar *et al.*, 2007).

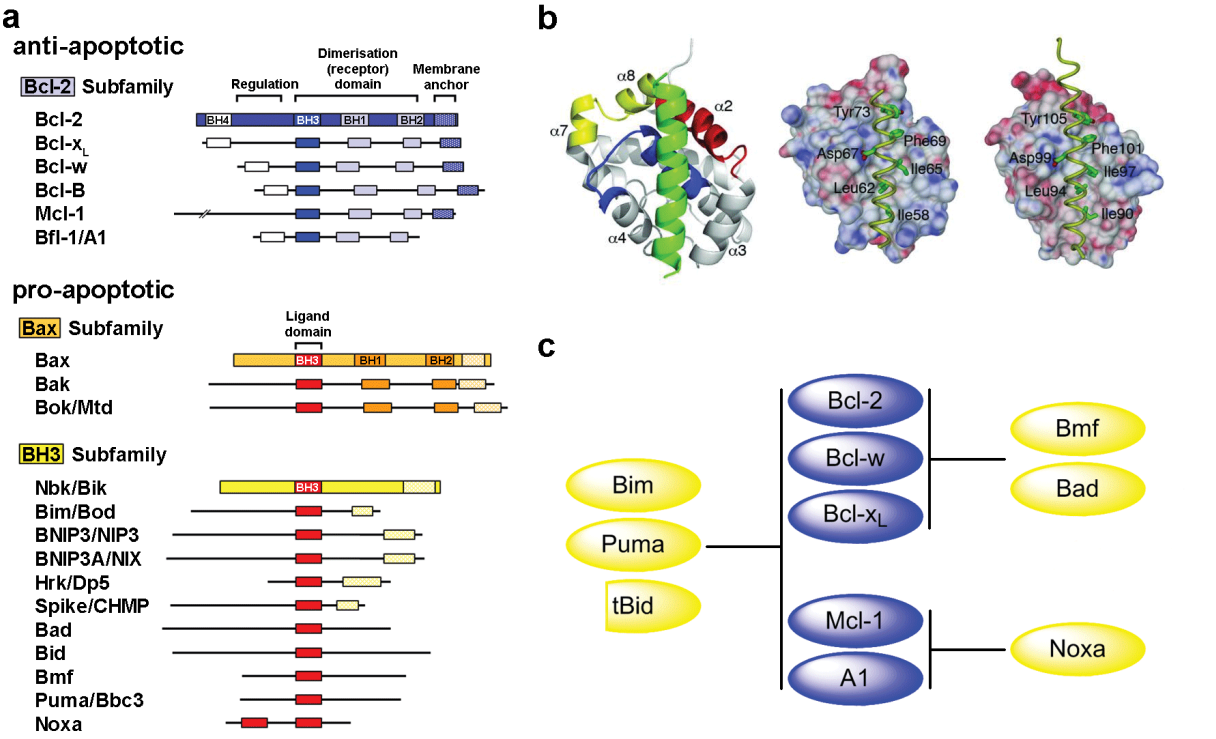

Figure 3. Bcl-2 family overview. (**a**) Anti- and pro-apoptotic members of the Bcl-2 family of proteins (excerpt). (**b**) X-ray structure of the interaction between Bim and Mcl-1; Bim BH3 peptide in green and the BH1, BH2, and BH3 regions of Mcl-1 in blue, yellow, and red, respectively (left). Bim BH3 complexed with Mcl-1 (middle) and Bcl-x_L (right) (Czabotar *et al.*, 2007). (**c**) Target selectivity of different Bcl-2 family proteins (modified from Chen *et al.*, 2005).

Bcl-2 family proteins can mostly be found at intracellular membranes where they are inserted with their carboxy-terminal hydrophobic tail, while BH3-only proteins are primarily localised in the cytosol (Krajewski *et al.*, 1993; Tanaka *et al.*, 1993). Multidomain protein Bak can be found at both the mitochondrial and ER membranes (Cheng *et al.*, 2003). Nbk, a member of the BH3-only subfamily, is inserted into the ER membrane by its transmembrane segment at the COOH-terminus and is able to induce mitochondrial cytochrome *c* release from its position at the ER (Germain *et al.*, 2002). Activation of mitochondria by Nbk is mediated only by Bax, because Bax homolog Bak is held in check by anti-apoptotic Mcl-1 (Gillissen *et al.*, 2003, 2007).

Although Bax contains a hydrophobic carboxy-terminal tail, inactive Bax is a cytosolic monomeric protein that, upon activation, changes its conformation. The internalised C-terminal anchor domain is released from the hydrophobic pocket formed by the BH1-3 domains and the protein then translocates to the mitochondrial outer membrane (Hsu *et al.*, 1997). The exact mechanism of Bak and Bax activation by BH3-only proteins is still under discussion (Danial and Korsmeyer, 2004; Youle and Strasser, 2008). Antiapoptotic proteins of the Bcl-2 family (Bcl-2, Bcl-x, Mcl-1, A1, Bcl-w, and Bcl-B) either bind to Bax and Bak and prevent oligomerisation, or are inhibited by binding to proapoptotic BH3-only proteins. The 'direct activation' hypothesis claims that a direct interaction between BH3-only proteins and Bak or Bax is necessary for their activation (Figure 4a) (Kuwana *et al.*, 2005). Recently, BH3

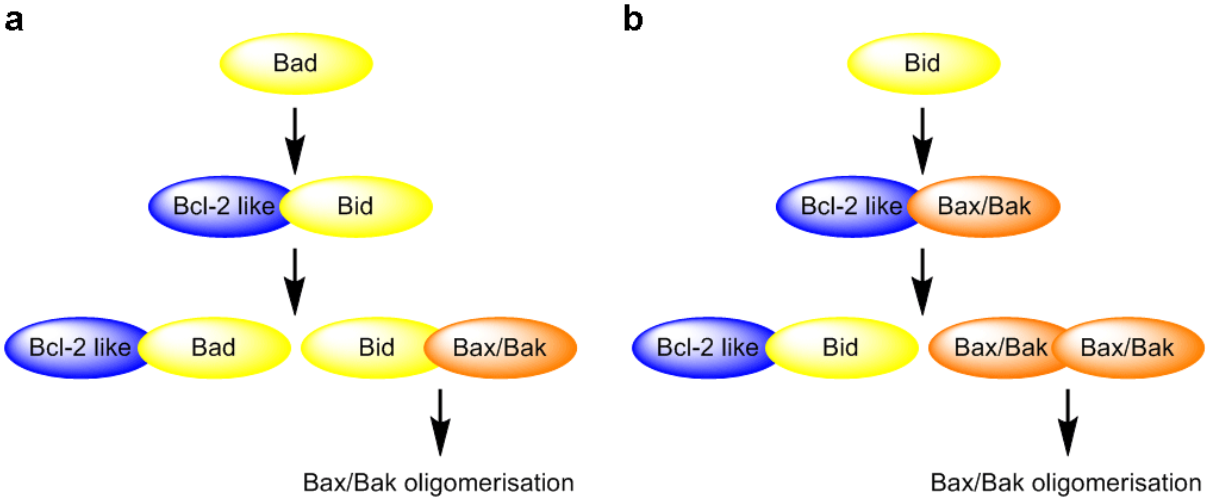

Figure 4. Models for Bax and Bak oligomerisation. (**a**) Direct activation model. BH3-only proteins can be divided into 'sensitizers' or 'derepressors' (e.g. Bad) that bind only to pro-survival proteins and 'activators' (e.g. Bim) that can also directly engage Bax and Bak. 'Sensitizers/derepressors' induce apoptosis by displacing 'activators' from pro-survival proteins, which then proceed to trigger Bax/Bak activation. (**b**) Displacement model. Pro-survival proteins inhibit Bax and Bak, perhaps through direct interaction as has been demonstrated for Bak. BH3-only proteins induce apoptosis by neutralizing pro-survival molecules and Bax/Bak activation occurs spontaneously in the absence of pro-survival activity (modified after van Delft and Huang, 2006).

domains of Bmf and Noxa were shown to induce mitochondrial outer membrane permeabilisation and apoptosis similar as the direct activators Puma, Bim, and Bid (Du *et al.*, 2011). The 'displacement' model proposes that BH3-only proteins bind to a complex of anti-apoptotic Bcl-2 and Bak or Bax, thereby replacing and activating Bak and Bax (Figure 4b) (Willis *et al.*, 2007).

1.2.1 BH3-only proteins

BH3-only proteins are important components in the regulation and activation of cell death (Daniel *et al.*, 2003). In response to different cell stress stimuli, different BH3-only proteins relay apoptosis signals to the mitochondria to induce apoptosis (Shibue and Taniguchi, 2006). BH3-only proteins are controlled by transcriptional and post-translational regulation. BH3-only genes under transcriptional control in mammals include *hrk* (harakiri), *noxa* (from latin 'damage'), *puma* (p53-upregulated mediator of apoptosis), *bim* (Bcl-2 interacting mediator of cell death), and *nbk/bik* (natural born killer / Bcl-2-interacting killer). *Noxa*, *puma*, and *nbk* are regulated by the tumour suppressor p53 (Oda *et al.*, 2000; Nakano and Vousden, 2001; Mathai *et al.*, 2002). BH3-only proteins regulated by post-translational mechanisms comprise of Bad (Bcl-2 antagonist of cell death), which is phosphorylated upon cellular stimulation with growth factors, Bid, that is N-myristoylated and cleaved by activated caspase-8, and Bmf (Bcl-2 modifying factor) and Bim (Bcl-2 interacting mediator of cell death), which are activated by sequestration from cytoskeletal structures inside the cell.

The amphipathic helix formed by the BH3 domain of BH3-only and Bax-like proteins binds to a hydrophobic groove on the surface of the anti-apoptotic Bcl-2 family members (Fesik, 2000). Although this nine amino acid long BH3 domain is highly conserved, it shows a specific target selectivity between pro-apoptotic BH3-only and anti-apoptotic Bcl-2 proteins (Figure 3c).

1.2.1.1 Bcl-2 modifying factor (Bmf)

The human *bmf* gene is located on chromosome 15q14 and loss of this site has been reported in lung and breast cancer (Wick *et al.*, 1996; Schmutte *et al.*, 1999). Bmf is regarded as a candidate tumour suppressor (Bouillet *et al.*, 2001; Puthalakath and Strasser, 2002). In this line of thought Bmf has been shown to be involved in mammary morphogenesis and to be repressed by oncogenic Ras (Schmelzle *et al.*, 2007). Bmf is constitutively expressed in

healthy tissues and is sequestered to myosin V motor complexes by association with the dynein light chain 2. Disruption of the actin cytoskeleton is thought to trigger release and activation of Bmf, initiating anoikis, i.e. apoptotic processes (Puthalakath *et al.*, 2001). Monoclonal antibodies specific for mouse Bmf have revealed the presence of multiple isoforms in most hematopoietic tissues with the highest levels found in immature T and B cells (Labi *et al.*, 2008). Until now, it is unclear how these isoforms arise, but alternative splicing of *bmf* has been reported to regulate its *in vivo* function. Two additional splice variants (*bmf II* and *bmf III*) were found to be expressed in normal and malignant human B cells (Morales *et al.*, 2004).

1.3 The $p14^{ARF}$ tumour suppressor

The *INK4b-ARF-INK4a* locus at chromosome 9p21.3 gives raise to three different proteins. Two structurally related proteins, $p15^{INK4b}$ and $p16^{INK4a}$, function as inhibitors of the cyclin-dependent kinase 4 (CDK4). The third transcript, $p14^{ARF}$, includes an alternate first exon 1β located about 20 kb upstream of the exon 1α, 2, and 3 of $p16^{INK4a}$ and contains an alternative reading frame (ARF), hence its name. Because of the alternative reading frame, $p16^{INK4a}$ and $p14^{ARF}$ do not share any amino acid homology and they have different functions within the cell (Figure 5).

The *INK4a-ARF* locus is second only to *p53* in the frequency of its disruption in human cancer (Haber, 1997). The tumour suppressor $p14^{ARF}$ is frequently inactivated in a wide spectrum of human cancer types, including colorectal, breast and pancreatic adenocarcinomas, malignant glioma, melanoma and non-Hodgkin's lymphoma (Sharpless and DePinho, 1999; Burri *et al.*, 2001). Simultaneous inactivation of p53 and $p14^{ARF}$ results in a broader tumour spectrum and more aggressive tumours than are observed with either knockout alone (Weber *et al.*, 2000).

Human ($p14^{ARF}$) and murine ($p19^{ARF}$) proteins are composed of 132 and 169 amino acids, respectively. They share about 50 % sequence homology and are both composed of more than 20 % arginine residues conferring them highly basic and having hydrophobic properties. There are no recognisable structural motifs in ARF proteins and the protein probably needs to form complexes with other molecules, both to be folded and for its charge to be neutralised at physiological pH (Ozenne *et al.*, 2010). Murine and human ARF contain a single internal methionine residue, which are absent in other species. Translational initiation from these

AUG codons produce a short form of the protein (smARF), which, when overexpressed, is supposed to localise to the mitochondria (Reef *et al.*, 2006). Full-length $p14^{ARF}$ possesses two nucleolar localisation signals (NoLS). The first one located in exon 1β plays a key role in the antiproliferative function as its deletion inhibits the ability of $p14^{ARF}$ to activate a checkpoint response via the Hdm-2 (human double minute 2) – p53 pathway (Zhang *et al.*, 1998; Rizos *et al.*, 2000; Sherr, 2006). The second one is involved in the ability of $p14^{ARF}$ to promote the sumoylation of its binding partners (Xirodimas *et al.*, 2002).

Ectopic expression of a variety of oncogenes such as Ras, c-myc, E1A and E2F1 upregulates $p14^{ARF}$ expression as part of a checkpoint response that limits cell cycle progression in response to hyperporoliferative signals (Sharpless, 2005). $P14^{ARF}$ expression is also increased after exposure to ionising or ultra violet radiation and genotoxic drugs and contributes to the DNA damage response that eliminates damaged cells from the proliferative pool (Sherr, 2006). It has also been shown that ARF expression is induced by viral infection and acts to reduce viral infectivity (García *et al.*, 2006).

Both mouse and human ARF are relatively stable proteins with estimated half-lifes ranging from approximately 1 to 8 hours. ARF turnover is still not completely understood, although two residues in exon 1β were found to be essential for $p14^{ARF}$ stability (di Tommaso *et al.*,

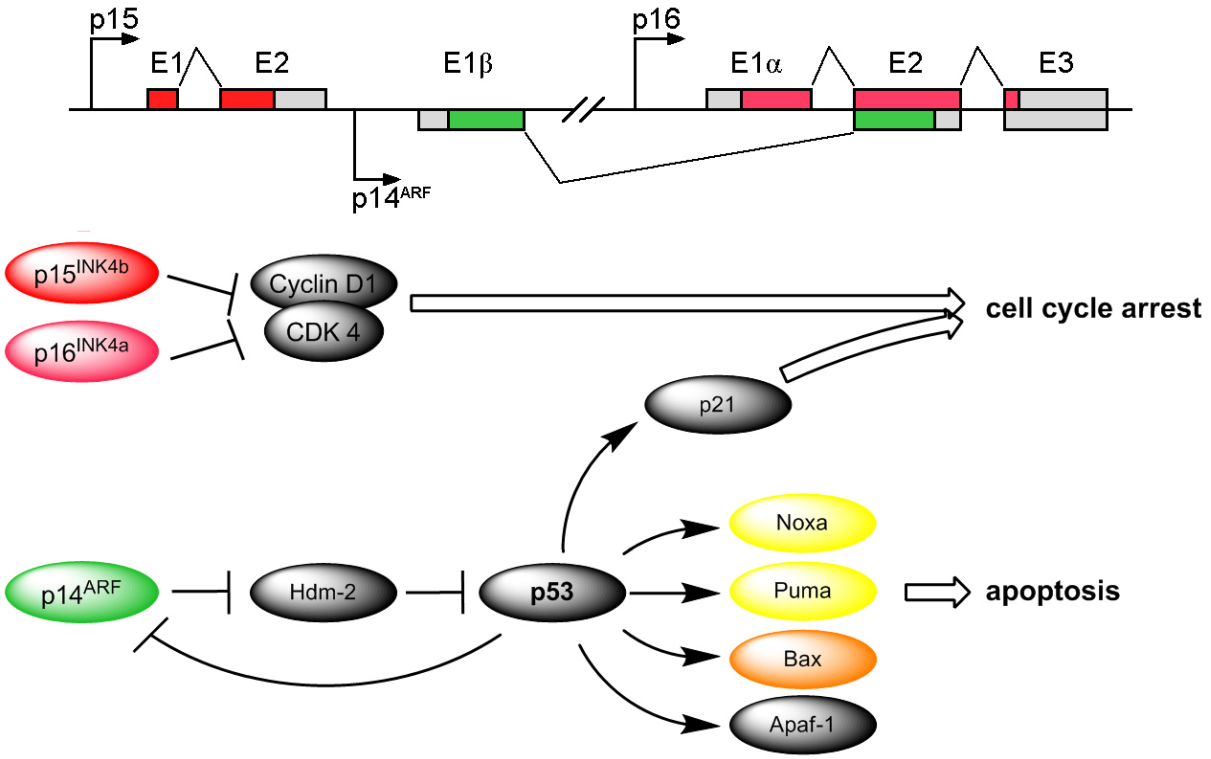

Figure 5. Schematics of the *INK4b-ARF-INK4a* locus. Activation of different pathways by transcribed genes: p15 and p16 inhibit the cyclin dependent kinase 4 (CDK4). $p14^{ARF}$ inhibits Hdm-2, thereby stabilising p53, leading to downstream transcription of pro-apoptotic proteins like Noxa, Puma, Bax, Apaf-1 and others.

2009). Some studies have shown, that ARF degradation depends, partially, on the proteasome and that, although it lacks lysine, ARF can undergo N-terminal ubiquitination independent of p53 and Hdm-2 (Pollice *et al.*, 2008). ARF is stable when expressed within the nucleolus, but turns over more rapidly in the nucleoplasm. In the nucleolus, ARF assumes a stable structure thanks to its sequestration by nucleophosmin (NPM1/B23) which prevents its nucleoplasmic degradation (den Besten *et al.*, 2005; Colombo *et al.*, 2006). From within the nucleolus ARF can attenuate translation by inhibiting RNA polymerase I and thereby ribosomal RNA (rRNA) synthesis (Sugimoto *et al.*, 2003).

To suppress aberrant cell growth in response to oncogene activation, ARF activates the transcription factor p53 by neutralising the inhibitory effects of the ubiquitin ligases Hdm-2 and ARF-BP1/Mule (ARF-binding protein 1 / Mcl-1-ubiquitin ligase E3). Both proteins are ubiquitin ligases for p53 and can inhibit its tumour suppressor functions. ARF interacts directly with Hdm-2 and blocks Hdm-2-mediated ubiquinilation, nuclear export and degradation of p53 by the proteasome (Sherr, 2006). P53 then triggers the expression of cell cycle inhibitory and pro-apoptotic genes, e.g. *puma* to induce apoptosis (Hemmati *et al.*, 2010). Although the ARF – p53 axis was proposed initially to constitute the main pathway of apoptosis induction, a number of publications clearly indicate, that ARF is able to restrict cell proliferation and induce cell death through p53-independent pathways (Lowe and Sherr, 2003). For example, expression of $p19^{ARF}$ induces a G_1 arrest in cells lacking p53 (Carnero *et al.*, 2000; Weber *et al.*, 2000). Loss of the cyclin-dependent kinase inhibitor p21, that is regulated by p53 (see Figure 5), disrupts this $p14^{ARF}$ induced G_1 arrest and increases the amount of apoptosis (Hemmati *et al.*, 2005). In double deficient p53/p21 cells, $p14^{ARF}$ expression results in a cell cycle arrest in the G_2 phase by targeting $p34^{cdc2}$ kinase, possibly representing an additional fail-safe mechanism preventing unrestrained proliferation (Normand *et al.*, 2005).

Our group showed, that p53 independent mitochondrial activation and subsequent induction of apoptosis by $p14^{ARF}$ is also independent of pro-apoptotic Bax and dependent of Bak in p53 deficient cells (Hemmati *et al.*, 2002; Müer *et al.*, 2011 submitted). Loss of Bax in cells can be functionally complemented by its homolog Bak, suggesting the induction of different pathways and BH3-only proteins (Hemmati *et al.*, 2006). One possible apoptotic pathway is targeting of C-terminal binding protein (CtBP) by ARF (Paliwal *et al.*, 2006; Kovi *et al.*, 2010).

Next to apoptosis, ARF plays an important role in induction of other types of cell death, e.g. autophagy. Although autophagy is a pro-survival mechanism where starving cells degrade their own cellular components through the lysosomal machinery for recycling purposes, deregulation of autophagy also plays a critical role in the initiation and progression of tumours (Pimkina and Murphy, 2009). Again, autophagy can be induced by ARF independent of p53 (Abida and Gu, 2008).

$p16^{INK4a}$/$p19^{ARF}$ genes also appear to be coregulated during aging. In rodents, $p19^{ARF}$ seems to play a predominant role in senescence entry, since in mouse embryonic fibroblasts (MEFs), the loss of the $p19^{ARF}$/p53, but not of the $p16^{INK4a}$/pRB axis, leads to spontaneous escape from senescence (Gil and Peters, 2006; Kim and Sharpless, 2006).

1.4 The p53 family of proteins

The p53 family consists of the tumour suppressor p53 (or tumour protein 53, TP53) and its two identified homologues, p63 and p73 (Kaghad *et al.*, 1997; Yang *et al.*, 1998). They share homology in their transactivation, DNA-binding, and oligomerisation domains with about 60 % amino acid identity in the DNA-binding domain (Melino *et al.*, 2003). The family members are differentially involved in the regulation of cell cycle and DNA-damage-induced apoptosis (Bénard *et al.*, 2003). Similar to *TP53*, the *TP73* and *TP63* genes each have two promoters (P1 and P2), and their transcripts undergo extensive splicing at the NH2- and COOH-termini. Splice variants that retain the N-terminal transactivation domain are named TA isoforms. TAp73, TAp63 and p53 share a set of target genes such as $p21^{waf1}$, *bax*, *puma*, and *noxa* to induce cell cycle arrest and apoptosis (Harms *et al.*, 2004; Perez and Pietenpol, 2007).

In general, the p53 tumour suppressor protein functions as a transcription factor that regulates the expression of stress response genes and mediates a variety of anti-proliferative processes. It is known to mediate its effect through the activation of genes regulating cell cycle checkpoints, DNA damage and repair response, and apoptosis (Stewart and Pietenpol, 2001).

In contrast, p63 is a putative oncogene and is required for the development and maintenance of stratified epithelium (Westfall and Pietenpol, 2004). It can bind to p53 DNA consensus sequences and induces apoptosis independent of p53 status when overexpressed in cells by triggering signalling via death receptors and the mitochondria (Gressner *et al.*, 2005). Endogenous p63 has been shown to be induced by many chemotherapeutic agents and

blocking its function might confer chemoresistance (Petitjean *et al.*, 2005). Interestingly, $p14^{ARF}$ has been shown to inhibit p63 mediated transactivation of p53 responsive genes (Calabrò *et al.*, 2004).

The high homology shared by p73 and p53 and the observation that p73 maps to chromosome 1p36.1, a region frequently deleted in several tumours, including neuroblastoma, colorectal cancer and breast cancer, initially suggested that p73 is a tumour suppressor. It is involved in neurogenesis, neuron survival and the inflammatory response (Irwin and Kaelin, 2001a). *TP73* is directly activated by E2F and can lead to the activation of pro-apoptotic genes in a p53-independent manner (Stiewe and Pützer, 2000).

Mutant p53 proteins form complexes with other transcription factors, such as p63 or p73, and either inactivate them or change their pattern of transcription, altering the properties of the cancer cell. Indeed, mutant p53/p73 complexes have been detected in cancer cells (Irwin *et al.*, 2003), and an altered chemotherapeutic response could be the result of an inactivation of p73 apoptotic functions (Irwin and Kaelin, 2001b). Both p63 and p73 are rarely mutated in cancer cells and therefore could be putative targets for novel anti-cancer therapeutics. Still, many questions remain about their roles in human tumourigenesis as data suggests that p63 and p73 have both tumour suppressive and oncogenic properties (Zaika and El-Rifai, 2006).

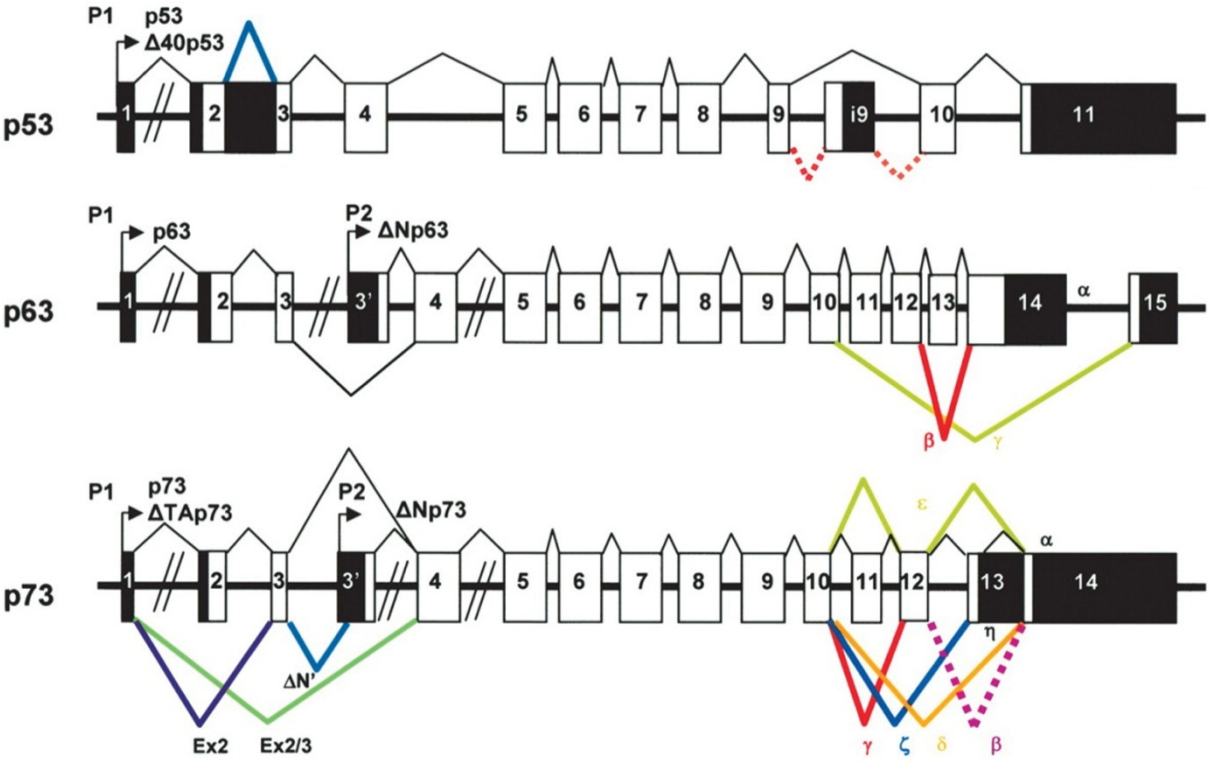

Figure 6. Overview of the p53 protein family. Structure of the human *p53*, *p63*, and *p73* genes and their multiple splice variants. Coding sequence in white; noncoding sequence in black (modified from Bourdon *et al.*, 2005).

2. Aim of the study

The $p14^{ARF}$ tumour suppressor plays a central role in the regulation of cell cycle arrest, apoptosis, and cellular senescence. Expression of cellular or viral oncogens leads to a rapid upregulation of $p14^{ARF}$ at the mRNA and protein level. Upon upregulation, cell cycle arrest and/or cell death is mediated via the $p14^{ARF}$/Hdm-2/p53 pathway. Apoptosis by this pathway is mainly executed via p53 mediated upregulation of Puma leading to mitochondrial activation (Hemmati *et al.*, 2010). Unfortunately, this pathway is not functional in most tumours because of mutations or deletions of p53. However, we previously showed, that $p14^{ARF}$ can also induce apoptosis and cell cycle arrest independent of p53 (Hemmati *et al.*, 2002, 2005), but the mechanism remains elusive.

The aim of this study was to analyse this mechanism by different approaches. First, the p53 family members p63 and p73 can be activated by $p14^{ARF}$ and contribute to programmed cell death induction in the absence of p53 (Yao and Chen, 2010; Slade and Horvat, 2011). Therefore, we wanted to analyse if these p53 homologs are able to compensate for loss of p53 in $p14^{ARF}$ induced apoptosis. Second, cellular organelles other than the mitochondria could be utilised to mediate $p14^{ARF}$ induced apoptosis. Next to the extrinsic and intrinsic mitochondrial pathway, induction of apoptosis via the endoplasmic reticulum (ER) has been reported. Comparative expression analysis of genes involved in the unfolded protein response (UPR), a mechanism to relay stress signals from the ER, by use of ER stressing drugs and $p14^{ARF}$ should be performed. Third, the BH3-only protein Puma plays an essential role in $p14^{ARF}$ induced apoptosis via p53. BH3-only proteins might also be involved in apoptosis induced by $p14^{ARF}$ in p53 deficient cells. Induction of BH3-only genes by $p14^{ARF}$ in p53 pro- and deficient cell lines and via the ER stress pathway should be addressed.

3. Materials and Methods

3.1 Materials

3.1.1 Tools

ABI7300	Applied Biosystems, Darmstadt, Germany
BD FACScan™	Becton Dickinson, Franklin Lakes, USA
centrifuge 5415C	Eppendorf, Hamburg, Germany
centrifuge Varifuge 3.0R	Heraeus Sepatech, Hanau, Germany
Curix 60	AGFA, Mortsel, Belgium
electroporator Gene Pulser II	Bio-Rad, München, Germany
gel apparatus MiniSub Cell	Bio-Rad, München, Germany
gel doc imager	Bio-Rad, München, Germany
incubator Certomat R / Certomat H	B. Braun Biotech International, Allentown, USA
laboratory scales BP210S	Satorius, Göttingen, Germany
PCR cycler GeneAmp PCR System 2400	Applied Biosystems, Norwalk, USA
pH meter CG825	Schott, Hofheim am Taunus, Germany
photometer GeneQuant II	Pharmacia Biotech, San Francisco, USA
Power Pac 300	Bio-Rad, München, Germany
precision scales BP3100S	Satorius, Göttingen, Germany
shaker Duomax 1030	Heidolph, Schwabach, Germany
Sonopuls GM70	Bandelin, Berlin, Germany
thermo shaker compact	Eppendorf, Hamburg, Germany
Vortex Genie II	Scientific Industries, Bohemia, USA

3.1.2 Chemicals

acetic acid	Merck, Darmstadt, Germany
agarose	Biozym, Hessisch-Oldendorf, Germany
ampicillin	AppliChem, Gatersleben, Germany
bacto agar	BD Biosciences, Heidelberg, Germany
β-mercaptoethanol	Carl Roth, Karlsruhe, Germany
boric acid	Carl Roth, Karlsruhe, Germany
bromphenol blue	Carl Roth, Karlsruhe, Germany
DMEM	Gibco, Karlsruhe, Germany
DMSO (dimethylsulfoxid)	Merck, Darmstadt, Germany
doxycycline hydrochlorid	Sigma, Taufkirchen, Germany

EDTA (ethylenediaminetetraacetic acid)	Carl Roth, Karlsruhe, Germany
ethanol	J. T. Baker, Griesheim, Germany
ethidiumbromid	Sigma, Taufkirchen, Germany
FCS (fetal calf serum)	Gibco, Karlsruhe, Germany
gel loading solution	Sigma, Taufkirchen, Germany
glycerol	J. T. Baker, Griesheim, Germany
HCl (hydrochloric acid)	Merck, Darmstadt, Germany
isopropanol	Carl Roth, Karlsruhe, Germany
kanamycin	Carl Roth, Karlsruhe, Germany
McCoy's 5A	Gibco, Karlsruhe, Germany
methanol	Carl Roth, Karlsruhe, Germany
NaCl (sodium chloride)	Carl Roth, Karlsruhe, Germany
Neomycin (G418)	Carl Roth, Karlsruhe, Germany
PBS (phosphate buffered saline)	Gibco, Karlsruhe, Germany
penicillin/streptomycin	Biochrom AG, Berlin, Germany
phenol-chloroform-isoamylalcohol	Carl Roth, Karlsruhe, Germany
puromycin	Carl Roth, Karlsruhe, Germany
SDS (sodium dodecyl sulfate)	Carl Roth, Karlsruhe, Germany
thapsigargin	A.G. Scientific, San Diego, CA, USA
tris base	Carl Roth, Karlsruhe, Germany
tris hydrochlorid	Carl Roth, Karlsruhe, Germany
trypsin-EDTA	Gibco, Karlsruhe, Germany
trypton	Carl Roth, Karlsruhe, Germany
tunicamycin	A.G. Scientific, San Diego, CA, USA
yeast extract	Carl Roth, Karlsruhe, Germany

3.1.3 Solutions, buffers and media

Antibiotics (1000x)	50 mg/ml Ampicillin; 30 mg/ml Kanamycin
LB medium	10 g Bacto-tryptone 5 g Bacto-yeast extract 10 g NaCl ad 1 l bidest H_2O; pH adjusted to 7.2; autoclave
LB agar	LB medium 15 g/l Bacto agar; autoclave

6x DNA loading buffer	0.2% Bromphenol blue 60% Glycerol 60 mM EDTA
10x Orange G DNA loading buffer	20 g Sucrose 100 mg Orange G ad 50 ml H_2O
10x TBE buffer	108 g Tris base 55 g Boric acid 40 ml 0.5 M EDTA; pH 8.0 ad 1 l H_2O
TE buffer	10 mM Tris-HCl 1 mM EDTA; pH 8.0
10x annealing buffer	10 mM Tris-HCl; pH 7.6 100 mM NaCl 1 mM EDTA
4x Laemmli buffer	8g SDS 40 ml Glycerin 40 ml 0.6 M Tris pH 6.8 80 mg bromophenol blue ad 80 ml bidest H_2O 20 ml β-mercaptoethanol
SDS-PAGE running buffer	25 mM Tris-HCl pH 8.3 190 mM Glycin 0.1% SDS
Western blotting running buffer	20 mM Tris 150 mM Glycin 20% methanol 0.08% SDS

3.1.4 Kits

ChIP Kit	Diagenode, Liege, Belgium
Invisorb Plasmid Maxi Kit	Invitek, Berlin, Germany
Invisorb Spin Plasmid Mini Two	Invitek, Berlin, Germany
QIAquick Gel Extraction	Qiagen, Hilden, Germany

3.1.5 Markers

rainbow molecular weight marker	GE Life Sciences, Fairfield, CT, USA
1 kb Plus DNA ladder	Invitrogen, Karlsruhe, Germany
100 bp DNA ladder	Invitrogen, Karlsruhe, Germany

3.1.6 Antibodies

β-actin (Ab-1) Mouse mAB (JLA20)	Merck, Darmstadt, Germany
ATF4/CREB-2 (C-20): sc-200	Santa Cruz Biotechnology, Santa Cruz, CA, USA
Bak NT (TC102)	Merck, Darmstadt, Germany
Bax NT, #06-499	Millipore, Billerica, MA, USA
BiP/GRP78 #610979	BD Biosciences, Heidelberg, Germany
CHOP/GADD153 (B-3): sc-7351	Santa Cruz Biotechnology, Santa Cruz, CA, USA
eIF2α-phospho (Ser51) #9721	Cell Signaling, Frankfurt, Germany
$p14^{ARF}$ (Clone 14P02)	Thermo Scientific, Bonn, Germany
p53 #554293	BD Biosciences, Heidelberg, Germany
p53 (PAb421) #OP03	Merck, Darmstadt, Germany
anti goat, #6165-05	Southern Biotech, Birmingham, AL, USA
anti mouse #1031-05	Southern Biotech, Birmingham, AL, USA
anti rabbit #4050-05	Southern Biotech, Birmingham, AL, USA
anti rat #3050-05	Southern Biotech, Birmingham, AL, USA
goat-anti-rabbit IgG (H+L) FITC labeled F(ab)2	Jackson Immuno Research, W. Grove, PA, USA
goat-anti-mouse IgG (H+L) FITC labeled F(ab)2	Jackson Immuno Research, W. Grove, PA, USA

If not stated otherwise, primary antibodies were used at a dilution of 1:1,000 and the secondary antibody at a dilution of 1:10,000.

3.1.7 Enzymes

restriction endonucleases (*Afe*I, *BamH*I, *Bgl*II, *Cla*I, *EcoR*I, *EcoR*V, *Hind*III, *Kpn*I, *Nde*I, *Nhe*I, *Not*I, *Pac*I, *Sac*II, *Spe*I, *Swa*I, *Xba*I, *Xho*I)	NEB, Frankfurt am Main, Germany

CrimsonTM Taq DNA polymerase (5 U/µl)	NEB, Frankfurt am Main, Germany
GoTaq® DNA polymerase (5 U/µl)	Promega, Mannheim, Germany
InviTaq polymerase	Invitek, Berlin, Germany
T4 DNA Ligase (100 U/µl)	Invitrogen, Karlsruhe , Germany

3.1.8 Oligonucleotides

Oligonucleotides for genotyping, sequencing, and ChIP assay were synthesised by BioTez GmbH (Berlin, Germany) or Tib MolBiol (Berlin, Germany). Primer and probes for RT-PCR (TaqMan) analysis were ordered from Tib Molbiol as complete gene expression assay or synthesised by BioTez GmbH.

TaqMan primer:

Name	Forward and reverse primer	Probe
p53	5'- AgT gTg gTg gTg CCC TAT gAg C -3' 5'- CgC CCA TgC Agg AAC TgT TAC -3'	6FAM-Tgg CTC TgA CTg TAC CAC CAT CCA CTA CAA CTA C--TMR
$p14^{ARF}$	5'- CCC TCg TgC TgA TgC TAC TgA ggA -3' 5'- ggC gCT gCC CAT CAT CAT gAC -3'	6FAM-AgC gTC TAg ggC AgC AgC CgC TTC CTA gAA--TMR
ATF4	5'- CAg TCC CTC CAA CAA CAg CAA -3' 5'- AAg TCg AAC TCC TTC AAA TCC ATT -3'	6FAM-Agg ATg CCT TCT CCg ggA CAg ATT g--TMR
ATF6	5'- TCT CTT TgC TgA ACT Cgg TTA TTT C -3' 5'- AAT TgT TTT CAT ACg TCT CAT TTg CT -3'	6FAM-CAg ACA CTg ATg AgC TgC AAT Tgg AA--TMR
CHOP	5'- ggA AAT gAA gAg gAA gAA TCA AAA AT -3' 5'- gTT CTg gCT CCT CCT CAg TCA -3'	6FAM-TTC ACC ACT CTT gAC CCT gCT TCT CTg g-TMR
eIF2α	5'- gAg gAT CAg AAg gAC TgT ACA Tgg T -3' 5'- TCT TCC CAg ATT CCC TTg gA -3'	6FAM-ATg gAC CAC CAC ATT TTA CAg AAA gCA CAg Tg--TMR
BiP/GRP78	5'- gCA ACC AAA gAC gCT ggA A -3' 5'- TgC CgT Agg CTC gTT gAT g -3'	6FAM-ATT gCT ggC CTA AAT gTT ATg Agg A--TMR
IRE1	5'- AAg CAg gAC ATC Tgg TAT gTT ATT gA -3' 5'- CgT ACA Tgg TgA Tgg TgT ATT CTg TT -3'	6FAM-TTg TCA TCg gCC TTT gCA gAT AgT CTC Tg--TMR
PERK	5'- gCA AAC CAg Agg TAT TTg ggA AT -3' 5'- ggT CTT ggTCCC ACT ggA AgA -3'	6FAM-ATg ATC ATT CCT TCC CTg gAT ggA gCC--TMR
XBP1u	5'- CAg TgA Agg AAg AAC CTg TAg AAg ATg AC -3' 5'- CAg TAg gCA ggA AgA Tgg CTT Tg -3'	6FAM-ATC TCA AAT CTg CTT TCA TCC AgC CAC TgC--TMR
XBP1u+s	5'- CgC TgA ggA ggA AAC TgA AAA A -3' 5'- TgT TCC AgC TCA CTC ATT CgA -3'	6FAM-AgC TCA gAC TgC CAg AgA TCg AAA gAA--TMR
BAD	5'- gCA CAg CAA CgC AgA TgC -3' 5'- AAg TTC CgA TCC CAC CAg gA -3'	6FAM-CCA gCT ggA CgC gAg TCT TCC Ag-TMR
BID	5'- CCA AgA Agg Tgg CCA gTC A -3' 5'- TCC TCA CgT Agg TgC gTA ggT -3'	6FAM-ACg CCg TCC TTg CTC CgT gAT gT
BIM	5'- CCA ggC CTT CAA CCA CTA TCT -3' 5'- CCA ATA CgC CgC AAC TCT T -3'	6FAM-CTT CAA TgA ggC Agg CTg AAC CTg C--TMR
BMF	5'- Tgg CAA CAT CAA gCA gAg gT -3' 5'- CTg CTg gTg TTg CTg CAC A -3'	6FAM-CAg ATT gCC CgA AAg CTT CAg Tg--TMR
BNIP3	5'- gAg gAA CAC gAg CgT CAT gA -3' 5'- Agg TgC Tgg Tgg Agg TTg TC -3'	6FAM-CCA TCT CTg CTg CTC TCT CAT TTg CTg g-TMR
HRK	5'- gCA ggC ggA ACT TgT Agg AA -3' 5'- TTT CTC CAA ggA CAC Agg gTT T -3'	6FAM-Cgg AgC CgA gAC CCA gCC g-TMR
NBK	5'- CAC AgC CTg ggT CTg gCT T -3' 5'- TTA AgT gTg gTg AAA CCg TCC A -3'	6FAM-CAT CCC TgA TgT CCT CAg TCT ggT CgTXT--PH
NOXA	5'- gCA AgA ACg CTC AAC CgA g -3' 5'- gCA gAA gAg TTT ggA TAT CAg -3'	6FAM-AAg TCg AgT gTg CTA CTC AA TCA--TMR
PUMA	5'- AgA CAA gAg gAg CAg CAg Cgg -3' 5'- ACC TAA TTg ggC TCC ATC TCg g -3'	6FAM-CTC ATC ATg ggA CTC CTg CCC TTA CCC--TMR
SPIKE	5'- CCT gCA AAg AAT ATg gTC AAg -3' 5'- CCC gCT gCT CAT ACA T -3'	6FAM-CAg AAA gCC TTg CgA gTT TTA AAg--TMR

ABL	5‘- Tgg AgA TAA CAC TCT AAg CAT AAC TAA Agg T -3‘ 5‘- gAT gTA gTT gCT Tgg gAC CCA -3‘	6FAM-CCA TTT TTg gTT Tgg gCT TCA CAC CAT T--TMR

Primer for ChIP-Assay:

Name	Forward primer	Reverse primer
NS	5‘- Agg CCA gTg ggA Agg CAg gT -3‘	5‘- CCC TTg gCA ATg ggg TCC TTT CC -3‘
RE1	5‘- AgA ATC CgC ACT ggC gAC gg -3‘	5‘- CTC ggg gCA TCC CgC AAA CA -3‘
RE2	5‘- gCA CCC TgC ACC CAC Tgg AC -3‘	5‘- CCg TCg CCA gTg Cgg ATT CT -3‘
RE3	5‘- TgA ggg CAg ACg CCA ggT TT -3‘	5‘- AAg Cgg AgC gCT CAA gAA gg -3‘
RE4	5‘- AgA CAg ggT TTC CCg TgT Tg -3‘	5‘- CTg gAg AAg gCC TCA ggg Ag -3‘
RE5	5‘- TAA gCT CTC CAg CTC AgC AC -3‘	5‘- TgC CTg TAA TCC CAg CTA CT -3‘

3.1.9 Vectors and Plasmids

For cloning and mutagenesis of genes and protein expression, a collection of vectors and plasmids available from the previous work in our laboratory has been used. All new constructs were analysed and verified by sequencing.

pGEM-T	Promega, Madison, WI, USA
pIRESneo3	Clontech, Cat #6988-1
pIRESpuro3	Clontech, Cat #631619
pCMV-p53	Clontech, Cat #6004-1
pCMV-Sport6_ATF4 (IRATp970B0515D)	cDNA ImaGenes, Berlin-Buch, Germany
pOTB7_DDIT3 (IRAUp969G0819D6)	cDNA ImaGenes, Berlin-Buch, Germany
pcDNA3-p14^{ARF}	provided by Philipp Hemmati
pAd1-Δ1Δ3+tTA	provided by Bernd Gillissen
pAd2 TrePro	provided by Bernd Gillissen. The insert contains a c-Myc epitope tag (EQKLISEEDL).
mPERK.ΔC.9E10.pCDNA.amp	provided by David Ron, Skirball Institute of New York University’s School of Medicine. The insert contains a c-Myc epitope tag (EQKLISEEDL) on its C-terminal end.
pGL3-Basic	Promega, Madison, WI, USA
pRL-TK	Promega, Madison, WI, USA

pIRESneo3-revMCS+*Xho*I and pIRESpuro3-revMCS+*Xho*I

Oligonucleotides containing restriction sites in a reverse order of pIRESneo3 and one added *Xho*I-site were designed (Fwd: 5′-CgA TAT CTC Cgg ATT CgA ATT Cgg ATC CAC Cgg TTA ACA ggC CTT AAg CgC TAg CCT CgA ggC-3′, Rev: 5′-ggC CgC CTC gAg gCT AgC gCT TAA ggC CTg TTA ACC ggT ggA TCC gAA TTC gAA TCC ggA gAT AT-3′) annealed and ligated into pIRESneo3 and pIRESpuro3 digested with *Cla*I and *Not*I.

pIRESneo3-revMCS+*Xho*I-mPERKΔC

Vectors mPERK.ΔC.9E10.pCDNA.amp and pIRESneo3-revMCS+*Xho*I were digested with *EcoR*I and *Xho*I. The truncated PERK fragment was then ligated into pIRESneo3-revMCS+*Xho*I.

pIRESneo3-p53 and pIRESneo3-ΔNp53

The p53 cDNA was cloned into pIRESneo3 by digesting pCMV-p53 with *Nde*I and *EcoR*I and ligated into pIRESneo3, thereby replacing part of the human cytomegalovirus major immediate early promoter ($P_{CMV\ IE}$) of pIRESneo3 by the one from pCMV-p53.

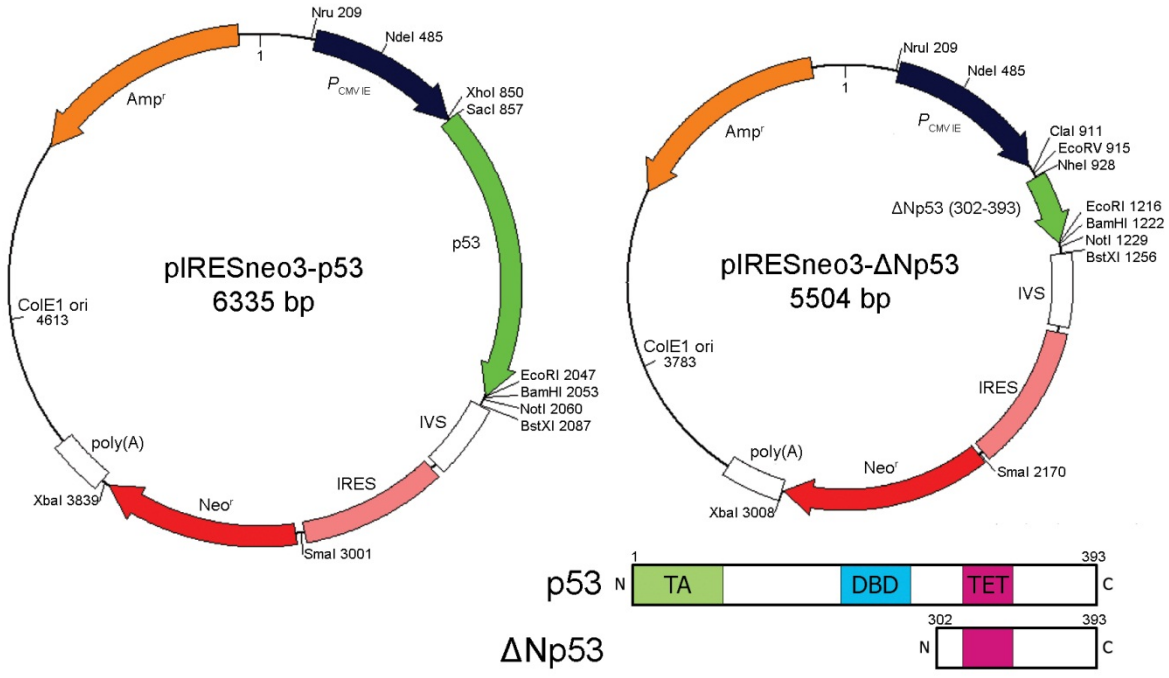

Figure 7. Schematics of pIRESneo3-p53 and pIRESneo3-ΔNp53 vectors. ΔNp53 contains amino acids 302-393 of full length p53. Abbreviations: transactivation domain (TA), DNA binding domain (DBD) and tetramerisation domain (TET).

Based on the work of Shaulian *et al.* we created a dominant negative p53 (ΔNp53) gene, lacking the transactivation and DNA binding domains (Shaulian *et al.*, 1992). The PCR product was raised by using a forward primer including a *Nhe*I site and the startcodon (`5′-TAg CTA gCA Tgg ggA gCA CTA AgC gAg C-3′`) and a reverse primer including an *EcoR*I site (`5′-ATA gAA TTC TCA gTC TgA gTC Agg CC-3′`) on pCMV-p53 as template. It was ligated into pGEM-T vector and analysed by sequencing. Correct clones were digested with *EcoR*I and *Nhe*I and ligated into the multiple cloning site of pIRESneo3.

pGL3-Basic(modMCS)

Oligonucleotides containing restriction sites of pGEM-T were designed (Fwd: `5′-CgA TAT CTC Cgg ATT CgA ATT Cgg ATC CAC Cgg TTA ACA ggC CTT AAg CgC TAg CCT CgA ggC-3′`, Rev: `5′-ggC CgC CTC gAg gCT AgC gCT TAA ggC CTg TTA ACC ggT ggA TCC gAA TTC gAA TCC ggA gAT AT-3′`) annealed and ligated into pGL3-Basic digested with *Kpn*I and *Hind*III.

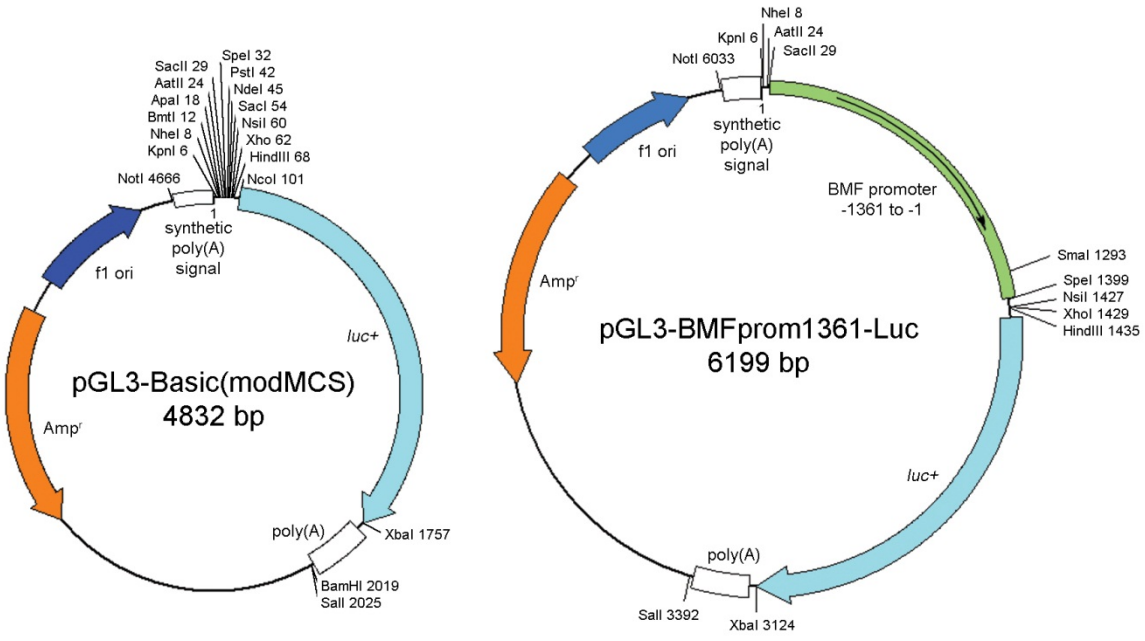

Figure 8. Schematics of pGL3-Basic(modMCS) and pGL3-BMFprom1361-Luc. Vectors with *bmf* promotor inserts from -1114 to -1, -821 to -1, -427 to -1, and -229 to -1 were cloned accordingly.

pGL3-BMFprom1361-Luc

Vector containing basepairs -1361 to -1 of the *bmf* promoter. PCR product raised from HCT116 wt genomic DNA with primers (Fwd: 5′-TAA gCT CTC CAg CTC AgC AC-3′, Rev: 5′-AAA ATA CgC CTg CTC ggg gC-3′) was ligated into pGEM-T vector. This vector was digested with *Sac*II and *Spe*I and the insert ligated into pGL3-Basic(modMCS).

pGL3-BMFprom229/427/821/1114-Luc

PCR products raised from pGL3-BMFprom1361-Luc with primers (Fwd 229: 5′-AgA ATC CgC ACT ggC gAC gg-3′, Fwd 427: 5′-gCA CCC TgC ACC CAC Tgg AC-3′, Fwd 821: 5′-TgA ggg CAg ACg CCA ggT TT-3′, Fwd 1114: 5′-AgA CAg ggT TTC CCg TgT Tg-3′, and Rev: 5′-AAA ATA CgC CTg CTC ggg gC-3′) were ligated into pGEM-T vector. pGEM-T vectors were then tested by sequence analysis, digested with *Sac*II and *Spe*I and inserts ligated into pGL3-Basic(modMCS).

pcDNA3.1(+)-CHOP and pcDNA3.1(+)-ATF4

pAd2 Vectors containing *chop* and *atf4* genes (see 2.1.10) were digested with *BamH*I and *Xba*I and ligated into pcDNA3.1(+) vector digested accordingly.

pcDNA3.1(+)-p14^{ARF}

pcDNA3-p14^{ARF} vector was digested with *BamH*I and *EcoR*I and ligated into pcDNA3.1(+) vector digested accordingly.

3.1.10 Adenoviruses

Ad5-CMV-LacZ	provided by Bernd Gillissen
Ad5-CMV-p14^{ARF}	provided by Philipp Hemmati
Ad5-CMV-p14$^{ARF}_{(Tet)}$	provided by Antje & Anja Richter

Ad5-CMV-ATF4$_{(Tet)}$ and Ad5-CMV-CHOP$_{(Tet)}$

Oligonucleotides containing *BamH*I and *Xba*I restriction sites were designed (ATF4 Fwd: 5′-TTC gAA TTC ggA TCC ATg ACC gAA ATg AgC-3′, ATF4 Rev: 5′-gAg CTC gAg TCT AgA CTA ggg gAC CCT TTT-3′; CHOP Fwd: 5′-TTC gAA TTC

ggA TCC ATg gCA gCT gAg TCA TTg CCT TTC TTC-3′, CHOP Rev: 5′-AgA TCT AgA TCA TgC TTg gTg CAg ATT CAC CAT TCg-3′). PCR products raised by these primers from pCMV-Sport6_ATF4 (IRATp970B0515D) and pOTB7_DDIT3 (IRAUp969G0819D6), respectively, were digested with *BamH*I and *Xba*I and ligated into pAd2 vectors digested accordingly. Shuttle plasmids pAd2 containing ATF4 and CHOP inserts were digested with *Pac*I and *Not*I and recombinated with *Cla*I digested pAd1-Δ1Δ3+tTA vector in *E. coli* BJ5183 cells. pAd1 containing ATF4 and CHOP inserts were transfected in HEK 293 cell lines by calcium phosphate precipitation. After plaque formation, supernatant was used to infect HEK 293 cells to amplify viruses. All viruses were banded in CsCl gradients, dialysed, and stored in aliquots.

3.1.11 Bacteria

Escherichia coli DH5α (Genotype: *fhu*A2, Δ(argF-lacZ)U169, *pho*A, *gln*V44, Φ80, Δ(*lac*Z)M15, *gyr*A96, *rec*A1, *rel*A1, *end*A1, *thi*-1, *hsd*R17), *Escherichia coli* SCS110 (Genotype: *rps*L, *thr*, *leu*, *end*A, *thi*-1, *lac*Y, *gal*K, *gal*T, *ara*, *ton*A, *tsx*, *dam*, *dcm*, *sup*E44, Δ(*lac-pro*AB)) and *Escherichia coli* JM109 (Genotype: *end*A1, *rec*A1, *gyr*A96, *thi, hsd*R17 (r_k^-, m_k^+), *rel*A1, *sup*E44, Δ(*lac-pro*AB), [F′ *tra*D36, *pro*AB, *laq*I^qZΔM15]) were used for transformations and plasmid amplifications.

Escherichia coli BJ5183 (Genotype: endA, scbBC, recBC, galK, met, thi-1, bioT, hsdR (Str)) were used for homologic recombinations.

3.1.12 Cell lines

All cells were kept in an incubator at 37 °C, 5% CO_2 and 95% humidity.

HEK293 is derived from human embryonal kidney cells which were transformed by adenovirus 5 (Ad5) (Graham *et al.*, 1977). They constitutively express Ad5 specific E1 proteins which allow replication and transcription of adenoviral DNA. The cell line is used for amplification and titration of human adenoviruses. Cells are grown in DMEM (Dulbecco's Modified Eagle Medium) supplemented with 10 % FCS (heat inactivated for 30 min at 56 °C), 100 U/ml penicillin and 0.1 µg/ml streptomycin.

DU145 was isolated from a human prostate adenocarcinoma metastatic in the brain (Stone *et al.*, 1978). Cells are grown in DMEM (Dulbecco's Modified Eagle Medium) supplemented with 10 % FCS (heat inactivated for 30 min at 56 °C), 100 U/ml penicillin and 0.1 µg/ml streptomycin.

HCT116 is a human colon carcinoma cell line isolated from a primary cell culture (Brattain *et al.*, 1981). Cells are grown in McCoy's 5A medium supplemented with 10 % FCS (heat inactivated for 30 min at 56 °C), 100 U/ml penicillin and 0.1 µg/ml streptomycin.

HCT116 wild type cells and their isogenic knock-out subline HCT116 $p53^{-/-}$ were kindly provided by Dr. Bert Vogelstein, Johns Hopkins Cancer Center, Baltimore, MD, USA. HCT116 $p53^{-/-}$ cells are resistant to neomycin and hygromycin-B (Bunz *et al.*, 1998).

3.1.13 Software

BioDraw Ultra v11.0	CambridgeSoft, Cambridge, MA, USA
BioEdit v7.0.5	Tom Hall, http://www.mbio.ncsu.edu
BLAST	NCBI, Bethesda, MD, USA
Ensembl	http://www.ensembl.org
GraphPad Prism v4.03	GraphPad Software, La Jolla, CA, USA
mfold	Michael Zuker, http://mfold.rna.albany.edu
Microsoft Office 2007	Microsoft, Redmond, WA, USA
Photoshop CS2	Adobe Systems, San Jose, CA, USA
Transfac	http://www.gene-regulation.com

3.2 Methods

3.2.1 Polymerase chain reaction (PCR)

To amplify DNA or to detect DNA after chromatin immunoprecipitation, polymerase chain reaction was performed. The DNA template was amplified in a mastermix containing a final concentration of 75 mM Tris-HCl, 20 mM $(NH_4)_2SO_4$, 0.01 % Tween-20, 1.5 mM $MgCl_2$, 0.25 mM of each dNTP, 0.25 mM of each primer, and H_2O with following program (as an example):

1. initial denaturation	5 min	94 °C	
2. denaturation	1 min	94 °C	steps 2 to 4
3. hybridisation	1 min	53 °C	were repeated
4. elongation	1 min	72 °C	30 times
5. final elongation	7 min	72 °C	
6. storage	∞	4 °C	

Hybridisation temperatures were calculated and set accordingly to every primer pair. Denaturation, hybridisation and elongation time was set as 1 min per 1000 bp.

3.2.2 DNA Electrophoresis

Electrophoretic separation, detection and sizing of DNA was performed by electrophoresis in 1 % agarose gels which were stained with 0.1 µg/ml ethidiumbromide (EtBr). DNA samples were mixed with 6x Loading Dye (GIBCO) or 10x Orange G Loading Dye. The 100 bp or 1 kb Plus DNA Ladder (Invitrogen) were used as a marker. Gels were run at 110 V for about 30 min in 1x TBE buffer.

3.2.3 Gel extraction

Gel extraction was performed according to the manual of the QIAquick Gel Extraction Kit. Briefly, gel slices were cut out, incubated with 3x volume QC buffer at 50 °C for 10 minutes. 1x volume isopropanol was added and solution loaded onto spin column. After a brief centrifugation at 2,000 rpm for 2 minutes, columns were washed with 750 µl PE buffer.

Additional centrifugation and elution in EB buffer resulted in purified PCR or DNA fragments.

3.2.4 Isolation of plasmid DNA

3 ml LB media supplemented with appropriate selection antibiotics were inoculated with a single colony and grown overnight at 37 °C on a shaker. Cells were centrifuged at 3,000 rpm for 10 min. Plasmid DNA was isolated using the QIAGEN Plasmid Mini Kit, which is based on a modified alkaline lysis procedure, followed by binding of plasmid DNA to an anion-exchange resin under appropriate low salt and pH conditions, according to the manufacturer's protocol. The DNA pellet was washed two times with 70 % ethanol and dissolved in 30 µl 1x TE buffer.

3.2.5 Measurement of DNA concentration

To measure the DNA concentration after a plasmid preparation or DNA extraction from an agarose gel, a GeneQuant II photomoter (Pharmacia Biotech) was used. By measuring the extinction at 260 nm (E260) and taking account of the dilution the DNA concentration can be calculated. E260 of 1 equates to a concentration of double stranded (ds) DNA of 50 µg/ml.

3.2.6 Enzymatic restriction of DNA

Type II restriction endonucleases and buffers were used according to protocol (New England Biolabs). For analytical restriction a volume of 15 µl was chosen; for a preparative restriction between 50 and 200 µl. Incubation for 1 h at a temperature of 37 °C or over night at room temperature was performed.

3.2.7 Ligation of DNA fragments

About 100 to 150 ng of vector as well as 2 to 3 times molar amount of insert was used for ligation. The reaction contained T4 ligase. Incubation for 1.5 to 2 h at 25 °C followed by heat inactivation of T4 ligase for 20 min at 60 °C. The ligation mix was transformed into *E. coli* cells by heat shock.

3.2.8 Mini- and Maxi-Prep of plasmid DNA from bacteria

For a mini prep, 3 ml LB media with antibiotic resistance was inoculated with *E. coli* DH5α cells expressing specific plasmid and cultured over night at 37 °C followed by centrifugation for 5 min at 13.000 rpm, the pellet was resuspended in 150 µl resuspension buffer. After adding 150 µl lysis buffer and incubation for 5 minutes at RT, another 150 µl neutralisation buffer was added and incubatied for 8 to 10 minutes on ice. Plasmid DNA was precipitated with 300 µl phenol/chloroform/isoamylalcohole (25/24/1). After 10 min centrifugation at 13,000 rpm, the upper phase was transfered to a new tube. DNA extraction was performed with 1 ml of ethanol (2x-3x parts of volume) and incubation at -70 °C for 15 min. After final centrifugation for 10 min at 13,000 rpm all liquid was removed and the pellet dried at room temperature for about 15 min. The dry pellet was resuspended in 30-50 µl H_2O.

Isolation of plasmid DNA was performed according to 'Invisorb Spin Plasmid Maxi Kit' by Invitek. 150 ml of LB media (with antibiotics) inoculated with E. coli cells carrying the plasmid were incubated over night at 37 °C in a shaker.

resuspension buffer	50 mM Tris/ HCl; pH 8.0 10 mM EDTA 100 µg/ml RNaseA
lysis buffer	200 mM NaOH 1 % (w/v) SDS
neutralisation buffer	3 M sodium acetate; pH 5.5

3.2.9 DNA sequencing

DNA sequencing was performed by utilising the dideoxynucleotide triphosphates (ddNTPs) chain-terminator method (Sanger *et al.*, 1977). DNA fragments with variable lengths which were terminated by four differently fluorescent dideoxynucleotides were separated electrophoretically. Sequencing was conducted by Invitek (Berlin, Germany) or by Thomas Pretzsch (AG Daniel, Virchow-Klinikum).

3.2.10 RNA extraction from cells

Total RNA was isolated according to the NucleoSpin® RNA II kit from Macherey-Nagel (Düren, Germany). Briefly cells were lysed in 350 µl buffer RA1 and 3.5 µl β-mercaptoethanol and lysate was filtrated through a NuceloSpin® Filter (violet ring) at 11,000 *g* for 1 min. 350 µl ethanol was added to the flowthrough and RNA was bound to the NuceloSpin® Column (blue ring) by centrifugation at 11,000 *g* for 1 min. To desalt the silica membrane 350 µl membrane desalting buffer was added and centrifuged at 11,000 *g* for 1 min. Then DNA was digested by 10 µl rDNase in 95 µl reaction buffer at room temperature for 15 min. Afterwards the silica membrane was washed and dried with buffers RA2 and RA3 and RNA was eluted in 40 µl RNase-free H_2O. Concentration was measured and RNA was stored at -80 °C.

3.2.11 cDNA synthesis from total RNA

5-10 g total RNA of each sample was mixed with 3 µl random hexamers (50 ng/µl). DEPC-treated water was added up to the final volume of 12 µl. Each sample was incubated at 70 °C for 10 min for primer hybridisation and chilled on ice for at least 1 min. Samples were briefly centrifuged and 8 µl of the reaction mix, containing 4 µl 5x first strand buffer (Gibco), 2 µl DTT (0.1 M), 1 µl dNTP mix (10 mM), 1 µl RNAse inhibitor (Rnasin 40 U), were added. Contents of the tubes were mixed and incubated at 25 °C for 5 min. 1 µl (200 U) of Superscript II RT was added before incubating the samples at 42 °C for 50 min. cDNA synthesis reaction samples containing random hexamers were first incubated at 25 °C for 10 min, followed by 50 min at 42 °C. The reaction was inactivated by incubating at 70 °C for 15 min. 1 µl (2 U) of RNAse H was added to remove RNA followed by incubating the tubes at 37 °C for 20 min. The cDNA was stored at -20 °C. The cDNA synthesis was verified by amplification of the β-actin gene via PCR with control primers provided by the manufacturer (RETROScript, Ambion).

3.2.12 Quantitative real-time PCR (qRT-PCR)

To detect and quantify (as absolute number of copies or relative amount when normalised to DNA input or additional normalising genes), we performed a qRT-PCR. Total cellular RNA was reverse transcribed into DNA. By using specific primer and FAM-TAMRA labeled probes (see 3.1.8) in a TaqMan® PCR we analysed the expression levels of genes compared to

the housekeeping gene *abl* in cell lines after treatment with drugs or infections with adenoviruses. The qPCR was performed in an Eppendorf realplex^2 Mastercycler epgradient S instrument (Eppendorf, Hamburg, Germany). 5 µl of TaqMan® Gene Expression Master Mix (Applied Biosystems, Darmstadt, Germany), 0.25 µl of forward and reverse primer, 0.3 µl of the probe, and 0.2 µl H_2O was added to 5 µl of the cDNA or 5 µl of the cDNA standard. All samples were measured in triplicates.

1. initial denaturation	7 min	94 °C	
2.	15 sec	94 °C	steps 2 and 3 were
3.	30 sec	61 °C	repeated 45 times

Results were normalised to the housekeeping gene *abl* and analysed by the ΔΔCt method to give fold induction as compared with untreated control samples.

3.2.13 Transfection of bacterial cells (heat shock)

DNA (10 µl for ligation or maximum for recombination) was added to *E. coli* and incubated on ice for 10-15 min before heat shocked at 42 °C for 90 sec. After another incubation on ice for 10 min 300 µl LB media was added and incubated at 37 °C for 20 min. Cells were plated out on LB agar with plasmid specific antibiotics (ampicillin or kanamycin).

3.2.14 Transfection of eucaryotic cells (electroporation)

Cells ($1x10^7$) were harvested and resuspended in 500 µl culture media without additives. 10 µg of plasmid was mixed with the cells and put into perforation vial (0.4 mm). Before and after electroperforation at 0.250 kV and 950 µF for 10 sec, cells were incubated at 37 °C for 10 min. Electroporated cells were seeded into a prewarmed T75 flask with full media and incubated for 2-3 days before media was replaced by selection media (1 µg/ml puromycin or 0.75 mg/ml neomycin [G418]). Bulk cultures were prepared for all cell lines.

3.2.15 Protein assay (Bradford)

A colorimetric protein assay, based on the Bradford method, was used for the measurement of protein concentration. This assay is based on a shift in the absorbance maximum when

Coomassie Brilliant Blue G-250 dye associates with proteins. The Lambert-Beer's Law is applied for quantification of protein by selecting an appropriate ratio of dye volume to sample concentration. At the assay pH, the dye molecules are doubly protonated and are present as the red cationic dye form. Binding of the dye to protein stabilizes the blue anionic dye form, detected at 595 nm. Dye binding requires a protein containing active basic or aromatic residues. 200 µl of Bradford reagent (Bio-Rad) was mixed with 5-7 µl of the sample, incubated for 30 min at room temperature and absorbance was determined at 595 nm. A calibration curve was established each time a protein assay was performed with bovine serum albumin dilutions of known concentrations. Using the standard curve, the concentration of each sample was determined according to its absorbance by interpolation (Bradford, 1976).

3.2.16 SDS polyacrylamide gel electrophoresis

Polyacrylamide gel electrophoresis of SDS-denatured proteins was performed according to the description of Laemmli (Laemmli, 1970). Electrophoresis was performed at 120 to 180 V in 1x TBE buffer.

3.2.17 Immunodetection of proteins - Western blot analysis

For detection of proteins using specific antisera, proteins were blotted first onto the Immobilon-P membrane (PVDF membrane; Millipore). Right after electrophoresis, gels were incubated in transfer buffer (150 mM glycine, 20 mM Tris, 10 % methanol). Electrophoretic transfer was performed in a semi-dry transfer apparatus (Gibco-BRL) with transfer buffer. Prehybridisation, hybridisation with primary and secondary antisera were carried out in 1x PBS containing 1 % v/v Tween 20 and 5 % dry skimmed milk. Specific antisera were used usually in a 1:1,000 dilution. Secondary antisera conjugated to horseradish peroxidase were used in a 1:10,000 dilution. After the hybridisation with the secondary antisera, the PVDF membranes were washed three times with 1x PBS containing 0.1 % v/v Tween 20. For visualisation of protein bands, the secondary antibodies were developed with ECL (enhanced chemiluminescence) reaction. The developing reagent was set up before the reaction freshly from stock solution. After incubation for 1 min in the developing reagent, PVDF membranes were exposed to an X-ray film (Kodak) for an appropriate time and developed in a Curix 60 processor (AGFA).

3.2.18 Analysing BAX/BAK N-terminal conformational change by flow cytometry

Cells were harvested by trypsination and washed once in PBS. About 75 % of cells were discarded and the rest centifugated for 5 min at 1,400 rpm. Cells were resuspended in 150 µl permeabilisation buffer and incubated on ice for 30 min. After centrifugation for 5 min at 1,400 rpm cells were washed in 200 µl wash buffer and after additional centrifugation the pellet was resuspended in 100 µl saponin buffer and 100 µl primary antibody BaxNT (Upstate, Lake Placid, #06-99) to a final concentration of 0.1 µg antibody for $1x10^5$ cells in 100 µl or BakNT (Oncogene, clone TC102) to a final concentration of 0.1 µg/ml for $1x10^5$ cells in 50 µl (1:1,000) and incubated for 30-60 min at 4 °C in the dark. Following centrifugation and washing once in saponin buffer, the pellet was resuspended in 100 µl saponin buffer and 100 µl secondary antibody at a dilution of 1:1,000 (BAX: goat-anti-rabbit IgG [H+L] FITC-labelled F[ab]2, Jackson Immuno Research, West Grove, PA, USA; BAK: mouse-anti-rabbit) and incubated for 30-60 min at 4 °C in the dark. The pellet was resuspended in 100 µl wash buffer after centrifugation and measured by flow cytometry (FL-1) on a BD FACScan™ within 60 min.

permeabilisation buffer	0.5 % Paraformaldehyde in 1x PBS
wash buffer	1 % FCS in 1x PBS
saponin buffer	1 % FCS and 0.1 % saponin in 1x PBS

3.2.19 Detection of genomic DNA fragmentation with propidium iodide (PI)

Apoptosis is characterised by the activation of endogenous endonucleases with subsequent cleavage of chromatin DNA into internucleosomal fragments of 180 bp and multiples therof. Propidium iodide intercalates with DNA and flow cytometry reveals apoptotic nuclei in the subdiploid region of the cell cycle histogram, allowing quantification of apoptosis in a given sample.

Cells were harvested by trypsination and spun for 5 min at 1,400 rpm. Pellets were transfered into 96-well round bottom plates. Supernatant was discarded and cells resuspended in 200 µl of 0.7 % CH_2O and incubated on ice or in fridge for 30 min. After another pelleting at 1,400 rpm for 5 min, pellets were resuspended in 150 µl ice-cold 70 % ethanol and incubated on ice for 20 minutes. Cells were pelleted and resuspended in 100 µl RNAse solution (20 µl RNAse in 50 ml PBS) and incubated at 37 °C for 30 min followed by centrifugation for 5 min

at 1,400 rpm. Pellets were resuspended in 200 µl PI solution (50 µg/ml), transfered to Luckham tubes and measured on a BD FACScan™ (FL-3 or FL-2).

3.2.20 AnnexinV-FITC/PI staining

During apoptosis, phosphatidylserin (PS) is translocated from the inside of the cell membrane to the outside. AnnexinV binds PS and by coupling with fluorescein isothiocyanate (FITC), cells can be measured on a BD FACScan™. In necrotic cells AnnexinV-FITC can bind to PS on the inside of the membrane. Double staining with PI, that can only enter necrotic cells, will reveal necrotic and others, distinctive from apoptotic cells.

3.2.21 Measuring breakdown of the mitochondrial membrane potential ($\Delta\Psi_m$)

JC-1 (Molecular Probes, Leiden, The Netherlands) is a lipophilic, cationic dye that can selectively enter into mitochondria and reversibly change color from green to red as the membrane potential increases. In healthy cells with high mitochondrial $\Delta\Psi_m$, JC-1 spontaneously forms complexes known as J-aggregates with intense red fluorescence. On the other hand, in apoptotic or unhealthy cells with low $\Delta\Psi_m$, JC-1 remains in the monomeric form, which shows only green fluorescence.

Cells were harvested, transfered into Eppendorf tubes (500 µl) and washed 1-2 times in PBS at RT. Tubes were centrifuged for 2 min at 1,300 rpm before supernatant was removed and JC-1 in 1x PBS was added to a final concentration of 2.5 µg/ml. After incubation at 37 °C for 30 min under gentle shaking, cells were centrifuged for 2 min at 1,300 rpm. Supernatant was removed and cells were washed twice in ice-cold PBS. The pellet was resuspended in 100 µl ice-cold PBS and cells were measured on a BD FACScan™ (FL-2 channel).

3.2.22 Cytochrome *c* release

Cells from a T25 flask were harvested by trypsination and washed twice in ice cold 1x PBS before the pellet was resuspended in 30 µl of ready made mito buffer. After incubation on ice for 3 min, cells were pelleted at 13,000 rpm for 15 min. Supernatant was transfered to a fresh tube and used for Western blot analysis.

ready made mito buffer	1 ml of mito-fridge buffer 7.5 µl Digitonin (100 mg/ml in H_2O) 7.5 µl PMSF (10 mM in ethanol)
mito-fridge buffer (stored at 4 °C)	50 mM Hepes; pH 7.4 10 mM KCl 2 mM $MgCl_2$ 1 mM EDTA

3.2.23 Chromatin Immunoprecipitation (ChIP)

To determine the location of transcription factor binding sites, a chromatin immunoprecipitation (ChIP) was performed. Briefly, $1x10^6$ HCT116 cells were infected with Ad-$p14^{ARF}$, Ad-$CHOP_{(Tet)}$, Ad-$ATF4_{(Tet)}$ or treated with tunicamycin or thapsigargin for 48h. Proteins were crosslinked to DNA by adding formaldehyde directly to culture medium to a final concentration of 1% and incubated for 10 minutes at 37 °C. Medium was aspirated and cells were harvested by trypsinisation. After centrifugation for 4 min at 2,000 rpm, the pellet was resuspended in 200 µl SDS Lysis buffer and incubated on ice for 10 min. The lysate was sonicated in a Sonopuls GM70 (Bandelin) ultrasonic generator 8 times for 20 sec á 50 cycles with at least 20 sec breaks on ice between every sonication. DNA was sheared into lengths between 200 and 1000 bp. The sonicated cell supernatant was diluted 10 fold in ChIP Dilution Buffer with protease inhibitors. About 1 % of the diluted lysate was kept to quantitate the amount of DNA for PCR. To reduce nonspecific background, cell supernatant was pre-cleared with 80 µl of Salmon Sperm DNA/Protein A Agarose-50 % slurry for 30 minutes at 4 °C with agitation. Agarose was pelleted by brief centrifugation and 10 µl antibody was added to the supernatant fraction and incubated over night at 4 °C with rotation. As a negative control, no antibody was added. To collect antibody/protein complexes, 60 µl of Salmon Sperm DNA/Protein A Agarose-50 % slurry was added and incubated for 30 min at 4 °C with rotation. After centrifugation at 700 to 1,000 rpm for 1 min at 4 °C, supernatant containing unbound, non-specific DNA was removed and the protein A agarose/antibody/protein complex was washed once with 1 ml Low Salt Immune Complex Wash Buffer, 1 ml High Salt Immune Complex Wash Buffer, 1 ml of LiCl Immune Complex Wash Buffer and washed twice with 1 ml of TE Buffer each for 5 min on a rotating platform followed by brief centrifugation Freshly prepared 250 µl Elution Buffer was added to the pelleted protein A

agarose/antibody/protein complex, vortexed and incubated at room temperature for 15 minutes with rotation. Agarose was spun down, supernatant transfered to a new tube and eluation repeated. 20 µl 5 M NaCl was added to combined eluates (~ 500 µl) and crosslinks reversed by heating at 65 °C for 4 h. Eluat was then used for PCR.

SDS Lysis Buffer	1 % SDS 10 mM EDTA 50 mM Tris-HCl; pH 8.1 before use add 1 tablet of 'complet' protease inhibitors to 100 ml
ChIP Lysis Buffer	0.01 % SDS 1.1 % Triton X-100 1.2 mM EDTA 16.7 mM Tris-HCl; pH 8.1 167 mM NaCL
Low Salt Immune Complex Wash Buffer	0.1 % SDS 1 % Triton X-100 2 mM EDTA 20 mM Tris-HCl; pH 8.1 150 mM NaCl
High Salt Immune Complex Wash Buffer	0.1 % SDS 1 % Triton X-100 2 mM EDTA 20 mM Tris-HCl; pH 8.1 500 mM NaCl
LiCl Immune Complex Wash Buffer	0.25 M LiCl 1 % NP-40 1% deoxycholate 1 mM EDTA 10 mM Tris-HCl; pH 8.1
TE Buffer	10 mM Tris-HCl; pH 8 1 mM EDTA

Elution Buffer	1 % SDS 0.1 M $NaHCO_3$
Salmon Sperm DNA/Protein A Agarose	600 µg sonicated Salmon Sperm DNA 1.5 mg BSA 4.5 mg recombinant Protein A ad 3 ml TE Buffer containing 0.05 % sodium azide

3.2.24 Luciferase Assay

To quantitate the transcriptional activation of promoter regions, different lengths of the BMF promoter were cloned in front of a luciferase gene (Figure 8). HCT116 wt and p53 knock out cells were transiently cotransfected with 25 ng pTK-RL and 400 ng pcDNA3.1+ containing $p14^{ARF}$, CHOP, and ATF4 as well as 100 ng pGL3-BMFprom427/821/1361-Luc constructs or 100 ng of empty pGL3(modMCS) and 500 ng of empty pcDNA3.1+ were used as negative controls.

According to the Promega (Madison, WI, USA) Dual-Luciferase Assay protocol, cells were lysed in 1x passive lysis buffer and transfered to a Greiner 96 flat bottom white polysterol plate. Produced light converted by the chemical energy of luciferin oxidation was measured in a Tecan infinity 200 micro plate reader. Here, 30 µl of luciferase assay substrate solved in luciferase assay buffer was added to each well and after 2 sec luminescence was measured. Afterwards the procedure was repeated with 30 µl of Stop & Glo® Reagent. Luciferase assay results were expressed as relative light units (RLU): the average of the *Photinus pyralis* firefly activity (from pGL3modMCS) observed divided by the average of the activity recorded from *Renilla* luciferase vector (pTK-RL).

3.2.25 siRNA

HCT116 cells were seeded in 6-well plates with $1x10^6$ cells/well. 24 h later siRNA was transfected using DharmaFECT 1 (Dharmacon, Thermo Scientific, Lafayette, CO, USA). After one additional day, cells were treated with tunicamycin and thapsigargin or transduced with 100 MOI Ad-LacZ and Ad-$p14^{ARF}$. Cells were harvested 48 h post treatment.

3.2.26 Statistics

For statistical analysis, GraphPad Prism 4.03 software was used. Expression values were compared using an unpaired *t* test to assess differences between two paired groups. The significance level was chosen as $p \leq 0.05$ (*) and $p \leq 0.01$ (**).

4. Results

4.1 p53 family independent induction of apoptosis by $p14^{ARF}$

To address the role of the p53-family of proteins in $p14^{ARF}$-induced apoptosis a dominant negative p53 protein (ΔNp53) was created, that lacks the first N-terminal 301 amino acids which contain the transactivation and DNA binding domains (Shaulian *et al.*, 1992). This protein binds to the oligomerisation domains of p53, p63, and p73 thereby inhibiting their binding capability to DNA, which, in turn, inhibits their transcriptional activity (Levrero *et al.*, 2000; Willis *et al.*, 2004).

As a model system we used HCT116 (HCT116 WT), a human colon carcinoma cell line, that is proficient for p53. The p53 knockout variant of HCT116 cells (HCT116 $p53^{-/-}$) was kindly provided by Dr. Bert Vogelstein (Bunz *et al.*, 1998). HCT116 WT cells were transfected with empty pIRESneo3 that was used as a vector control (HCT116 VC) and with pIRESneo3 carrying ΔNp53 (HCT116 ΔNp53). These cell lines were subjected to Western blot analysis to verify successful transfection (Figure 9a). Cells were then treated mock (Co) or transduced with adenoviral constructs, either expressing the β-galactosidase gene (LacZ) as a virus negative control or $p14^{ARF}$ (ARF). Virus was added at 50 multiplicities of infection (MOI), i.e. the amount of virions (in this case 50) added per cell. After 24, 48, and 72 h cells were harvested and apoptosis was determined by measuring the extent of fragmentated genomic DNA by flow cytometry.

Cell lines transduced with Ad-$p14^{ARF}$ show similar percentages of hypodiploid cells with no statistical differences, reaching about 25 % apoptotic cells at 72 h compared to 7.5 % and less apoptotic cells in LacZ or mock treated cells (Figure 9b). A similar extent of apoptosis after expression of $p14^{ARF}$ could be detected at all time points (Figure 9c). Mock treated or Ad-LacZ infected cells showed less than 8 % hypodiploid cells at all time points (data not shown). 48 h post treatment, events leading to apoptosis, e.g. conformational change of Bak or Bax, loss of mitochondrial membrane potential ($\Delta\Psi_m$), and release of cytochrome *c* from the mitochondrial intermembrane space into the cytosol were measured. Flow cytometry with anti-Bak N-terminal (NT) or anti-Bax NT antibodies, which specifically recognise the NT-exposed conformation of Bax or Bak revealed no statistical differences in cells transduced with ARF (Figure 9d, e). Around 20 to 25 % of ARF treated cells showed a conformational change. Mock or LacZ treated cell lines showed about 5 to 10 % Bak- and Bax-NT activation.

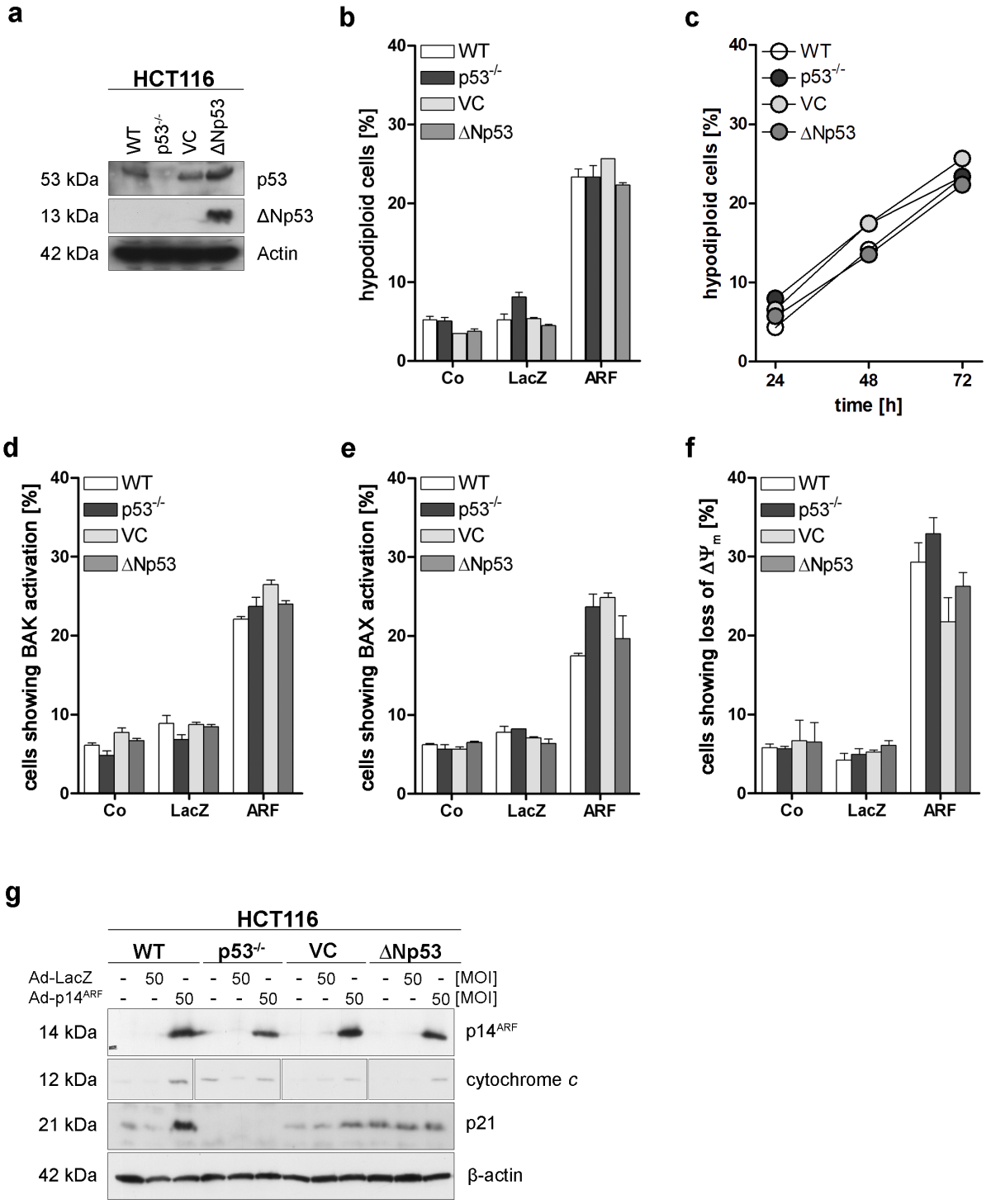

Figure 9. p53-family independent induction of apoptosis by p14^{ARF} in HCT116 cell lines. (**a**) Western blot showing expression status of p53 and ΔNp53 in HCT116 WT, p53$^{-/-}$, VC, and ΔNp53 cell lines. (**b**) Hypodiploid, i.e. apoptotic cells 72 h after mock, LacZ or ARF treatment. (**c**) Apoptotic levels in these cell lines after adenoviral overexpression of p14^{ARF}. Apoptosis was measured by flow-cytometric analysis of genomic DNA fragmentation 24, 48, and 72 h after infection. (**d-f**) HCT116 cell lines showing Bak- and Bax-activation and loss of mitochondrial membrane potential after 48 h. Bars represent mean ± s.d. (n=3). (**g**) HCT116 cell lines were mock treated or transduced with the adenoviral constructs Ad-p14^{ARF} or Ad-LacZ as indicated at a MOI of 50. Cells were harvested 24, 48, and 72 h after infection and were studied by Western blot analysis for the expression of p14^{ARF}, p21 and release of cytochrome *c*. Equal loading was confirmed by reprobing with an antibody against β-actin.

A similar amount of cells also showed $\Delta\Psi_m$ (Figure 9f). The lowest value of $\Delta\Psi_m$ was aproximately 25 % in VC and the highest value of $\Delta\Psi_m$ was about 35 % in $p53^{-/-}$ cells. All other $\Delta\Psi_m$ values varied around 30 %. Breakdown of the mitochondrial membrane potential should lead to release of cytochrome *c*, therefore cell lines were treated and harvested as before and were subjected to Western blot analysis for the expression of $p14^{ARF}$, p21, and β-actin. Cytosolic protein extract was analysed for levels of cytochrome *c* (Figure 9g). Release of cytochrome *c* could be detected in all cell lines treated with $p14^{ARF}$. Upregulation of p21 could only be detected in HCT116 WT and VC cell lines. Loss of p53 or inhibition of p53 by ΔNp53 also inhibited p21 induction, verifying the dominant negative effect of the ΔNp53 protein.

Comparing HCT116 ΔNp53 to the other HCT116 cell lines tested, no significant differences in levels of apoptosis induction, Bak- and Bax-NT activation, $\Delta\Psi_m$, or release of cytochrome *c* could be detected, indicating that $p14^{ARF}$-induced apoptosis is independent of the p53 family.

Similar results were found in the prostate carcinoma cell line DU145 (Figure 10). In this cell line Bax is lost and both allels of *p53* are mutated. Mutants $p53^{223Leu}$ and $p53^{274Phe}$ differ from wild-type p53 in their conformation and transactivation ability (Isaacs *et al.*, 1991). Here, wild-type p53 as well as ΔNp53 (both in pIRESneo3) were stably transfected into DU145

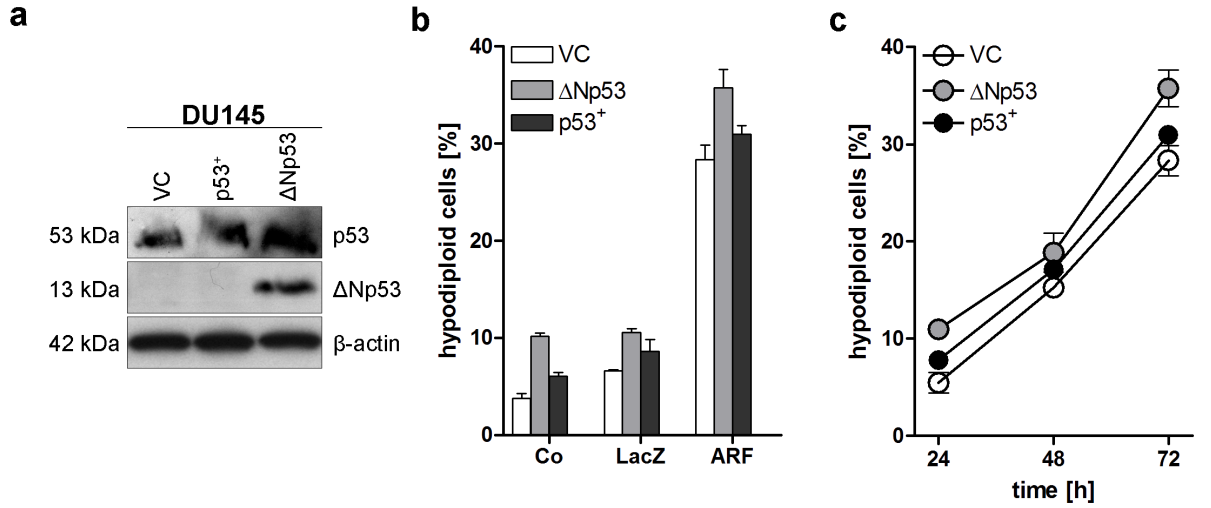

Figure 10. p53-family independent induction of apoptosis by $p14^{ARF}$ in DU145 cell lines. (**a**) Western blot showing expression status of p53 and ΔNp53 in DU145 VC, ΔNp53, and $p53^{+}$ cell lines. Equal loading was confirmed by reprobing with an antibody against β-actin. (**b**) Hypodiploid, i.e. apoptotic cells 72 h after mock, LacZ or ARF treatment. (**c**) Apoptotic levels in these cell lines after adenoviral expression of $p14^{ARF}$. Hypodiploid cell content, i.e. apoptosis, was measured by flow-cytometric analysis of genomic DNA fragmentation 24, 48, and 72 h after $p14^{ARF}$ infection.

cells and termed DU145 $p53^{+}$ and DU145 ΔNp53, respectively (Figure 10a). These cell lines were treated mock or infected with either 50 MOI of Ad-LacZ as control or Ad-$p14^{ARF}$. After 72 h about 30 to 35 % of ARF-infected cells were apoptotic, compared to about 5 to 10 % of mock or LacZ treated cells (Figure 10b). No difference between apoptotic cells upon $p14^{ARF}$ treatment could be measured after 24, 48, and 72 h (Figure 10c).

These results indicate, that $p14^{ARF}$ can induce apoptosis irrespective of a wildtype or a mutated p53 family.

4.2 Involvement of cellular organelles in $p14^{ARF}$ induced apoptosis

We previously showed that $p14^{ARF}$ induced apoptosis is executed via the mitochondrial death pathway. However, several reports show that other organelles might be involved. Therefore we specifically addressed the involvement of the endoplasmic reticulum (ER) in p53-independent apoptosis triggered by $p14^{ARF}$ in DU145 cell lines. In addition to expressing anti-apoptotic Bcl-2 targeted to either the ER or the mitochondrial membranes by a specific carboxy-terminal tail-anchor sequence. As such, Bcl-2 cb5 is a fusion protein retaining the cytoplasmic domain of Bcl-2 and the insertion sequence from the endoplasmic reticulum specific isoform of cytochrome b5. Bcl-2 ActA carries the mitochondria specific insertion sequence from the ActA protein from Listeria (Zhu *et al.*, 1996). Both Bcl-2 proteins and an empty vector (VC) as negative control were expressed in DU145 mock or DU145 Bax cells and were then assayed for their apoptosis sensitivity following expression of $p14^{ARF}$ (Figure 11). Time- (a and b, left) and dose-dependent (a and b, right) analysis of all cell lines after infection with Ad-$p14^{ARF}$ showed similar levels of apoptosis in Bax proficient versus Bax deficient cells dependent on Bcl-2 status. The time-dependent graphs showed about 20 % apoptotic VC cells 48 h post infection with 25 MOI Ad-$p14^{ARF}$. After 96 h about 35-40 % VC cells were apoptotic. Expression of Bcl-2 ActA in mock cells inhibited apoptosis with about 10 % apoptotic cells at all time points. Levels of apoptotic cells in Bcl-2 cb5 expressing cells were about 15 % at all measured time points. In Bax reexpressing cells induction of $p14^{ARF}$ increased apoptosis from about 8 % in Bcl-2 ActA cell lines at 48 h to about 12 % at 96 h. A similar increase from about 14 % to 20 % in Bcl-2 cb5 expressing Bax cells could be detected.

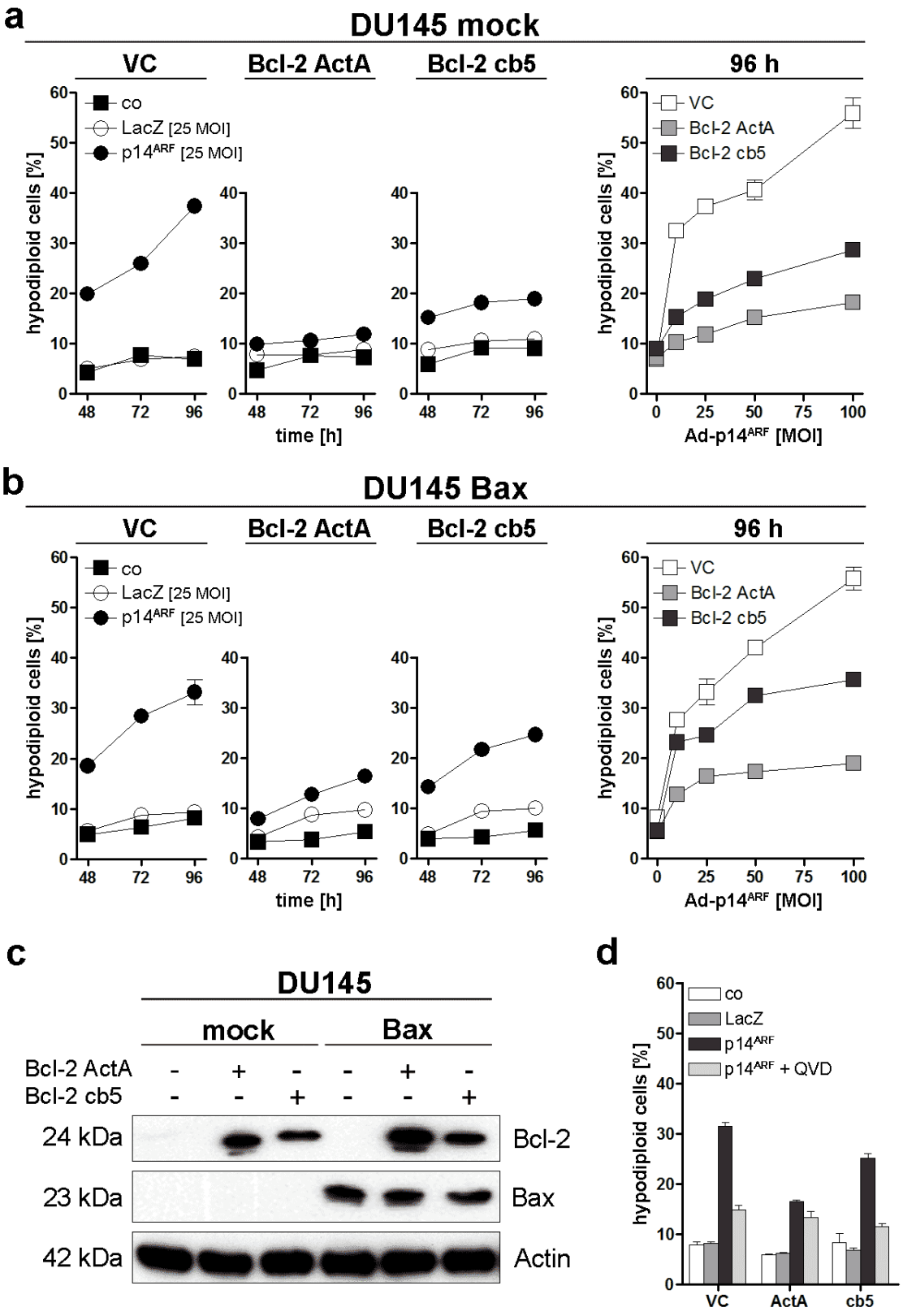

Figure 11. Organelle specific targeting of Bcl-2 to mitochondria and ER inhibits or attenuates p14^{ARF}-induced apoptosis, respectively. (**a, b**) DU145 mock and Bax reexpressing cells expressing Bcl-2 ActA, Bcl-2 cb5 or an empty vector (VC) were treated mock or infected with Ad-LacZ or Ad-p14^{ARF}. Time- (left) and dose-dependent (right) graphs. (**c**) Western blot of analysed cell lines. (**d**) DU145 Bax cells transfected with Ad-p14^{ARF} and incubated with the caspase inhibitor Q-VD-OPh. Hypodiploid cell content, i.e. sub-G1 DNA content was measured by FACS. Bars represent mean ± s.d. (n=3).

The dose-dependent curve showed induction of apoptosis after 96 h in control cells up to 55 % with 100 MOI of Ad-p14^{ARF} independent of Bax status. Mitochondria-targeted Bcl-2 inhibited apoptosis. Here, only 15 % of cells showed a hypodiploid DNA content with 100 MOI p14^{ARF}. Bcl-2 cb5 also inhibited apoptosis to some degree, which is, however inferior compared to Bcl-2 ActA expressing cells. About 25 % (in mock) and about 35 % (in Bax) of the cells showed apoptosis with 100 MOI Ad-p14^{ARF}.

When we infected cells with 50 MOI Ad-p14^{ARF} and at the same time added the caspase inhibitor Quinolyl-Valyl-O-methylaspartyl-(2,6-difluorophenoxy)-methyl ketone (Q-VD-OPh), levels of apoptosis could be reduced significantly in VC and Bcl-2 cb5 expressing cells (Figure 11d). Incubation with QVD in Bcl-2 ActA did not have a significant effect, levels of apoptotic cells were reduced from about 16 % to about 13 %, indicating that induction of apoptosis by Ad-p14^{ARF} in DU145 cell lines can be attenuated by Bcl-2 targeted to the ER, pointing to a mechanism at this cellular organelle relaying signals to induce apoptosis. Furthermore, apoptosis upon expression of p14^{ARF} is independent of pro-apoptotic Bax and, as expected, can be inhibited by caspase inhibitors.

4.3 Induction of BH3-only proteins by p14^{ARF}

As shown before (see 4.2), ER- and mitochondria-localised Bcl-2 can inhibit p14^{ARF}-induced apoptosis. We previously showed that the BH3-only protein Puma plays a central role in mediating p14^{ARF} induced apoptosis. BH3-only proteins are likely targets relaying signals to the ER as well as mitochondria. To this end, we analysed the induction of pro-apoptotic BH3-only genes across the entire family after expression of p14^{ARF} compared to Ad-LacZ infected or untreated cells by quantitative RT-PCR (Figure 13).

Treatment with 50 MOI Ad-p14^{ARF} led to an induction of Bim, Noxa, Puma, and Spike in HCT116 WT cells. 72 h after treatment, Bim is induced 4-fold as compared to control or LacZ treated cells. Noxa is induced about 2.5-fold after 48 h, while only about 1.5-fold at 24 and 72 h. Puma is induced 5-fold after 24 and 48 h. Its induction declines to 2.5-fold at 72 h. Spike induction decreases over time from about 3.5-fold at 24 h over 2-fold at 48 h to 1.5-fold at 72 h. The mRNA expression of all other BH3-only genes are not altered significantly.

A similar result can be observed in HCT116 VC cells. Again, Bim, Noxa, Puma, and Spike are induced. Bim is induced up to 2.5-fold at 72 h. Noxa is induced also 2.5-fold at 48 and

72 h. Puma is induced around 3-fold at 24 and 48 h and 1.5-fold after 72 h. Spike is induced about 3-fold after 48 h. Other BH3-only genes are not induced significantly.
In HCT116 $p53^{-/-}$ cells, Bim is induced 3-fold after 48 h. Bmf is induced 3-fold after 48 and 72 h. Noxa is induced up to 5-fold after 48 h and 3-fold after 72 h. Spike is induced about 4-fold after 48 h. The other BH3-only genes are not affected significantly.
In HCT116 ΔNp53 cells Bim is induced up to 2-fold after 48 and 72 h. Bmf is induced up to 3.5-fold after 48 h and 2-fold after 72 h. Noxa is induced 4-fold after 48 h and 1.5-fold after 72 h. Spike is induced 4-fold after 48 h and 2-fold after 72 h.

Comparing p53 pro- and deficient cell lines, i.e. knockout lines or cells expressing dominant negative p53, we can clearly see upregulation of Puma in p53 proficient cell lines. Interestingly, Bmf is upregulated only in p53 deficient or inhibited cell lines. Bim, Noxa, and Spike are induced independent of p53 family status. To verify qRT-PCR data in the case of Bmf, Westernblot analysis was performed (Figure 12). Indeed, downregulation of Bmf by $p14^{ARF}$ can be detected in p53 proficient HCT116 WT cell lines, while in p53 deficient cell line Bmf is induced.

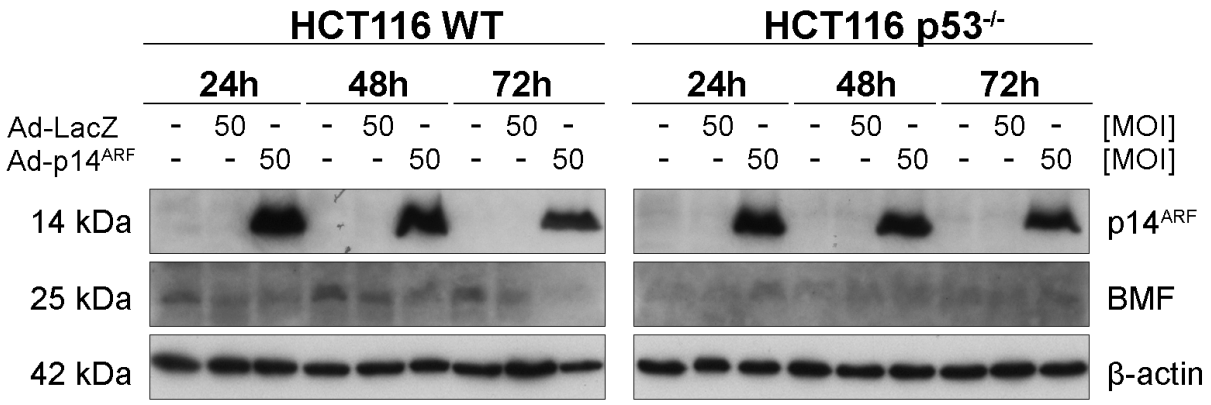

Figure 12. Induction of Bmf in p53 deficient HCT116 cells by Ad-$p14^{ARF}$. Western blot showing expression status of Bmf in HCT116 WT and $p53^{-/-}$ cell lines after 24, 48, and 72 h of forced expression of Ad-$p14^{ARF}$. 50 MOI of Ad-LacZ was used as virus control. Equal loading was confirmed by reprobing with an antibody against β-actin.

In the case of Puma, the $p14^{ARF}$ – p53 signalling axis was analysed extensively (Hemmati *et al.*, 2010). The mechanism behind the induction of Bmf by $p14^{ARF}$ in p53 deficient cell lines on the other hand is not known so far.

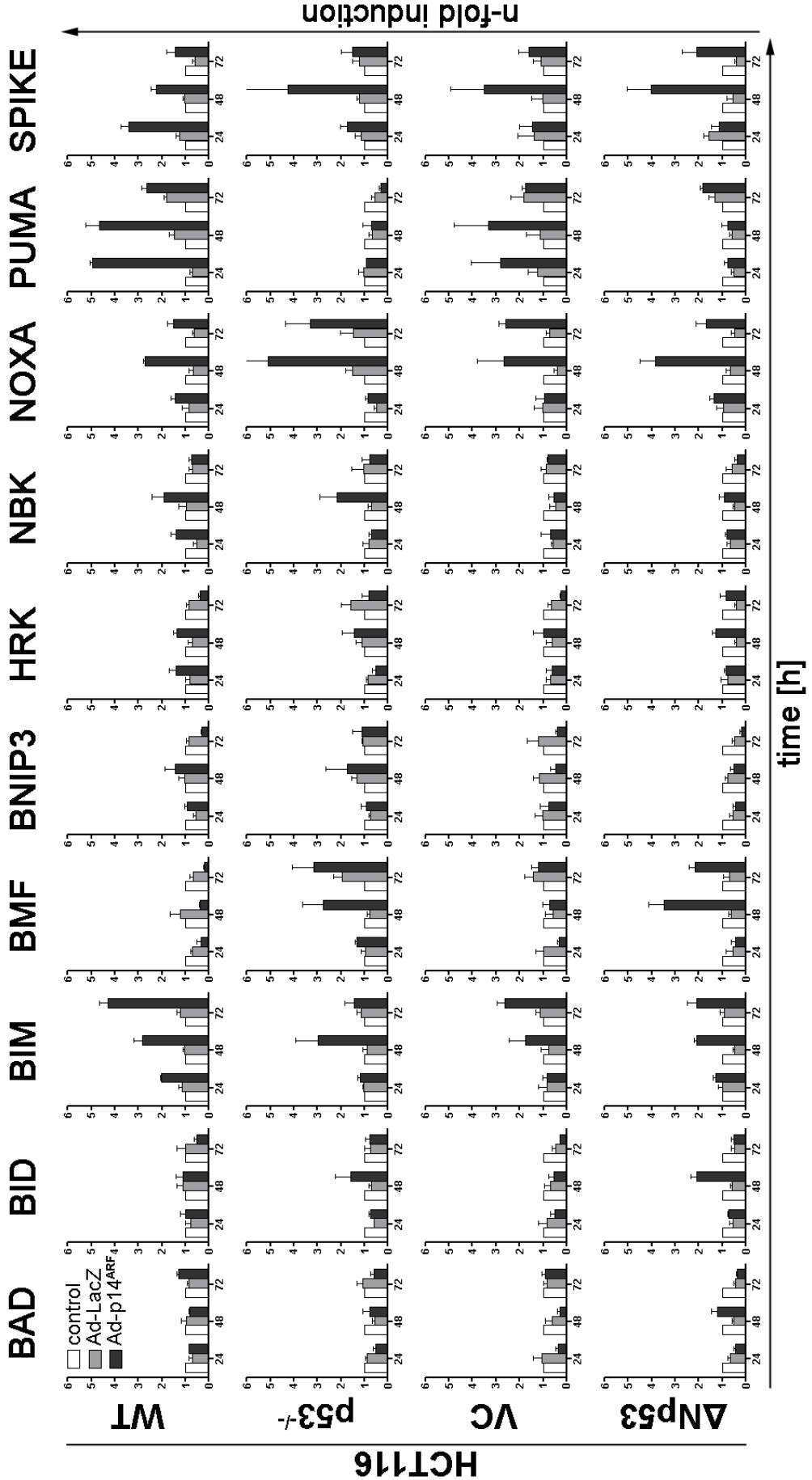

Figure 13. Quantitative RT-PCR of BH3-only family members in HCT116 cell lines after $p14^{ARF}$-induction. HCT116 WT, p53 knockout ($p53^{-/-}$), VC and ΔNp53 cell lines were infected with 50 MOI Ad-LacZ as internal virus control (light grey) and Ad-$p14^{ARF}$ (dark grey). Changes of mRNA levels were measured after one to three days. Data mean ± s.d. of three independent measurements. Bars represent mean ± s.d. (n=3).

4.4 Induction of genes triggering the UPR by ER stress and p14^{ARF}

Bcl-2 at the ER can inhibit reduced intracellular Ca^{2+} oscillations, thereby limiting the redistribution of Ca^{2+} from the ER to the mitochondria (Baffy *et al.*, 1993; Magnelli *et al.*, 1994). Bcl-2 can also interact with ER-bound BH1-3 multidomain proteins Bak and Bax which have been shown to modulate unfolded protein response (UPR) signalling (Hetz *et al.*, 2006). The UPR attempts to increase the folding capacity of the ER through the induction of key proteins involved in chaperoning, protein folding, and degradation pathways (Szegezdi *et al.*, 2003). If the stress exceeds a certain limit or occurs prolonged, an apoptotic program is activated.

ER stress can be chemically induced by different drugs: Tunicamycin (TUN) blocks *N*-glycan biosynthesis by inhibiting the formation of a lipid-linked oligosaccharide precursor, leading to an aggregation of unfolded proteins within the ER (Elbein, 1987). Thapsigargin (THA) raises cytosolic Ca^{2+} levels by inhibiting sarco / endoplasmic reticulum Ca^{2+} ATPases (SERCA), i.e. Ca^{2+} pumps, which maintain calcium ion homeostasis and signalling (Rogers *et al.*, 1995).

To analyse the induction of UPR genes, quantitative real-time PCR was performed for the chaperone BiP/GRP78, the three sensors PERK, ATF6, IRE1 and their downstream targets eIF2α, ATF4, CHOP, and XBP1. Levels of XBP1 can be detected either for unspliced, full length XBP1 (XBP1u) or both spliced and unspliced (XBP1u+s) mRNA. HCT116 cell lines were mock treated or transduced with 50 MOI Ad-LacZ or Ad-p14^{ARF} and prepared for qRT-PCR after 24, 48, and 72 h (Figure 14). These results were compared to HCT116 WT cells treated with 1 and 5 µg/ml TUN or THA that were harvested after 6, 12, 24, 48, and 72 h (Figure 15).

48 and 72 h post transduction with Ad-p14^{ARF} HCT116 WT, p53-/-, VC, and ΔNp53 cell lines displayed a 2-3 fold upregulation of PERK and a slight upregulation of eIF2α. WT, VC, and p53 also show an up to 20 fold upregulation of CHOP after 72 h. The levels of BiP, ATF4, ATF6, IRE1 and both XBP1 mRNAs were not significantly affected when compared to mock treated and LacZ infected cells.

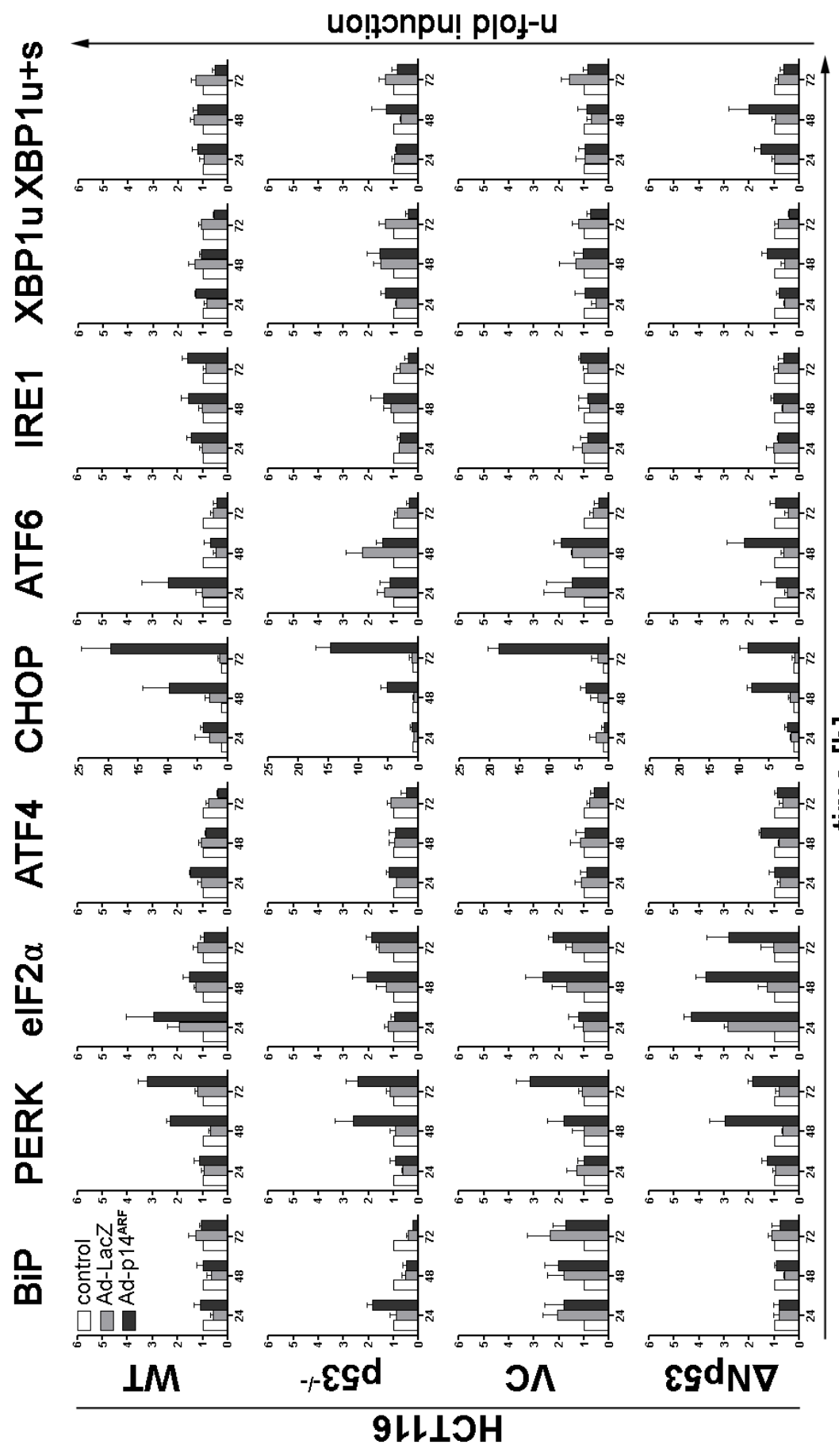

Figure 14. **Quantitative RT-PCR of UPR specific genes in HCT116 cell lines after expression of p14^{ARF} in HCT116 WT cells.** Cells were harvested at indicated time points post infection. Fold-change was calculated as ratio of treated to untreated cells. Value of untreated cells (control; white) were set to 1 at all time points. HCT116 cells transduced with the LacZ control virus (light grey) and with Ad-p14^{ARF} (dark grey). Bars represent mean ± s.d. (n=3).

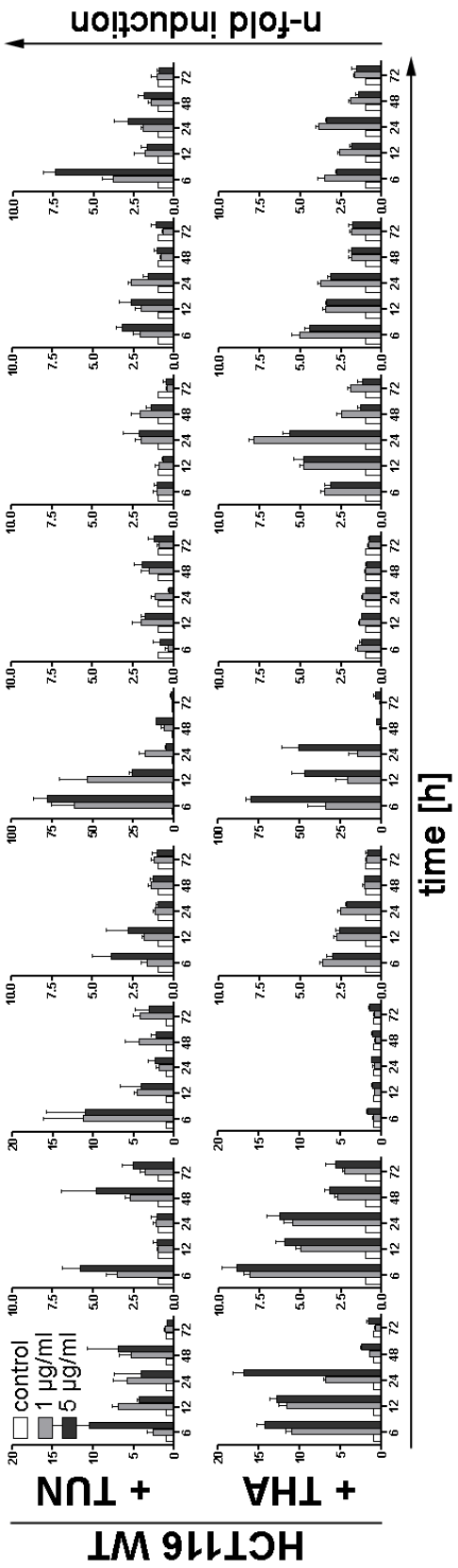

Figure 15. Quantitative RT-PCR of UPR specific genes in HCT116 cell lines after treatment with tunicamycin or thapsigargin. WT cells. Cells were harvested at indicated time points post infection. Fold-change was calculated as ratio of treated to untreated cells. Value of untreated cells (control; white) were set to 1 at all time points. Fold-change in HCT116 WT cells treated with 1 µg/ml (light grey) or 5 µg/ml (dark grey) of either tunicamycin or thapsigargin. Bars represent mean ± s.d. (n=3).

Both tunicamycin and thapsigargin induced a strong immediate response at the first time point at 6 h that lasted up to 48 h. BiP was readily induced 10 to 15-fold after 6 h and fell to basal levels after 48 to 72 h.

Tunicamycin treated cells showed upregulation of PERK at 6, 48, and 72 h with about 5-fold induction. Its downstream target eIF2α showed highest upregulation after 6 h with levels around 10-fold induced in cells treated with either 1 or 5 µg/ml. These levels decrease over time and end at about 2.5-fold induction after 72 h. Levels of ATF4 are slightly increased at 6 and 12 h and fall back to basal levels at 24 h and thereafter. CHOP mRNA is induced 75-fold after 6 h and decrease over time up to about 12-fold induction at 48 h before reaching basal levels at 72 h. There is also a slight induction of ATF6 and IRE1 detectable, with induction levels not over 2.5-fold. XBP1u is induced 2.5-fold between 6 and 24 h while XBP1u+s reaches 7.5-fold induction at 6 h and decreases to levels around 2-fold from 12 to 48 h before reaching basal levels at 72 h.

Similar to tunicamycin thapsigargin induces PERK upregulation to a much higher extend. Here, at 6 h levels of 7.5-fold induction are reached that gradually decrease over time to 2.5-fold induction after 72 h. Different to tunicamycin, there is no upregulation of eIF2α. Instead, thapsigargin induces IRE1 levels starting 3-fold at 6 h up to 7.5-fold at 24 h in cells treated with 1 µg/ml of the drug.

Although we could not detect any stress response, i.e. induction of BiP/GRP78 upon $p14^{ARF}$ treatment, UPR downstream targets PERK and CHOP showed a strong induction independent of p53 over time. Although upregulation of CHOP could also be achieved by ATF6, we could not detect any upregulation of XBP1, another target of this transcription factor, after overexpression of $p14^{ARF}$. Upregulation of XBP1 and its splice form is only visible in ER stressed cells after treatment with tunicamycin and thapsigargin. In comparison ER stress induced by tunicamycin and thapsigargin leads to an immediate upregulation of BiP/GRP78 and early upregulation of PERK and its downstream targets eIF2α, ATF4, and CHOP. Also, dependent on the drug, ATF6 or IRE are upregulated and the amount of the XBP1 splice form increases.

Different to the induction of ER stress and induction of UPR genes by tunicamycin and thapsigargin, $p14^{ARF}$ does not induce ER stress but activates only the PERK-CHOP pathway, which will be analysed in more detail in the following.

4.5 Inhibition of apoptosis by dominant negative mPERKΔC

The kinase activity of PERK can be abrogated by expression of a dominant negative isoform. This isoform was shown to inhibit phosphorylation of eIF2α following various stresses, including hypoxia (Brewer and Diehl, 2000; Koumenis *et al.*, 2002). A plasmid containing truncated murine PERK (mPERKΔC) that lacks the protein kinase domain and has a myc-tag epitope was kindly provided by Dr. David Ron.

Murine PERK has an identity of 87.2 % to its human homolog on the protein level. Introduction of mPERKΔC in HCT116 WT cells and expressing 50 MOI of $p14^{ARF}$ led to a significant decrease of hypodiploid cells compared to HCT116 WT and VC cell lines. HCT116 WT and VC cell lines display 5-8 % of hypodiploid cells after mock or LacZ treatment and about 30 % hypodiploid cells after $p14^{ARF}$ expression. HCT116 mPERKΔC cell lines also show about 5-8 % of hypodiploid cells after mock or LacZ treatment. $p14^{ARF}$ treated cells show about 20 % of hypodiploid cells (Figure 16b).

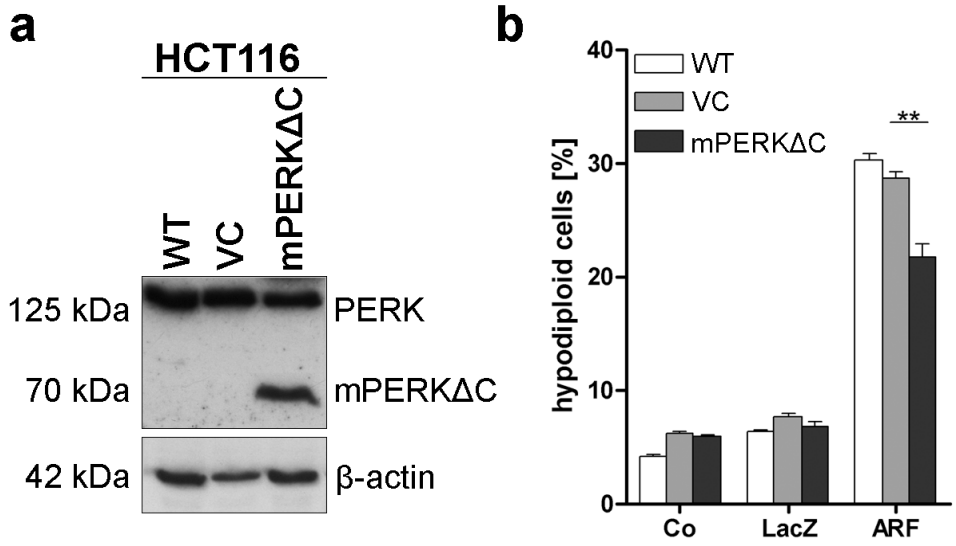

Figure 16. Dominant negative murine PERK inhibits $p14^{ARF}$-induced apoptosis. (**a**) Western blot showing expression status of PERK and mPERKΔC in HCT116 WT, VC, and mPERKΔC cell lines. (**b**) Hypodiploid, i.e. apoptotic cells 72 h after mock, LacZ or ARF treatment. Bars represent mean ± s.d. (n=3).

Inhibition of PERK by mPERKΔC significantly attenuates apoptosis induction by Ad-$p14^{ARF}$ in p53 wild-type cell lines. In these cell lines, Puma activation via p53 is likely responsible for induction of apoptosis. In p53 deficient HCT116 cell lines Puma cannot be upregulated and the effect of inhibiting PERK on the amount of hypodiploid cells should be stronger.

4.6 Inhibition of apoptosis by PERK and ATF4 siRNA

To validate the mPERKΔC results, HCT116 WT and p53$^{-/-}$ cell lines were treated with control, PERK, and ATF4 siRNA and transduced with 100 MOI of either Ad-LacZ as virus control or Ad-p14^{ARF}. 48 h post infection, cells were analysed by flow cytometry and the amount of hypodiploid, i.e. apoptotic cells was measured (Figure 17).

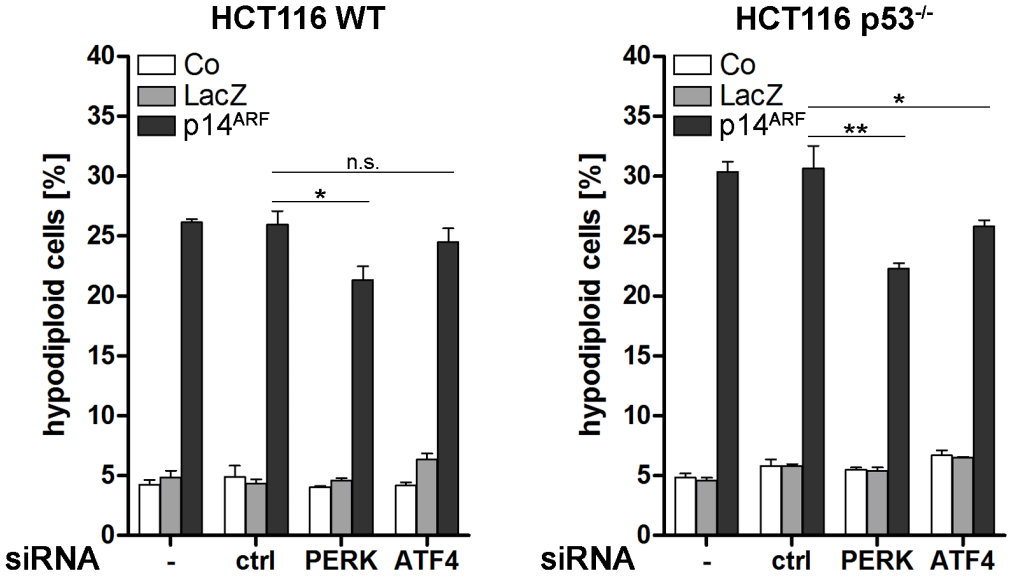

Figure 17. Inhibition of apoptosis by PERK and ATF4 siRNA. HCT116 WT and p53 deficient cells were incubated with no, unspecific control (ctrl), PERK and ATF4 siRNA before infection with 100 MOI Ad-LacZ and Ad-p14^{ARF}. Hypodiploid, i.e. apoptotic cells were measured 48 h post infection by flow-cytometric analysis of genomic DNA fragmentation. Bars represent mean ± s.d. (n=3).

Untreated and ctrl siRNA treated HCT116 WT cells display about 27 % of hypodiploid cells after expression of p14^{ARF}. Downregulation of PERK by siRNA leads to a significant reduction of apoptosis, as only 22% of p14^{ARF} infected cells are apoptotic. Downregulation of ATF4 shows no significant difference to ctrl siRNA treated cells. A similar result can be seen in HCT116 p53 deficient cell lines. Here, forced expression of p14ARF leads to about 30 % hypodiploid cells without and ctrl siRNA. After treatment with PERK siRNA, about 22 % of the cells are apoptotic, which is a very significant decrease when compared to ctrl treated cells. Also, downregulation of ATF4 by siRNA leads to a significant decrease of apoptotic cells. About 25 % of the cells are hypodiploid.

These data indicate that downregulation of PERK leads to a stronger effect in p53 deficient cell lines, where induction of apoptosis is not dependent of Puma. In HCT116 p53$^{-/-}$ cells, signal transduction via the PERK-eIF2α-ATF4 pathway seems to be more undisturbed as in

WT cells, where downregulation of ATF4 does not show a significant impact on inhibition of apoptosis.

4.7 Specific phosphorylation of eIF2α by $p14^{ARF}$

The eukaryotic initiation factor 2α is required in the initiation of translation and is phosphorylated by PERK. Another cellular kinase called PKR (serine-threonine kinase protein kinase R) or DAI (double-stranded RNA-activated inhibitor of translation) is present in a latent form in most cells. It is activated by low concentrations of double-stranded RNA, generated during viral infections by symmetrical transcription of the virus genome (Maran and Mathews, 1988). Upon binding of dsRNA it is activated and phosphorylates eIF2α at Ser51 to inhibit viral protein synthesis. Due to approximations in calculating the virus titer of Ad-LacZ and Ad-$p14^{ARF}$ significant deviations in MOI could occur between both viruses which could mask DAI activation. To rule out artificial adenoviral phosphorylation of eIF2α and to equalise the MOIs we used a regulatory adenovirus Ad-$p14^{ARF}{}_{(Tet)}$. It contains repetitive tet operator sequences (tetO) followed by a human minimal CMV promoter and the gene for $p14^{ARF}$. In the absence of tetracycline (Tet) or a derivative (doxycycline), the transactivator protein binds to the tetO sequences and activates ARF protein expression. Binding of Tet to the tTA protein inhibits $p14^{ARF}$ protein expression by reducing tTA affinity for the tetO sequences (Loew *et al.*, 2010).

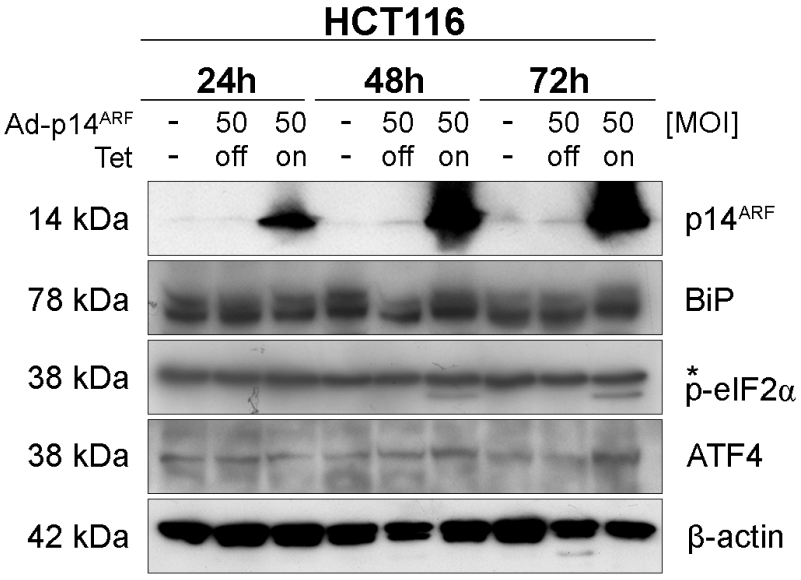

Figure 18. Specific phosphorylation of eIF2α and subsequent induction of ATF4 by Ad-$p14^{ARF}{}_{(Tet)}$ in HCT116 cell lines. Western blot showing the expression status of proteins after transduction with Ad-$p14^{ARF}{}_{(Tet)}$ under 'off' (with doxycyline) and 'on' (without doxycycline) conditions after 24, 48, and 72 h. Equal loading was confirmed by reprobing with an antibody against β-actin. * unspecific band.

HCT116 WT and $p53^{-/-}$ cell lines were mock treated or were transduced with Ad-$p14^{ARF}_{(Tet)}$ in the presence or absence of doxycyclin in the culture media. Cells were harvested 24, 48, and 72 h post infection and were tested for expression of 14^{ARF}, BiP, phosphorylation of eIF2α, and ATF4 by Western blot analysis (Figure 18).

The Western blot shows stable induction of $p14^{ARF}_{(Tet)}$ only under 'on' condition at all time points. Levels of BiP/GRP78 do not change when compared to untreated cells or cells under 'off' condition. After 48 and 72 h phosphorylation of eIF2α can be detected. Inhibition of cap-dependent translation by phosphorylated eIF2α also leads to an induction of downstream transcription factor ATF4. An increase in ATF4 levels can be detected after 48 and 72 h of $p14^{ARF}$ induction. Activation of ATF4 should also lead to an induction of CHOP.

4.8 Induction of apoptosis by ER stressors, Ad-$ATF4_{(Tet)}$ and Ad-$CHOP_{(Tet)}$

To further dissect the PERK – CHOP pathway, we created additional inducible adenoviruses Ad-$ATF4_{(Tet)}$ and Ad-$CHOP_{(Tet)}$. Both proteins are upregulated after ER stress when eIF2α is phosphorylated and global cap-dependent translation is inhibited (Ma *et al.*, 2002; Harding *et al.*, 2003).

ATF4 and CHOP were tested for their ability to induce apoptosis in HCT116 WT and $p53^{-/-}$ cell lines. Results were compared to cells treated with tunicamycin and thapsigargin (Figure 19).

Expression of 25 MOI Ad-$ATF4_{(Tet)}$ and Ad-$CHOP_{(Tet)}$ leads to induction of apoptosis after 72 h. About 15 % of the cells show a hypodiploid cell content, compared to 2-3 % of untreated cells. Cells transduced with an adenovirus under 'off' conditions (with doxycyclin in the culture media) show slightly increased levels of apoptotic cells compared to control cells. Low MOI of Ad-$ATF4_{(Tet)}$ and Ad-$CHOP_{(Tet)}$ have a similar effect after 72 h as 1 µg/ml tunicamycin after 48 h. As seen in the Western blot, withdrawal of doxycyclin does allow for a strong induction of ATF4 or CHOP. However, at 48 h CHOP can be detected even under 'off' condition, suggesting some leakiness of the tet-system.

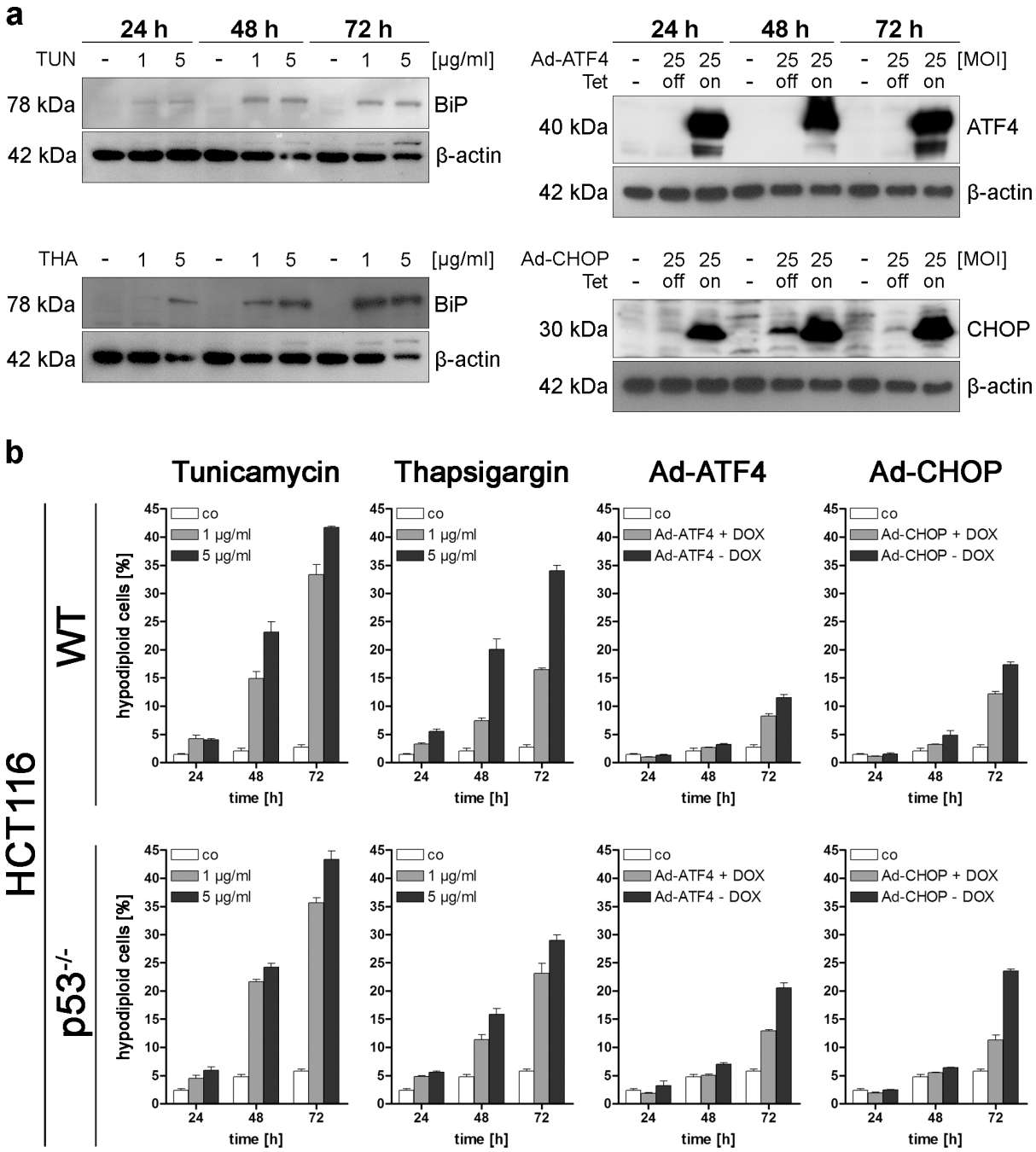

Figure 19. Induction of apoptosis by ER stress inducing agents tunicamycin and thapsigargin compared to Ad-ATF4$_{(Tet)}$ and Ad-CHOP$_{(Tet)}$ in HCT116 cell lines. (**a**) HCT116 WT and p53$^{-/-}$ cell lines were treated with 1 and 5 µg/ml tunicamycin and thapsigargin or were incubated with 25 MOI of Ad-ATF4$_{(Tet)}$ and Ad-CHOP$_{(Tet)}$ with ('off') or without ('on' condition) doxycyclin. Western blots showing induction of BiP after treatment with tunicamycin and thapsigargin or induction of either ATF4 or CHOP after adenoviral infection. Equal loading was confirmed by reprobing with an antibody against β-actin (**b**) Measurement of hypodiploid cells after 24, 48, and 72 h by FACS. Bars represent mean ± s.d. of three measurements.

4.9 Induction of BH3-only proteins by ER stressors, Ad-ATF4$_{(Tet)}$ and Ad-CHOP$_{(Tet)}$

BH3-only proteins play a major role in induction of apoptosis via the mitochondrial pathway. It was already known that ER stress triggers apoptosis by activating BH3-only proteins Puma (Reimertz *et al.*, 2003), Noxa (Li *et al.*, 2006), and Bim (Puthalakath *et al.*, 2007). We were especially interested in upregulation of BH3-only family members that are involved in the PERK pathway. Therefore, we treated HCT116 WT cells with 1 and 5 µg/ml thapsigargin or tunicamycin, and compared data with cells transduced with 25 MOI Ad-ATF4$_{(Tet)}$ and Ad-CHOP$_{(Tet)}$. Quantitative RT-PCR for BH3-only genes was performed after 24, 48, and 72 h post treatment (Figure 20).

Treatment of HCT116 WT with tunicamycin leads to a dose dependent upregulation of Bmf mRNA increasing over time with about 2-fold induction after 24 h up to 4-fold at 72 h. Noxa is upregulated 3-fold after 72 h, while Puma is induced about 3.5-fold at all time points. Levels of Spike decrease from about 2.5-fold induction at 24 and 48 h to 0.5-fold at 72 h. There is no significant upregulation of the other BH3-only genes. Thapsigargin also induces the same genes but leads to stronger inductions overall. Bmf is induced up to 2-fold at 48 h and reaches up to 4-fold induction at 72 h. Levels of Noxa and Puma start at about 5.5-fold after 24 h and decrease to about 2.5-fold induction after 72 h. Spike is induced 3-fold at 48 h. Interestingly, 1 µg/ml thapsigargin induces Bim more strongly than 5 µg/ml. Here, levels from 2-fold at 24 h up to 3-fold at 72 h are reached. Bid and Nbk levels are downregulated after 48 h and decline to around 0.5-fold until 72 h. Adenoviral expression of ATF4 induced Bmf mRNA up to 4-fold after 72 h. Levels of Bad, Nbk and Noxa are downregulated. Other mRNA levels are not induced significantly. Expression of CHOP only induced Bmf mRNA. Levels of Bmf increase to 3-fold at 48 h and up to 4-fold after 72 h. All other tested mRNAs were downregulated by Ad-CHOP$_{(Tet)}$.

A strong upregulation of Bmf can be detected in HCT116 WT cells after treatment with tunicamycin, thapsigargin, and after adenoviral expression of ATF4 or CHOP. When compared to the induction of Bmf by p14^{ARF} (see 4.3), induction could only be detected in p53 deficient cell lines. To corroborate the role of p53 in this context, we repeated the experiment in HCT116 p53$^{-/-}$ cell lines (Figure 21).

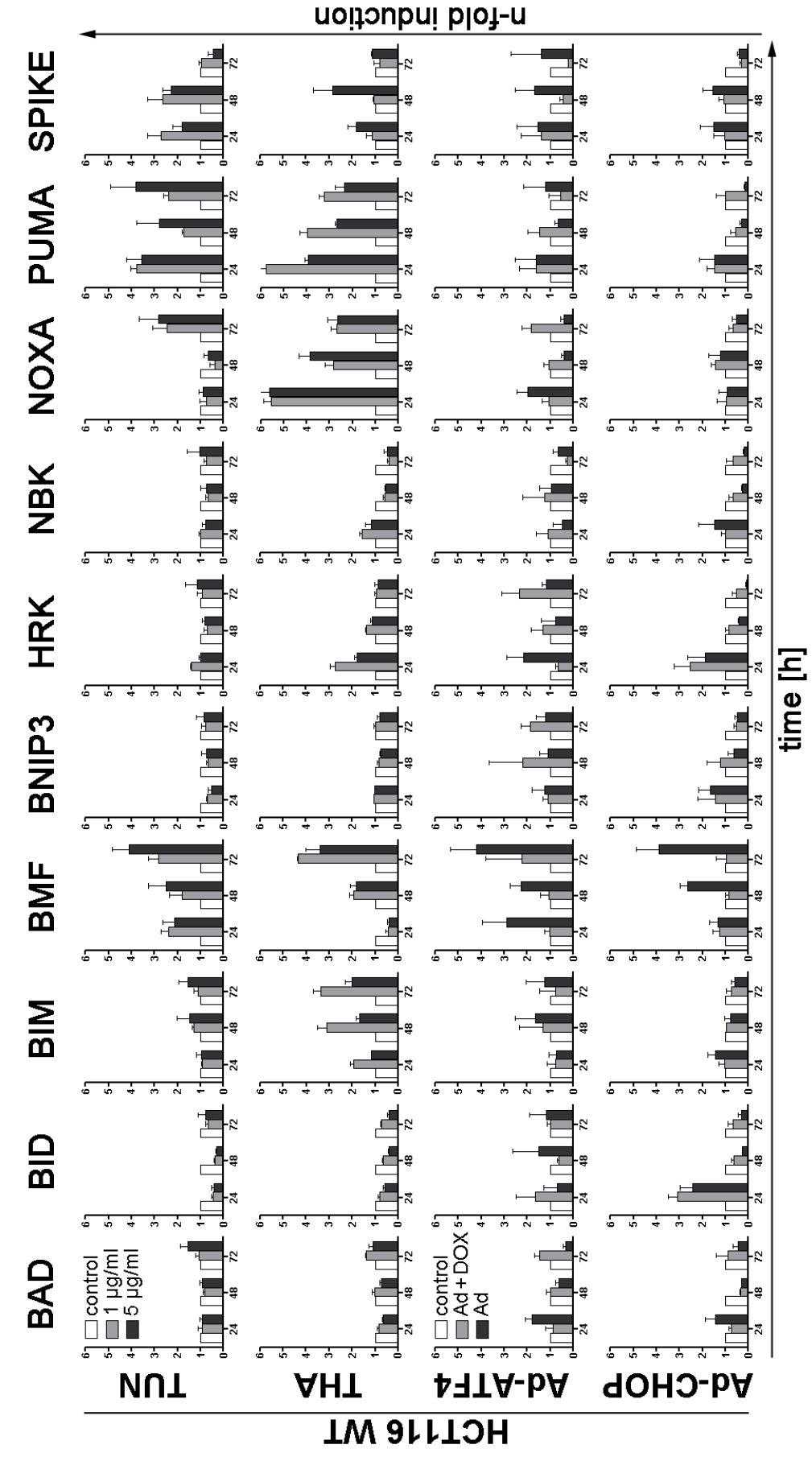

Figure 20. Quantitative real-time PCR data of BH3-only mRNA induction after incubation with tunicamycin (TUN), thapsigargin (THA) or adenoviral expression of ATF4 and CHOP. HCT116 WT cells were incubated with TUN and THA at concentrations of 1 and 5 µg/ml as well as infected with adenoviruses expressing ATF4 and CHOP. Real-time data of BH3-only mRNA was measured 24, 48 and 72 h post treatment or infection. Untreated cells as control set to 1 (white), cells treated with TUN and THA at a concentration of 1 µg/ml (light grey) and cells treated with TUN and THA at a concentration of 5 µg/ml (dark grey). Cells infected with Ad-$ATF4_{(Tet)}$ and Ad-$CHOP_{(Tet)}$ under 'off-condition' (light grey) and 'on-condition' (dark grey). Bars represent mean ± s.d. (n=3).

Similar to HCT116 WT cells, treatment with 5 µg/ml tunicamycin in HCT116 p53$^{-/-}$ cells induced Bmf gradually over time from about 3-fold at 24 h to about 7-fold at 72 h. Induction of Noxa ranges between 3 to 6-fold induction at all time points, similar to Puma with 4 to 6-fold induction. Treatment with thapsigargin led to 4 to 5-fold induction of Bim after 48 and 72 h. Induction of Bmf increased from 1.5-fold at 24 h for both concentrations to about 6 to 7-fold at 72 h. Noxa showed a similar induction as Bmf and levels of Puma increased from about 5-fold at 24 h to about 15-fold at 72 h independent of the thapsigargin concentration. Adenoviral expression of ATF4 led to a strong induction of Bmf to about 15-fold at 72 h and a slight increase in Noxa and Puma levels at 48 and 72 h. Expression of CHOP only induced

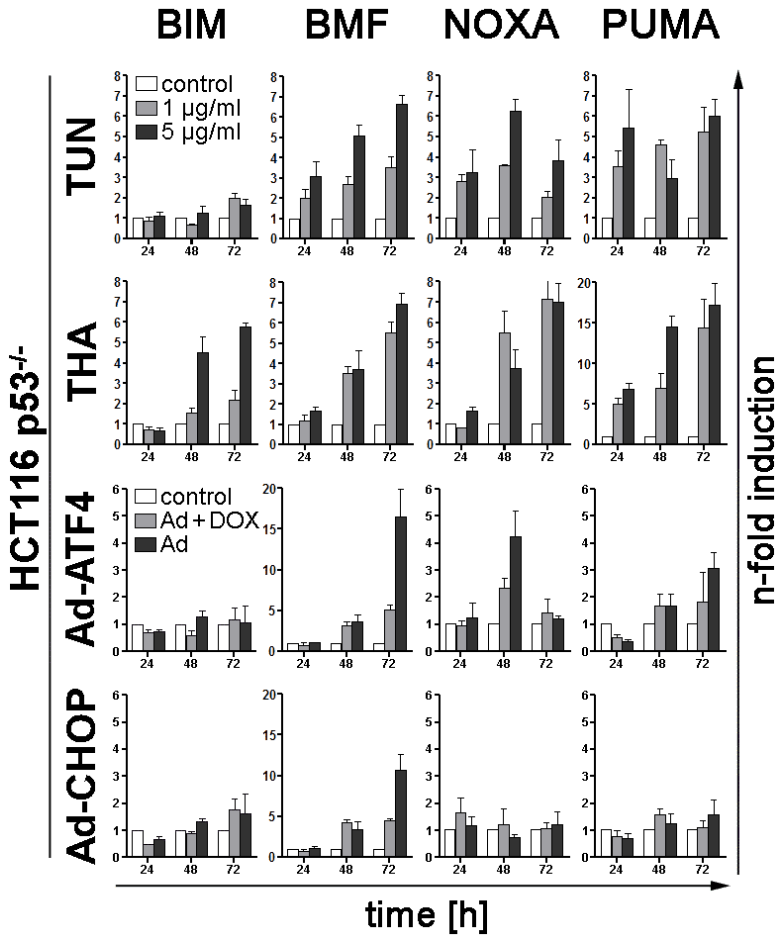

Figure 21. Quantitative RT-PCR of HCT116 p53$^{-/-}$ cells after treatment with tunicamycin and thapsigargin or infection with Ad-ATF4$_{(Tet)}$ and Ad-CHOP$_{(Tet)}$. HCT116 p53-/- cells were incubated with TUN and THA at concentrations of 1 and 5 µg/ml as well as infected with adenoviruses expressing ATF4 and CHOP. Real-time data of BH3-only mRNA was measured 24, 48 and 72 h post treatment or infection. Untreated cells as control set to 1 (white), cells treated with TUN and THA at a concentration of 1 µg/ml (light grey) and cells treated with TUN and THA at a concentration of 5 µg/ml (dark grey). Cells infected with Ad-ATF4$_{(Tet)}$ and Ad-CHOP$_{(Tet)}$ under 'off-condition' (light grey) and 'on-condition' (dark grey). Bars represent mean ± s.d. (n=3).

Bmf levels from about 5-fold at 48 h to about 10-fold at 72 h. Levels of other BH3-only mRNAs were unaffected at all time points investigated.

These data indicate that similar to Bim, Noxa, and Puma, Bmf can be implicated in mediating apoptosis triggered by the ER. In particular, this response is most prominent in cells void of p53.

4.10 Inhibition of apoptosis by Bmf siRNA in p53 pro- and deficient HCT116 cells

To analyse the function of Bmf after ER stress we downregulated Bmf by siRNA. Cells were seeded and incubated with control and Bmf siRNA for 24 h before treatment with tunicamycin and thapsigargin (Figure 22).

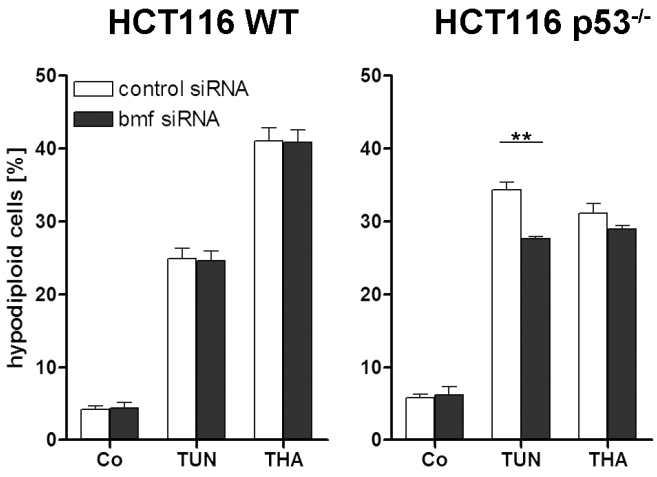

Figure 22. Downregulation of Bmf by siRNA. HCT116 WT and p53$^{-/-}$ cells were incubated with control and Bmf siRNA. 24 h later cells were treated with 5 µg/ml tunicamycin and thapsigargin. Bars represent mean ± s.d. (n=3).

Tunicamycin and thapsigargin treated HCT116 WT cells show about 25 and 40 % hypodiploid cells, respectively. Addition of Bmf siRNA had no impact. In p53 deficient HCT116 cells, treatment with tunicamycin leads to about 35 % of apoptotic cells, while treatment with thapsigargin induces apoptosis in about 30 % of the cells. When Bmf is downregulated in tunicamycin treated cells, the amount of hyplodiploid cells is significantly reduced to about 27 % (p=0.0036). In thapsigargin treated cells, the amount of apoptotic cells is reduced slightly to about 28 %.

4.11 Bmf translation after phosphorylation of eIF2α

Activation of the PERK–CHOP pathway eventually leads to the induction of Bmf. When global cap-dependent initiation of translation is inhibited by phosphorylation of eIF2α by PERK, translation of Bmf should also be inhibited. To analyse if Bmf circumvents translational inhibition, we analysed the promoter regions of different species for conserved homologies and structures. A comparison of the 5' UTR of *bmf* from human (accession NM_001003940), dog (*Canis familiaris*; XM_843970) and rat (*Rattus norvegicus*; NM_139258) showed 88.2 % and 82 % identity between human and dog, and human and rat, respectively. Secondary structures of the RNA predicted by the mFOLD program (Zuker, 2003) showed nearly identical structures between human and dog 5' UTR even in regions of lower sequence identity (Figure 23), leading us to the assumption, that this structural conservation might be part of a mechanism by which translational inhibition can be circumvented.

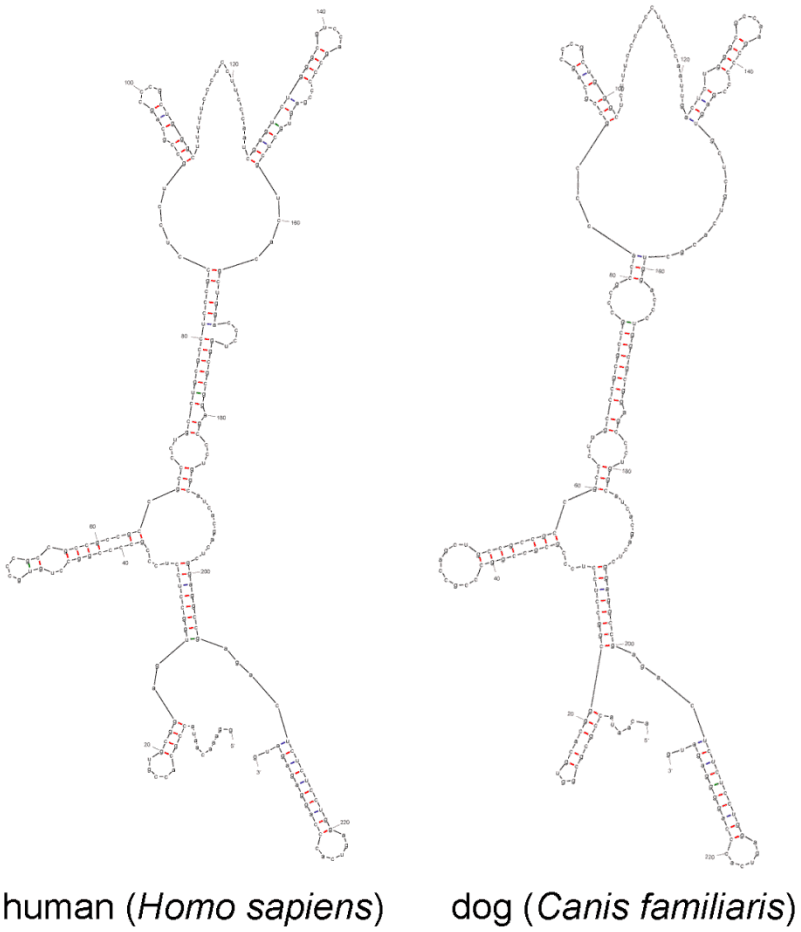

Figure 23. Secondary structure of *bmf* 5' UTR of human and dog. Secondary structures of the 5' UTR of *bmf* were calculated with the mFOLD program.

4.12 *bmf* promoter binding studies and transcriptional activity

The differential regulation of Bmf in p53 pro- versus deficient cells suggests that p53 acts as repressor for *bmf*. To further analyse this hypothesis, we carried out an additional *in silico* analysis of the *bmf* promoter region. The sequence of *bmf* (ENSG00000104081) was taken from the ensemble.org website (see Appendix for full sequence). No p53 response elements (5'-RRRCWWGYYY-3'; el-Deiry *et al.*, 1992) were found in the promoter region. Instead we identified putative binding sites for transcription factors ATF4 (5'-TGACGTMR-3'; Lin and Green, 1988) and CHOP (5'- RRRTGCAATMCCC -3'; Ubeda *et al.*, 1996) within the first 1500 bp of the 5' upstream *bmf* promoter region (Figure 24).

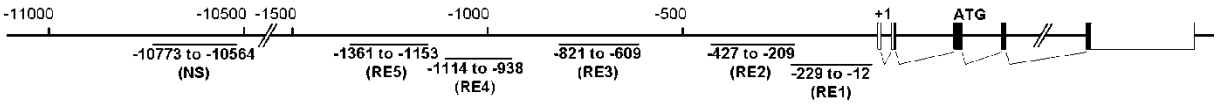

Figure 24. *bmf* promotor region (not to scale). Putative binding sites with corresponding ChIP PCR fragments (RE1 to RE5 and nonspecific; NS). BMF mRNA and exons (ENSG00000104081) in bigger boxes, coding region in black. All numbers relative to transcription initiation site (TIS; +1).

To verify binding of ATF4 and CHOP to the identified sites, a chromatin immunoprecipitation (ChIP) assay was performed (Figure 25). HCT116 WT and p53 knockout cells were treated mock or infected with Ad-p14^{ARF}. Additionally, HCT116 WT cells were treated with tunicamycin and thapsigargin or infected with Ad-ATF4$_{(Tet)}$ and Ad-CHOP$_{(Tet)}$. Immunoprecipitation with antibodies against ATF4 and CHOP and subsequent PCR for promoter sequences -229 to -12 (region 1; RE1), -427 to -209 (RE2), -821 to -609 (RE3), -1114 to -938 (RE4), -1361 to -1153 (RE5), as well as an nonspecific region -10773 to -10564 (NS) was performed. Untreated cells were used as controls.

Mock treated HCT116 WT cells show binding of ATF4 to regions RE1, RE2, RE4, and RE5. After induction of p14^{ARF} binding could be detected in regions RE2, RE4, and RE5 although signals were weaker compared to mock treated cells. In tunicamycin treated cells, regions RE2, RE4, and RE5, while in thapsigargin treated cells, regions RE2 and RE4 could be detected. Regions RE1, RE2, and RE4 could be amplified after expression of ATF4 and CHOP, with stronger signals in ATF4 infected cells.

In mock treated HCT116 WT cells after precipitation with CHOP antibody, signals could be detected in RE1 and RE4. After induction with p14^{ARF}, regions RE1, RE2, RE4, and RE5

could be amplified. In cells treated with tunicamycin, binding of CHOP could be detected in RE2, RE4, and RE5. RE1, RE2, and RE4 in thapsigargin treated cells. Induction of ATF4 led to signals in RE2 and RE4; induction of CHOP to signals in RE2, RE4, and RE5.

In p53 deficient untreated HCT116 cells, regions RE2 and RE4 can be amplified after

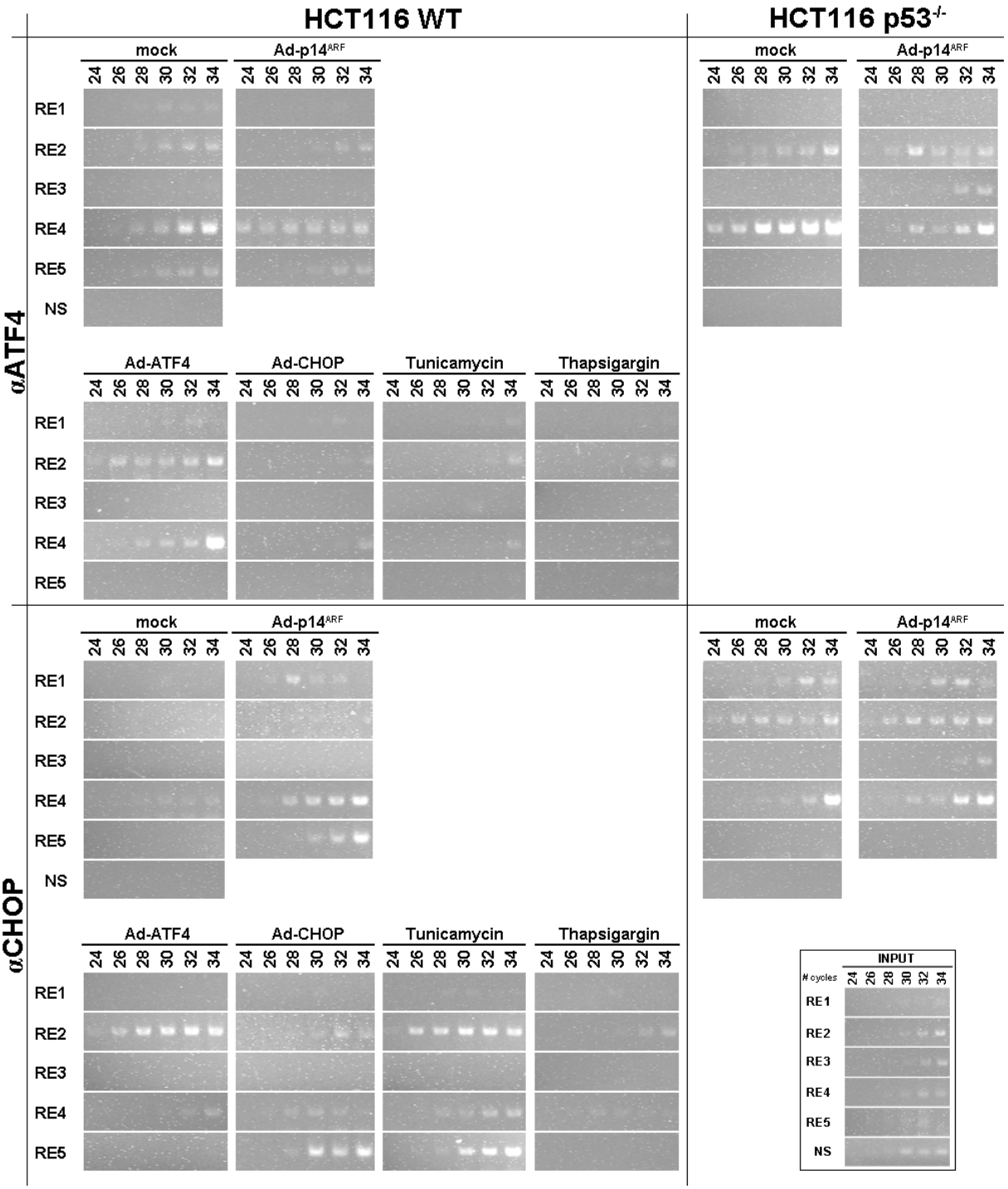

Figure 25. Chromatin immunoprecipitation against ATF4 and CHOP in HCT116 WT and p53$^{-/-}$ cell lines. Chromatin of cells treated mock, transfected with Ad-p14^{ARF}, Ad-CHOP$_{(Tet)}$, and Ad-ATF4$_{(Tet)}$ under 'on' condition or treated with tunicamycin and thapsigargin were precipitated with antibodies against ATF4 and CHOP and subjected to PCR with primers for identified binding regions (RE1 to RE5) of ATF4 and CHOP. Number of cycles as indicated. Input shows PCR before chromatin immunoprecipitation.

immunoprecipitation with an antibody against ATF4. After induction of $p14^{ARF}$, regions RE2, RE3, and RE4 could be detected. In $p53^{-/-}$ cells precipitated with an antibody against CHOP, regions RE1, RE2 and RE4 can be detected in mock treated cells. Expression of $p14^{ARF}$ leads to signals in regions RE1, RE2, RE3, and RE4.
Overall, signals in p53 deficient cells were stronger when compared to WT cells. Signals in RE3 for both ATF4 and CHOP could only be detected in p53 knockout cells. Signals in RE5 could only be detected in HCT116 WT cells.

Binding of ATF4 and CHOP to distinct or same regions could show co-localisation or -binding of these bZIP family transcription factors. Specific signals in the PCR for RE3 for ATF4 and CHOP after induction of $p14^{ARF}$ in p53 cell lines might point to this region as potential repressor or co-factor binding site in p53 proficient cell lines.

To analyse the transcriptional activity of $p14^{ARF}$, ATF4, and CHOP as well as drugs tunicamycin and thapsigargin cotransfection of different pGL3-constructs with an internal control for the luciferase activity plus additional transfection with pcDNA-constructs was performed in a luciferase assay (Figure 26).

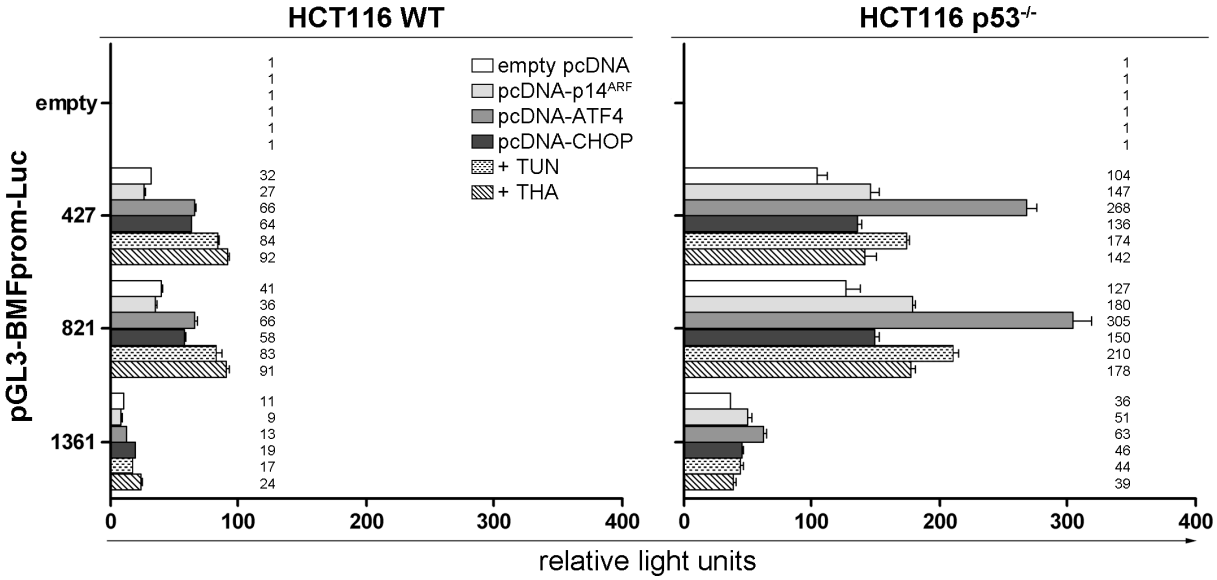

Figure 26. Luciferase Assay. HCT116 WT and p53-/- cell lines were transfected with pGL3modMCS constructs. Cell lines were cotransfected with pGL3-BMF promoter constructs as well as pcDNA or treated with 3 µg/ml tunicamycin or thapsigargin. Relative light units was calculated as luciferase activity divided by activity of cotransfected pRL-TK vector. Numbers represent mean of triplicates. Bars represent mean ± s.d.

HCT116 WT and $p53^{-/-}$ cell lines were transfected with pGL3-constructs containing no, 427 bp (RE1 - RE2), 821 bp (RE1 - RE3), or the first 1361 bp (RE1 - RE5) of the *bmf* promoter. Additionally, pRL-TK as internal luciferase control as well as pcDNA-constructs coding for $p14^{ARF}$, ATF4, and CHOP were cotransfected. Alternatively, 3 µg/ml of tunicamycin or thapsigargin was added to transfected cells without pcDNA.

The empty pGL3 vector is not activated by either cotransfection with other pcDNAs or tunicamycin and thapsigargin in both cell lines. The ratio and therefore the amount of relative light units (RLU) of empty pGL3 to pRL-TK is 1. The first 427 bp of the *bmf* promoter, containting RE1 and RE2, cotransfected with empty pcDNA led to a RLU of 32 in HCT116 WT cells. Cotransfection with $p14^{ARF}$ slightly reduced RLU, while ATF4 and CHOP doubled RLU to 66 and 64, respectively. Incubation with tunicamycin and thapsigargin nearly triples RLU to 84 and 92, respectively. Addition of RE3 (821 bp) changes RLU only slightly compared to 427 bp. The full length construct (1361 bp; containing regions 1-5) reduces RLU in HCT116 WT cell lines to about 11 with empty pcDNA3. Cotransfection with CHOP or treatment with tunicamycin and thapsigargin raises RLU to values of 19, 17, and 24, respectively.

In p53 deficient HCT116 cells, cotransfection with empty pcDNA3.1(+) leads to a three times higher RLU compared to p53 proficient cells with all promoter fragments. Also cotransfection with $p14^{ARF}$ in pcDNA leads to an increase of RLU with all promoter constructs compared to empty pcDNA. Expression of ATF4 leads to overall highest RLUs with 268 for regions RE1 and RE2 (427 bp) and 305 for 821 bp. Expression of CHOP alone increases RLU only slightly when compared to empty pcDNA constructs. Here, levels of 136 and 150 RLU are reached for constructs with 427 and 821 bp, respectively. Drug treatment with tunicamycin and thapsigargin also increases RLU. Tunicamycin treated cells display 174 RLU for the 427 bp construct and 210 RLU for the 821 bp construct. Thapsigargin treatment leads to 142 and 178 RLU in 427 and 821 bp constructs, respectively. Relative light units for the 1361 bp construct are about 36 for empty pcDNA and are only increased to 51 after ARF expression and 63 after ATF4 expression. CHOP expression (46 RLU), tunicamycin (44 RLU), and thapsigargin (39 RLU) treatment do not show a significant increase.

Interestingly, $p14^{ARF}$ expression in HCT116 WT cells reduces transcriptional activity by about 15 % independent of the length of the promoter fragment. In HCT116 $p53^{-/-}$ cells, $p14^{ARF}$ induces transcriptional activity. Both ChIP- and luciferase assay show the difference of binding and transcriptional activity in p53 pro- and deficient cells. Further analysis of RE3, a putative ATF4 binding site, should lead to the p53-dependent factors that are responsible for the difference in regulation.

5. Discussion

5.1 $p14^{ARF}$ induces p53 family independent apoptosis

The $p14^{ARF}$ – Hdm-2 – p53 pathway which induces apoptosis by a Puma-dependent mechanism is inactivated in over 50 % of all cancers mainly because of mutated or loss of p53. However, we previously showed, that the forced expression of $p14^{ARF}$ in human cancer cells can also trigger apoptosis and cell cycle arrest in a p53 independent manner. We set out to further explore the underlying signalling pathways, by focusing on the p53 homologs p63 and p73, as all p53 family members are able to regulate cell cycle and apoptosis after DNA damage. Neither p63 nor p73 is targeted by inactivating mutations in human cancers (Moll and Slade, 2004) and could be utilised to convey $p14^{ARF}$-induced cell death. However, it has been shown, that $p14^{ARF}$ inhibits p63-mediated transactivation and transrepression through direct interaction (Calabrò *et al.*, 2004), leaving p73 as a possible candidate for $p14^{ARF}$-induced apoptosis. Both p53 and p73 have been shown to contribute to chemosensitivy of tumours (Lunghi *et al.*, 2009) and both together with $p14^{ARF}$ are forming a network that is still able to induce apoptosis even when one partner is inactivated (Nicholson *et al.*, 2001). The interaction of p53-family proteins and their transcriptional activity has been analysed extensively. Mutations in p53 itself influences the regulatory ability of other family members, e.g. $p53^{Arg72}$ can bind and inhibit p73 activity (Irwin *et al.*, 2003). Especially the tetramerisation domain of p53 was thought to interact with the tetramerisation domains of p63 and p73, thereby interfereing with binding of the protein complexes to DNA and subsequent inhibiting their transcriptional activity.

Overexpression of the p53 tetramerisation domain should be able to interfere stoichiometrically with all splice variants carrying a homologuous domain. The newly created stable cell line expressing this tetramerisation domain (ΔNp53) displays no upregulation of p21 after induction of $p14^{ARF}$, confirming that we successfully disabled p53 family proteins. Our data clearly show a similar induction pattern of BH3-only mRNAs by $p14^{ARF}$ in p53 deficient cells as well as in p53 proficient cells (Figure 13). Therefore, inhibition of p53 homologs by expression of ΔNp53 does not inhibit $p14^{ARF}$ induced apoptosis. Thus, induction of apoptosis must be relayed by other means which are as fast and efficient as the Hdm-2–p53 signalling pathway since no difference in the amount of apoptosis could be detected in p53 family proficient and deficient cell lines (Figure 9 and Figure 10).

5.2 p14^{ARF}-induced apoptosis utilises pathways of the mitochondria and the ER

Apoptosis upon adenoviral expression of p14^{ARF} is executed via the mitochondria by activation of Bax and Bak, breakdown of the mitochondrial membrane potential, cytochrome *c* release (Figure 9), and by activation of caspases (Figure 10). Bcl-2 localised to the mitochondria is able to inhibit apoptosis and Bcl-2 family proteins have been shown to prevent all mitochondrial changes (Gross *et al.*, 1999; Shimizu and Tsujimoto, 2000).

We have demonstrated here, that Bcl-2 localised to the ER also attenuates p14^{ARF}-induced apoptosis (Figure 10), suggesting a connection of the ARF signalling pathway to this cellular organelle. Interestingly, according to literature, apoptosis induced by c-myc or DNA-damage through irradiation can also be inhibited by ER-targeted Bcl-2 (Lee *et al.*, 1999; Rudner *et al.*, 2001). The tumour suppressor p14^{ARF} is induced by both mechanisms (Zindy *et al.*, 1998; Lee *et al.*, 2005), thus, our data suggests p14^{ARF} being the common factor connecting these signalling pathways to the ER.

At the ER different mechanisms of inhibition of p14^{ARF} induced proteins by Bcl-2 are possible: First, direct inhibition of ER localised pro-apoptotic Bcl-2 family members. Inhibition of Bak or BH3-only proteins or inhibition of Bax translocalisation to the mitochondria by ER localised Bcl-2 has been shown before (Wei *et al.*, 2001; Zhang and Armstrong, 2007). Second, inhibition/interaction with non-Bcl-2 family members involved in ER stress, e.g. BiP or the transducers PERK, IRE1, and ATF6. Third, by interaction with the inositol 1,4,5-trisphosphate receptor (IP_3R) Bcl-2 is able to inhibit Ca^{2+} release from the ER (Rong *et al.*, 2008). The actual mechanism has not been elucidated, yet.

Based on our data, we cannot distinguish clearly between a parallel or consecutive activation of ER and mitochondria. If it is the former, the ER must be targeted first, relaying signals to the mitochondria which then leads to the activation of the intrinsic apoptosis pathway. By parallel activation of the organelles initial mitochondrial changes could be enhanced by signalling from the ER.

5.3 Induction of the PERK – CHOP pathway by p14^{ARF}

The most direct way to activate the ER would be by induction of ER stress by changes of Ca^{2+} homeostasis or the accumulation of unfolded proteins as induced by thapsigargin and tunicamycin, respectively. This leads to immediate induction of the UPR and its hallmark reporter BiP/GRP78 (Figure 14 and Figure 19) as well as all transducer proteins, i.e. PERK, ATF6, and IRE1. The ability of tunicamycin to trigger the accumulation of unfolded proteins

in the ER leads to the induction of the transducer proteins, while thapsigargin also activates pathways activated by changes in Ca^{2+} concentrations.

Our quantitative RT-PCR data shows, that expression of $p14^{ARF}$ does not lead to an induction of BiP/GRP78, i.e. ER stress, but exclusively upregulation of PERK, thereby only activating one specific pathway of the UPR when compared to tunicamycin and thapsigargin, which induce also ATF6 and IRE1. After $p14^{ARF}$ expression we also detect upregulation of eIF2α and CHOP, which are downstream components of the PERK pathway. However, the transcription factor ATF4, which is part of the PERK–CHOP signalling axis is not transcriptionally upregulated. According to literature, ATF4 exhibits a short half-life and low translation efficiency under normal conditions. After phosphorylation of eIF2α ATF4 translation is increased and proteasomal degradation is reduced (Rzymski *et al.*, 2009). Since no transcriptional upregulation of *atf4* but *chop* can also be detected by qRT-PCR after treatment with tunicamycin and thapsigargin, our data suggests that $p14^{ARF}$ solely activates the PERK–eIF2α–ATF4–CHOP pathway. Such selective activation of single branches of the UPR have been reported (Ma *et al.*, 2010) and especially the downstream consequences of the PERK pathway, i.e. the ISR are induced by different stress stimuli, e.g. amino acid deprivation, infection with double-stranded RNA viruses, heme deficiency, oxidative stress, and hypoxia (Brostrom and Brostrom, 1998; Brewer *et al.*, 1999; Williams, 1999; Harding *et al.*, 2000; Koumenis *et al.*, 2002; Rutkowski and Kaufman, 2003). Furthermore, the PERK-CHOP pathway is induced independent of the p53-family and was reported to lead to cell cycle arrest and/or apoptosis (Matsumoto *et al.*, 1996; Maytin *et al.*, 2001; Sauane *et al.*, 2008).

Inhibition of PERK by expressing its dominant negative variant significantly abrogates $p14^{ARF}$ induced cell death in p53 proficient HCT116 WT cells (Figure 16). This effect is even stronger in p53 deficient cells treated with PERK siRNA, where downregulation of ATF4 also inhibits apoptosis significantly (Figure 17). In these cells, the effect of downregulation of PERK Induction of apoptosis via the PERK pathway is likely to be executed by extended expression of downstream transcription factors ATF4 and CHOP (Figure 19) and is then achieved by pro-apoptotic Bcl-2 family members, i.e. BH3-only proteins. BH3-only proteins are sensors relaying apoptotic signals to mitochondria and their involvement is discussed in the next chapter. Interestingly, CHOP is able to inhibit anti-apoptotic Bcl-2 (Matsumoto *et al.*, 1996). Whether or not downregulation of Bcl-2 is as equally important as upregulation of BH3-only proteins has to be analysed in upcoming studies.

Induction of PERK signalling pathways by $p14^{ARF}$ might work as fail-safe mechanisms that function independent of the p53-family. Interestingly, PERK-mediated activation of the glycogen synthetase kinase-3β (GSK-3β) has been shown to phosphorylate p53, leading to its degradation via the proteasome (Qu *et al.*, 2004), and may act as a possible regulatory mechanism in p53 proficient cells.

5.4 Role of BH3-only proteins in ER-mediated induction of apoptosis

Induction of ER stress by tunicamycin and thapsigargin leads to upregulation of Bim, Bmf, Noxa, and Puma. BH3-only proteins Bim, Noxa, and Puma have already been shown to be involved in induction of apoptosis by ER stress (Reimertz *et al.*, 2003; Li *et al.*, 2006; Puthalakath *et al.*, 2007). Bim mediates cell death induced by ER stress via translocation to reticular membranes (Morishima *et al.*, 2004) and ER stress can selectively activate Puma and Noxa at the transcription level (Li *et al.*, 2006).

Our qRT-PCR data reveals Bmf as a novel candidate involved in mediating ER stress (Figure 20 and Figure 21). Its transcriptional regulation is discussed in more detail in the next chapter. Downregulation of *bmf* by siRNA leads to a small, but significant, reduction of apoptosis in cells treated with tunicamycin and a small reduction in cells treated with thapsigargin (Figure 22). Both drugs induce ER stress by different mechanisms, which could explain the differences in upregulation of BH3-only proteins and subsequent susceptibility to a reduction of Bmf. However, inhibition of apoptosis by knockdown of Bmf functions only in p53 deficient cells. In p53 proficient cells induction of the BH3-only proteins Bim, Noxa, and Puma seem to be the main regulators of apoptosis. In p53 proficient cell lines induction of Puma by $p14^{ARF}$ is the main pathway for apoptosis (Hemmati *et al.*, 2010). Here, Puma is able to inhibit all anti-apoptotic Bcl-2 family members (Chen *et al.*, 2005), thereby releasing and activating Bax & Bak to induce apoptosis. Interestingly, expression of $p14^{ARF}$ in p53 deficient cell lines leads to induction of Noxa and Bmf. Noxa selectively binds only to anti-apoptotic Mcl-1 and A1, while Bmf has a greater affinity to Bcl-2, Bcl-x_L, and Bcl-w (Chen *et al.*, 2005). Therefore, activation of both BH3-only proteins by $p14^{ARF}$ leads to release and activation of Bax & Bak and seems to compensate for Puma, which is not induced in p53 deficient cells. Further dissection and specific activation of the pathways, especially the p53 independent induction of Noxa by $p14^{ARF}$, will help to understand underlying mechanisms.

5.5 Bmf gene regulation

Induction of *bmf* by $p14^{ARF}$ can only be observed in p53 deficient cell lines (Figure 12 and Figure 13). Loss of p53 increases binding of the transcription factors ATF4 and CHOP to the *bmf* promoter (Figure 25) and enhances overall transcriptional activity (Figure 26) after induction of $p14^{ARF}$. Our promoter analysis of *bmf* revealed no binding sites of p53, thus a direct role of this transcription factor in *bmf* regulation seems implausible. Nevertheless, p53 might be involved indirectly by inducing repressors or co-factors that inhibit binding to or transcriptional activity of *bmf*. Our *in silico* promoter analysis revealed binding sites for different transcription factors, next to involved factors ATF4 and CHOP.

Binding sites for the CtBP-interacting basic Kruppel-like factor (BKLF) were shown to inhibit transcription of *nbk* and ARF reversed CtBP-associated repression (Kovi *et al.*, 2010). One binding site of BKLF is also found at position -401 (relative to TIS) of the *bmf* promoter, but the luciferase assay shows no significant induction of transcriptional activity in p53 proficient cells upon $p14^{ARF}$ expression, supporting our theory that p53-dependent repressors have a stronger effect on *bmf* transcription.

ATF4 seems to be the main transcription factor of *bmf* by specifically binding to the region 2 of the *bmf* promoter (Figure 25). ATF4 can dimerise with a number of transcription factors, including FIAT (factor-inhibiting ATF4-mediated transcription), Nrf2 (nuclear factor [erythroid-derived 2]-like 2), NF-IL6, AP-1 (activator protein 1), and Maf (macrophage activating factor) family members (Tanaka *et al.*, 1998; Hai and Hartman, 2001; He *et al.*, 2001). While ATF4 seems to be the important transcription factor, induction of CHOP by ATF4 might also regulate *bmf* transcription, as interaction of CHOP with ATF4 can regulate gene induction (Su and Kilberg, 2008). CHOP itself also binds to similar sites in the *bmf* promoter as ATF4 and a CHOP-C/EBP heterodimer has been reported to bind to an unique DNA sequence different from classical C/EBP binding sites (Ubeda *et al.*, 1996). Other bZIP proteins from the same family, i.e. ATF2 and ATF3, were shown to be involved in the regulation of CHOP as well (Averous *et al.*, 2004). These heteromeric complexes between ATF and CHOP proteins provide the potential for variable DNA binding specifities, as well as inhibitory complexes, allowing for differential regulation in the presence or absence of p53 (Tsukada *et al.*, 2011).

Taken together, we propose that Bmf is upregulated via the PERK-ATF4-CHOP signalling pathway, by activation of transcription factors ATF4 and CHOP and Bmf induction is inhibited indirectly by p53. However, expression of ATF4 and CHOP leads to a moderate

amount of apoptosis in p53 deficient cells when compared to expression of $p14^{ARF}$, suggesting that there are other pathways which must be accountable for the difference. In p53 deficient cell lines Bmf is the only BH3-only induced by ATF4 and CHOP via the PERK pathway, induction of 'stronger' BH3-only proteins, i.e. Bim, Noxa, and Puma, by other UPR pathways could explain these differences.

Since phosphorylation of eIF2α by PERK inhibits cap-dependent translation of proteins, upregulation of Bmf is only reasonable if translation of this BH3-only protein can also occur by a cap-independent mechanism. Our assumption about a conserved element in the 5' UTR of the mRNA was supported by a paper in November 2010. Here, Grespi *et al* showed that *bmf* contains an IRES element and an upstream CUG site by which translation will start (Grespi *et al.*, 2010). Whether or not Noxa or other BH3-only proteins are also translated by cap-independent mechanisms has to be analysed in upcoming studies.

5.6 Involvement of the ER as an energy saving mechanism

Ribosome biogenesis is the major biosynthetic and energy consuming activity of eukaryotic cells. It is sensitive to the availability of nutrients and growth factors and is coupled to cell cycle progression through regulation of Hdm-2/p53 signalling (Deisenroth and Zhang, 2011). Within the nucleolus nucleophosmin (NPM1) is involved in many processes leading to the processing and assembly of ribosomes, e.g. shuttling between the nucleus and cytoplasm to bind nucleic acids and to transport preribosomal particles (Borer *et al.*, 1989; Yun *et al.*, 2003). A knockdown of NPM1 inhibits the processing of preribosomal RNA (Itahana *et al.*, 2003; Grisendi *et al.*, 2005).

ARFs nucleolar localisation (Rizos *et al.*, 2000) makes for a possible regulator of this mechanism and it was already shown, that $p14^{ARF}$ interacts with NPM1 thereby inhibiting biogenesis of ribosomal RNA and retarding processing of 47/45S and 32S precursors. Subsequent reduction of ribosome levels lead to overall reduction of translation of proteins. By a parallel activation of the PERK-CHOP signalling pathway, $p14^{ARF}$ leads to inhibition of cap-dependent translation through phosphorylation of eIF2α, thereby also reducing the amount of protein translation. The inhibition of rRNA synthesis and protein translation might function as an energy saving mechanism initiated by $p14^{ARF}$. Additionaly, phosphorylation of eIF2α mediates the polyglutamine-induced LC3 conversion, an essential step for autophagy induction, i.e. inducing a process that by degradation of a cell's own components will

reallocate nutrients away from unnecessary processes (Kouroku *et al.*, 2007). Interestingly, *NPM1* mutations associate inversely with the occurrence of CCAAT/enhancer-binding protein-α *(CEBPA)* mutations in patients with acute myeloid leukemia (AML) (Verhaak *et al.*, 2005). CEBPA can interact with CHOP, which is induced by $p14^{ARF}$ via the PERK pathway. ARF might be one of the links/regulators, which keeps the network between these inversely correlated mutations in balance to retain its ability to influence the translation of proteins and therefor energy levels.

5.7 A cap-independent network regulating apoptosis

If inhibition of translation is an energy saving mechanism, basic regulation of homeostasis has to be maintained even under conditions of reduced protein translation. Interestingly, many genes involved in the intrinsic apoptotic pathway possess mRNAs carrying IRES elements or reinitiate translation by uORF mechanisms, circumventing regular cap-dependent translation and leaving a nearly intact network even under conditions of global inhibition of protein translation. Among these proteins, we find Bcl-2, cIAP, and XIAP (Coldwell *et al.*, 2000), which keep apoptosis in check. Also, during apoptosis, a reduction of translation initiation caused by caspase cleavage of several of the factors required for the cap-dependent scanning mechanism can be detected (Spriggs *et al.*, 2005).

Activation of the PERK–CHOP pathway by $p14^{ARF}$ leads to induction and translation of ATF4 by a cap-independent uORF mechanism. As ATF4 induces CHOP, which is known to inhibit anti-apoptotic Bcl-2, the homeostasis between pro- and anti-apoptotic factors is changed. Additional upregulation of transcription and IRES-mediated translation of Bmf might increase this imbalance and contributing to apoptotic cell death.

5.8 Model of $p14^{ARF}$ induced activation of apoptosis

Our findings of apoptosis induction by $p14^{ARF}$ are summarised in the following model (Figure 27). Next to the canonical pathway via stabilisation of p53 by Hdm-2 and induction of Puma (left), $p14^{ARF}$ also activates the PERK–CHOP pathway, leading to induction of Bmf in p53 deficient cells (right). While Puma is able to inhibit all anti-apoptotic Bcl-2 family members, Bmf inhibits Bcl-2, Bcl-x_L, and Bcl-w. The p53 independent induction of Noxa, probably via a different signalling pathway at the ER might then be responsible for inhibition of anti-apoptotic Mcl-1 and A1.

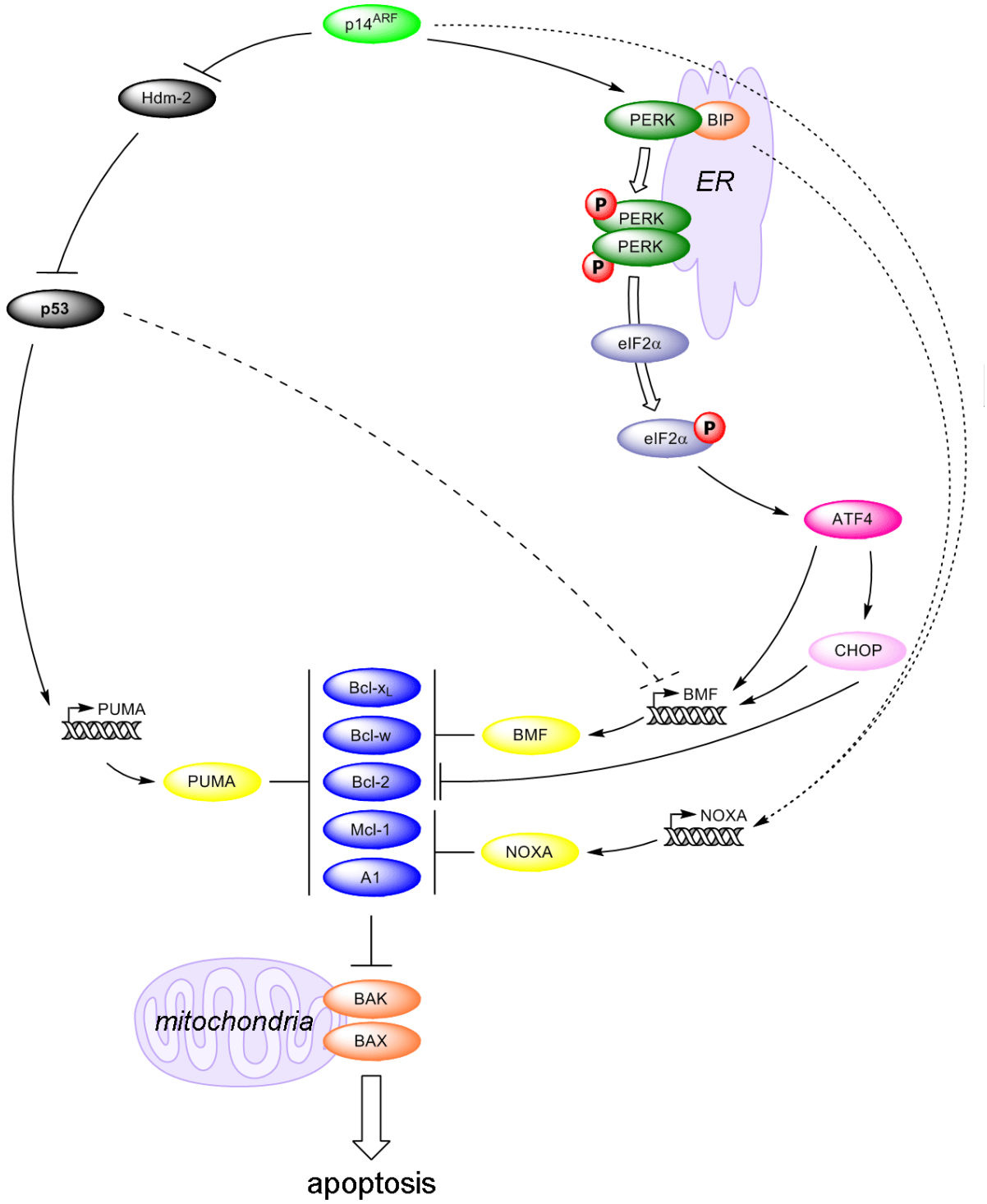

Figure 27. Model of p14^{ARF}-induced activation of apoptosis. Expression of p14^{ARF} leads to activation of the PERK – CHOP pathway, which is one branch of the so called unfolded protein response (UPR). Phosphorylation of eIF2α by PERK-induced p14^{ARF} and subsequent stabilisation of ATF4 and upregulation of CHOP leads to downregulation of anti-apoptotic Bcl-2 and induction of pro-apoptotic *bmf* (right). Additional, p53 independent induction of *noxa* will increase changes in the homeostasis between pro- and anti-apoptotic proteins and eventually results in induction of apoptosis by activation of mitochondria via Bak and Bax. In p53 proficient cells transcription of *bmf* is inhibited and activation of mitochondria is regulated by induction of BH3-only protein Puma (left).

5.9 Outlook

In this thesis we presented evidence for a novel signalling connection between the tumour suppressor $p14^{ARF}$ and the ER. Complex protein networks within and between cellular organelles are responsible for maintaining homeostasis with several control mechanisms ensuring and enforcing specific conditions. Each organelle can sense stressful and pathogenic alterations and initiates local or global responses leading to adaptation or, once a critical threshold of damage has been reached, cell death (Ferri and Kroemer, 2001).

The newly found connection between $p14^{ARF}$ and the induction of the PERK–eIF2α–ATF4–CHOP signalling cascade shows a pathway emanating from the ER that will activate and/or amplify events at the mitochondria. The pro-apoptotic Bmf, which is induced by the PERK pathway is the sole BH3-only protein known so far that carries an IRES element and can circumvent inhibition of cap-dependent translation initiated by the integrated stress response (ISR). Bmf might therefore be involved in apoptosis induction by diverse stimuli.

Further analysis on the impact of $p14^{ARF}$ to execute pathways from other cellular organelles, e.g. the Golgi apparatus or lysosomes, will reveal if $p14^{ARF}$ is a general transducer of cell death by activating different pathways at the same time. Activation of the PERK-CHOP pathway by $p14^{ARF}$ connects signalling networks that are not only involved in tumorigenesis but also in development of diabetic, cardiovascular, and other diseases. Targeted activation/deactivation of factors in these networks will open possibilities to treat these illnesses.

6. Summary

In tumour cells, BH3-only proteins are the main regulator of apoptotic cell death and are regulated by p53-dependent and -independent signalling. We have shown here, that induction of apoptosis by expression of the tumour suppressor $p14^{ARF}$ may function independently of the canonical Hdm-2 – p53 pathway.

In addition, we showed, that $p14^{ARF}$-induced apoptosis can be inhibited by Bcl-2 localised to the ER. Therefore we analysed this cellular organelle to detect the factors relaying apoptotic signals. By use of quantitative real-time PCR, we found, that expression of $p14^{ARF}$ leads to activation of the PERK branch of the unfolded protein response (UPR), without causing characteristical ER stress, i.e. induction of the chaperone BiP/GRP78. Downstream events of PERK lead to attenuation of cap-dependent protein translation and upregulation of transcription factors ATF4 and CHOP. Adenoviral overexpression of these transcription factors and analysis of induction of BH3-only genes revealed, that *bmf* is induced by these proteins. In an *in silico* promoter analysis of *bmf* we identified putative binding sites for ATF4 and CHOP. Additional promoter analysis via ChIP and reporter studies with a luciferase assay showed binding and transcriptional activation of the *bmf* promoter by ATF4 and CHOP, further verifying our model. Bmf is the only member of the BH3-only family that is induced by these transcription factors. We found, that the conserved structure of the 5' UTR of the Bmf mRNA serves as an IRES element which is used to circumvent the global cap-dependent translation activated by the PERK pathway.

PERK is one of three transducer proteins involved in UPR and is activated by ER stress. Here, next to the already in ER-mediated induction of apoptosis implied BH3-only proteins Bim, Noxa, and Puma, pro-apoptotic Bmf plays an important role. Further dissection of the other UPR branches will reveal by which mechanisms those BH3-only proteins are induced.

Induction of *bmf* by $p14^{ARF}$ is also achieved via the PERK/eIF2α/ATF4/CHOP signalling axis but is negatively regulated in p53 proficient cells. This pathway could play the role of a 'fail-safe' mechanism that allows cells, even after loss of p53, to undergo apoptosis induced by upregulation of $p14^{ARF}$ by oncogenes.

References

Abida, W.M., and Gu, W. (2008). p53-Dependent and p53-independent activation of autophagy by ARF. Cancer Res. *68*, 352–357.

Averous, J., Bruhat, A., Jousse, C., Carraro, V., Thiel, G., and Fafournoux, P. (2004). Induction of CHOP expression by amino acid limitation requires both ATF4 expression and ATF2 phosphorylation. J. Biol. Chem. *279*, 5288–5297.

Baffy, G., Miyashita, T., Williamson, J.R., and Reed, J.C. (1993). Apoptosis induced by withdrawal of interleukin-3 (IL-3) from an IL-3-dependent hematopoietic cell line is associated with repartitioning of intracellular calcium and is blocked by enforced Bcl-2 oncoprotein production. J. Biol. Chem. *268*, 6511–6519.

Banner, D.W., D'Arcy, A., Janes, W., Gentz, R., Schoenfeld, H.J., Broger, C., Loetscher, H., and Lesslauer, W. (1993). Crystal structure of the soluble human 55 kd TNF receptor-human TNF beta complex: implications for TNF receptor activation. Cell *73*, 431–445.

Bénard, J., Douc-Rasy, S., and Ahomadegbe, J.-C. (2003). TP53 family members and human cancers. Hum. Mutat. *21*, 182–191.

Bence, N.F., Sampat, R.M., and Kopito, R.R. (2001). Impairment of the ubiquitin-proteasome system by protein aggregation. Science *292*, 1552–1555.

den Besten, W., Kuo, M.-L., Williams, R.T., and Sherr, C.J. (2005). Myeloid leukemia-associated nucleophosmin mutants perturb p53-dependent and independent activities of the Arf tumor suppressor protein. Cell Cycle *4*, 1593–1598.

Boldin, M.P., Mett, I.L., Varfolomeev, E.E., Chumakov, I., Shemer-Avni, Y., Camonis, J.H., and Wallach, D. (1995). Self-association of the "death domains" of the p55 tumor necrosis factor (TNF) receptor and Fas/APO1 prompts signaling for TNF and Fas/APO1 effects. J. Biol. Chem. *270*, 387–391.

Borer, R.A., Lehner, C.F., Eppenberger, H.M., and Nigg, E.A. (1989). Major nucleolar proteins shuttle between nucleus and cytoplasm. Cell *56*, 379–390.

Bouillet, P., Cory, S., Zhang, L.C., Strasser, A., and Adams, J.M. (2001). Degenerative disorders caused by Bcl-2 deficiency prevented by loss of its BH3-only antagonist Bim. Dev. Cell *1*, 645–653.

Bourdon, J.-C., Fernandes, K., Murray-Zmijewski, F., Liu, G., Diot, A., Xirodimas, D.P., Saville, M.K., and Lane, D.P. (2005). p53 isoforms can regulate p53 transcriptional activity. Genes Dev. *19*, 2122–2137.

Bradford, M.M. (1976). A rapid and sensitive method for the quantitation of microgram quantities of protein utilizing the principle of protein-dye binding. Anal. Biochem. *72*, 248–254.

Brattain, M.G., Fine, W.D., Khaled, F.M., Thompson, J., and Brattain, D.E. (1981). Heterogeneity of malignant cells from a human colonic carcinoma. Cancer Res. *41*, 1751–1756.

Brewer, J.W., and Diehl, J.A. (2000). PERK mediates cell-cycle exit during the mammalian unfolded protein response. Proc. Natl. Acad. Sci. U.S.A. *97*, 12625–12630.

Brewer, J.W., Hendershot, L.M., Sherr, C.J., and Diehl, J.A. (1999). Mammalian unfolded protein response inhibits cyclin D1 translation and cell-cycle progression. Proc. Natl. Acad. Sci. U.S.A. *96*, 8505–8510.

Brostrom, C.O., and Brostrom, M.A. (1998). Regulation of translational initiation during cellular responses to stress. Prog. Nucleic Acid Res. Mol. Biol. *58*, 79–125.

Bunz, F., Dutriaux, A., Lengauer, C., Waldman, T., Zhou, S., Brown, J.P., Sedivy, J.M., Kinzler, K.W., and Vogelstein, B. (1998). Requirement for p53 and p21 to sustain G2 arrest after DNA damage. Science *282*, 1497–1501.

Burri, N., Shaw, P., Bouzourene, H., Sordat, I., Sordat, B., Gillet, M., Schorderet, D., Bosman, F.T., and Chaubert, P. (2001). Methylation silencing and mutations of the p14ARF and p16INK4a genes in colon cancer. Lab. Invest. *81*, 217–229.

Calabrò, V., Mansueto, G., Santoro, R., Gentilella, A., Pollice, A., Ghioni, P., Guerrini, L., and La Mantia, G. (2004). Inhibition of p63 transcriptional activity by p14ARF: functional and physical link between human ARF tumor suppressor and a member of the p53 family. Mol. Cell. Biol. *24*, 8529–8540.

Carnero, A., Hudson, J.D., Price, C.M., and Beach, D.H. (2000). p16INK4A and p19ARF act in overlapping pathways in cellular immortalization. Nat. Cell Biol. *2*, 148–155.

Cheng, E.H.Y., Sheiko, T.V., Fisher, J.K., Craigen, W.J., and Korsmeyer, S.J. (2003). VDAC2 inhibits BAK activation and mitochondrial apoptosis. Science *301*, 513–517.

Chen, L., Willis, S.N., Wei, A., Smith, B.J., Fletcher, J.I., Hinds, M.G., Colman, P.M., Day, C.L., Adams, J.M., and Huang, D.C.S. (2005). Differential targeting of prosurvival Bcl-2 proteins by their BH3-only ligands allows complementary apoptotic function. Mol. Cell *17*, 393–403.

Coldwell, M.J., Mitchell, S.A., Stoneley, M., MacFarlane, M., and Willis, A.E. (2000). Initiation of Apaf-1 translation by internal ribosome entry. Oncogene *19*, 899–905.

Colombo, E., Martinelli, P., Zamponi, R., Shing, D.C., Bonetti, P., Luzi, L., Volorio, S., Bernard, L., Pruneri, G., Alcalay, M., et al. (2006). Delocalization and destabilization of the Arf tumor suppressor by the leukemia-associated NPM mutant. Cancer Res. *66*, 3044–3050.

Crompton, M. (2000). Mitochondrial intermembrane junctional complexes and their role in cell death. J. Physiol. (Lond.) *529 Pt 1*, 11–21.

Czabotar, P.E., Lee, E.F., van Delft, M.F., Day, C.L., Smith, B.J., Huang, D.C.S., Fairlie, W.D., Hinds, M.G., and Colman, P.M. (2007). Structural insights into the degradation of Mcl-1 induced by BH3 domains. Proc. Natl. Acad. Sci. U.S.A. *104*, 6217–6222.

Danial, N.N., and Korsmeyer, S.J. (2004). Cell death: critical control points. Cell *116*, 205–219.

Daniel, P.T. (2000). Dissecting the pathways to death. Leukemia *14*, 2035–2044.

Daniel, P.T., Schulze-Osthoff, K., Belka, C., and Güner, D. (2003). Guardians of cell death: the Bcl-2 family proteins. Essays Biochem. *39*, 73–88.

Davis, R.J. (2000). Signal transduction by the JNK group of MAP kinases. Cell *103*, 239–252.

Deisenroth, C., and Zhang, Y. (2011). The Ribosomal Protein-Mdm2-p53 Pathway and Energy Metabolism: Bridging the Gap between Feast and Famine. Genes Cancer *2*, 392–403.

van Delft, M.F., and Huang, D.C.S. (2006). How the Bcl-2 family of proteins interact to regulate apoptosis. Cell Res. *16*, 203–213.

Deng, J., Harding, H.P., Raught, B., Gingras, A.-C., Berlanga, J.J., Scheuner, D., Kaufman, R.J., Ron, D., and Sonenberg, N. (2002). Activation of GCN2 in UV-irradiated cells inhibits translation. Curr. Biol. *12*, 1279–1286.

Du, H., Wolf, J., Schafer, B., Moldoveanu, T., Chipuk, J.E., and Kuwana, T. (2011). BH3 domains other than Bim and Bid can directly activate Bax/Bak. J. Biol. Chem. *286*, 491–501.

de Duve, C. (1963). The Lysosome Concept. Ciba Foundation Symposium Lysosomes 1–35.

Elbein, A.D. (1987). Inhibitors of the biosynthesis and processing of N-linked oligosaccharide chains. Annu. Rev. Biochem. *56*, 497–534.

el-Deiry, W.S., Kern, S.E., Pietenpol, J.A., Kinzler, K.W., and Vogelstein, B. (1992). Definition of a consensus binding site for p53. Nat. Genet. *1*, 45–49.

Ferri, K.F., and Kroemer, G. (2001). Organelle-specific initiation of cell death pathways. Nat. Cell Biol. *3*, E255–E263.

Fesik, S.W. (2000). Insights into programmed cell death through structural biology. Cell *103*, 273–282.

Finlay, C.A., Hinds, P.W., and Levine, A.J. (1989). The p53 proto-oncogene can act as a suppressor of transformation. Cell *57*, 1083–1093.

Fischer, H., Koenig, U., Eckhart, L., and Tschachler, E. (2002). Human caspase 12 has acquired deleterious mutations. Biochem. Biophys. Res. Commun. *293*, 722–726.

Frisch, S.M., and Francis, H. (1994). Disruption of epithelial cell-matrix interactions induces apoptosis. J. Cell Biol. *124*, 619–626.

Ganten, D., and Ruckpaul, K. (2007). Grundlagen der Molekularen Medizin (Springer).

García, M.A., Collado, M., Muñoz-Fontela, C., Matheu, A., Marcos-Villar, L., Arroyo, J., Esteban, M., Serrano, M., and Rivas, C. (2006). Antiviral action of the tumor suppressor ARF. Embo J. *25*, 4284–4292.

Germain, M., Mathai, J.P., and Shore, G.C. (2002). BH-3-only BIK functions at the endoplasmic reticulum to stimulate cytochrome c release from mitochondria. J. Biol. Chem. *277*, 18053–18060.

Gil, J., and Peters, G. (2006). Regulation of the INK4b-ARF-INK4a tumour suppressor locus: all for one or one for all. Nat. Rev. Mol. Cell Biol. *7*, 667–677.

Gillissen, B., Essmann, F., Graupner, V., Stärck, L., Radetzki, S., Dörken, B., Schulze-Osthoff, K., and Daniel, P.T. (2003). Induction of cell death by the BH3-only Bcl-2 homolog Nbk/Bik is mediated by an entirely Bax-dependent mitochondrial pathway. Embo J. *22*, 3580–3590.

Gillissen, B., Essmann, F., Hemmati, P.G., Richter, A., Richter, A., Oztop, I., Chinnadurai, G., Dörken, B., and Daniel, P.T. (2007). Mcl-1 determines the Bax dependency of Nbk/Bik-induced apoptosis. J. Cell Biol. *179*, 701–715.

Golks, A., Brenner, D., Fritsch, C., Krammer, P.H., and Lavrik, I.N. (2005). c-FLIPR, a new regulator of death receptor-induced apoptosis. J. Biol. Chem. *280*, 14507–14513.

Graham, F.L., Smiley, J., Russell, W.C., and Nairn, R. (1977). Characteristics of a human cell line transformed by DNA from human adenovirus type 5. J. Gen. Virol. *36*, 59–74.

Grespi, F., Soratroi, C., Krumschnabel, G., Sohm, B., Ploner, C., Geley, S., Hengst, L., Häcker, G., and Villunger, A. (2010). BH3-only protein Bmf mediates apoptosis upon inhibition of CAP-dependent protein synthesis. Cell Death Differ. *17*, 1672–1683.

Gressner, O., Schilling, T., Lorenz, K., Schulze Schleithoff, E., Koch, A., Schulze-Bergkamen, H., Lena, A.M., Candi, E., Terrinoni, A., Catani, M.V., et al. (2005). TAp63alpha induces apoptosis by activating signaling via death receptors and mitochondria. Embo J. *24*, 2458–2471.

Grisendi, S., Bernardi, R., Rossi, M., Cheng, K., Khandker, L., Manova, K., and Pandolfi, P.P. (2005). Role of nucleophosmin in embryonic development and tumorigenesis. Nature *437*, 147–153.

Gross, A., McDonnell, J.M., and Korsmeyer, S.J. (1999). BCL-2 family members and the mitochondria in apoptosis. Genes Dev. *13*, 1899–1911.

Haber, D.A. (1997). Splicing into senescence: the curious case of p16 and p19ARF. Cell *91*, 555–558.

Hai, T., and Hartman, M.G. (2001). The molecular biology and nomenclature of the activating transcription factor/cAMP responsive element binding family of transcription factors: activating transcription factor proteins and homeostasis. Gene *273*, 1–11.

Han, E.-S., Muller, F.L., Pérez, V.I., Qi, W., Liang, H., Xi, L., Fu, C., Doyle, E., Hickey, M., Cornell, J., et al. (2008). The in vivo gene expression signature of oxidative stress. Physiol. Genomics *34*, 112–126.

Harding, H.P., Novoa, I., Zhang, Y., Zeng, H., Wek, R., Schapira, M., and Ron, D. (2000). Regulated translation initiation controls stress-induced gene expression in mammalian cells. Mol. Cell *6*, 1099–1108.

Harding, H.P., Zhang, Y., Zeng, H., Novoa, I., Lu, P.D., Calfon, M., Sadri, N., Yun, C., Popko, B., Paules, R., et al. (2003). An integrated stress response regulates amino acid metabolism and resistance to oxidative stress. Mol. Cell *11*, 619–633.

Harms, K., Nozell, S., and Chen, X. (2004). The common and distinct target genes of the p53 family transcription factors. Cell. Mol. Life Sci. *61*, 822–842.

Heath-Engel, H.M., Chang, N.C., and Shore, G.C. (2008). The endoplasmic reticulum in apoptosis and autophagy: role of the BCL-2 protein family. Oncogene *27*, 6419–6433.

He, C.H., Gong, P., Hu, B., Stewart, D., Choi, M.E., Choi, A.M., and Alam, J. (2001). Identification of activating transcription factor 4 (ATF4) as an Nrf2-interacting protein. Implication for heme oxygenase-1 gene regulation. J. Biol. Chem. *276*, 20858–20865.

Hemmati, P.G., Gillissen, B., von Haefen, C., Wendt, J., Stärck, L., Güner, D., Dörken, B., and Daniel, P.T. (2002). Adenovirus-mediated overexpression of p14(ARF) induces p53 and Bax-independent apoptosis. Oncogene *21*, 3149–3161.

Hemmati, P.G., Güner, D., Gillissen, B., Wendt, J., von Haefen, C., Chinnadurai, G., Dörken, B., and Daniel, P.T. (2006). Bak functionally complements for loss of Bax during p14ARF-induced mitochondrial apoptosis in human cancer cells. Oncogene *25*, 6582–6594.

Hemmati, P.G., Müer, A., Gillissen, B., Overkamp, T., Milojkovic, A., Wendt, J., Dörken, B., and Daniel, P.T. (2010). Systematic genetic dissection of p14ARF-mediated mitochondrial cell death signaling reveals a key role for p21CDKN1 and the BH3-only protein Puma/bbc3. J. Mol. Med. *88*, 609–622.

Hemmati, P.G., Normand, G., Verdoodt, B., von Haefen, C., Hasenjäger, A., Güner, D., Wendt, J., Dörken, B., and Daniel, P.T. (2005). Loss of p21 disrupts p14 ARF-induced G1 cell cycle arrest but augments p14 ARF-induced apoptosis in human carcinoma cells. Oncogene *24*, 4114–4128.

Hetz, C., Bernasconi, P., Fisher, J., Lee, A.-H., Bassik, M.C., Antonsson, B., Brandt, G.S., Iwakoshi, N.N., Schinzel, A., Glimcher, L.H., et al. (2006). Proapoptotic BAX and BAK modulate the unfolded protein response by a direct interaction with IRE1alpha. Science *312*, 572–576.

Hitomi, J., Katayama, T., Eguchi, Y., Kudo, T., Taniguchi, M., Koyama, Y., Manabe, T., Yamagishi, S., Bando, Y., Imaizumi, K., et al. (2004a). Involvement of caspase-4 in endoplasmic reticulum stress-induced apoptosis and Abeta-induced cell death. J. Cell Biol. *165*, 347–356.

Hitomi, J., Katayama, T., Taniguchi, M., Honda, A., Imaizumi, K., and Tohyama, M. (2004b). Apoptosis induced by endoplasmic reticulum stress depends on activation of caspase-3 via caspase-12. Neurosci. Lett. *357*, 127–130.

Hsu, Y.T., Wolter, K.G., and Youle, R.J. (1997). Cytosol-to-membrane redistribution of Bax and Bcl-X(L) during apoptosis. Proc. Natl. Acad. Sci. U.S.A. *94*, 3668–3672.

Irwin, M.S., and Kaelin, W.G. (2001a). p53 family update: p73 and p63 develop their own identities. Cell Growth Differ. *12*, 337–349.

Irwin, M.S., and Kaelin, W.G., Jr (2001b). Role of the newer p53 family proteins in malignancy. Apoptosis *6*, 17–29.

Irwin, M.S., Kondo, K., Marin, M.C., Cheng, L.S., Hahn, W.C., and Kaelin, W.G., Jr (2003). Chemosensitivity linked to p73 function. Cancer Cell *3*, 403–410.

Isaacs, W.B., Carter, B.S., and Ewing, C.M. (1991). Wild-type p53 suppresses growth of human prostate cancer cells containing mutant p53 alleles. Cancer Res. *51*, 4716–4720.

Itahana, K., Bhat, K.P., Jin, A., Itahana, Y., Hawke, D., Kobayashi, R., and Zhang, Y. (2003). Tumor suppressor ARF degrades B23, a nucleolar protein involved in ribosome biogenesis and cell proliferation. Mol. Cell *12*, 1151–1164.

Kaghad, M., Bonnet, H., Yang, A., Creancier, L., Biscan, J.C., Valent, A., Minty, A., Chalon, P., Lelias, J.M., Dumont, X., et al. (1997). Monoallelically expressed gene related to p53 at 1p36, a region frequently deleted in neuroblastoma and other human cancers. Cell *90*, 809–819.

Kerr, J.F., Wyllie, A.H., and Currie, A.R. (1972). Apoptosis: a basic biological phenomenon with wide-ranging implications in tissue kinetics. Br. J. Cancer *26*, 239–257.

Kim, W.Y., and Sharpless, N.E. (2006). The regulation of INK4/ARF in cancer and aging. Cell *127*, 265–275.

Koumenis, C., Naczki, C., Koritzinsky, M., Rastani, S., Diehl, A., Sonenberg, N., Koromilas, A., and Wouters, B.G. (2002). Regulation of protein synthesis by hypoxia via activation of the endoplasmic reticulum kinase PERK and phosphorylation of the translation initiation factor eIF2alpha. Mol. Cell. Biol. *22*, 7405–7416.

Kouroku, Y., Fujita, E., Tanida, I., Ueno, T., Isoai, A., Kumagai, H., Ogawa, S., Kaufman, R.J., Kominami, E., and Momoi, T. (2007). ER stress (PERK/eIF2alpha phosphorylation) mediates the polyglutamine-induced LC3 conversion, an essential step for autophagy formation. Cell Death Differ. *14*, 230–239.

Kovi, R.C., Paliwal, S., Pande, S., and Grossman, S.R. (2010). An ARF/CtBP2 complex regulates BH3-only gene expression and p53-independent apoptosis. Cell Death Differ. *17*, 513–521.

Kozutsumi, Y., Segal, M., Normington, K., Gething, M.J., and Sambrook, J. (1988). The presence of malfolded proteins in the endoplasmic reticulum signals the induction of glucose-regulated proteins. Nature *332*, 462–464.

Krajewski, S., Tanaka, S., Takayama, S., Schibler, M.J., Fenton, W., and Reed, J.C. (1993). Investigation of the subcellular distribution of the bcl-2 oncoprotein: residence in the nuclear envelope, endoplasmic reticulum, and outer mitochondrial membranes. Cancer Res. *53*, 4701–4714.

Krammer, P.H., Behrmann, I., Daniel, P., Dhein, J., and Debatin, K.M. (1994). Regulation of apoptosis in the immune system. Curr. Opin. Immunol. *6*, 279–289.

Krueger, A., Schmitz, I., Baumann, S., Krammer, P.H., and Kirchhoff, S. (2001). Cellular FLICE-inhibitory protein splice variants inhibit different steps of caspase-8 activation at the CD95 death-inducing signaling complex. J. Biol. Chem. *276*, 20633–20640.

Kuwana, T., Bouchier-Hayes, L., Chipuk, J.E., Bonzon, C., Sullivan, B.A., Green, D.R., and Newmeyer, D.D. (2005). BH3 domains of BH3-only proteins differentially regulate Bax-mediated mitochondrial membrane permeabilization both directly and indirectly. Mol. Cell *17*, 525–535.

Labi, V., Erlacher, M., Kiessling, S., Manzl, C., Frenzel, A., O'Reilly, L., Strasser, A., and Villunger, A. (2008). Loss of the BH3-only protein Bmf impairs B cell homeostasis and accelerates gamma irradiation-induced thymic lymphoma development. J. Exp. Med. *205*, 641–655.

Laemmli, U.K. (1970). Cleavage of structural proteins during the assembly of the head of bacteriophage T4. Nature *227*, 680–685.

Lane, D.P. (1992). Cancer. p53, guardian of the genome. Nature *358*, 15–16.

Lee, C., Smith, B.A., Bandyopadhyay, K., and Gjerset, R.A. (2005). DNA damage disrupts the p14ARF-B23(nucleophosmin) interaction and triggers a transient subnuclear redistribution of p14ARF. Cancer Res. *65*, 9834–9842.

Lee, S.T., Hoeflich, K.P., Wasfy, G.W., Woodgett, J.R., Leber, B., Andrews, D.W., Hedley, D.W., and Penn, L.Z. (1999). Bcl-2 targeted to the endoplasmic reticulum can inhibit apoptosis induced by Myc but not etoposide in Rat-1 fibroblasts. Oncogene *18*, 3520–3528.

Leist, M., and Jäättelä, M. (2001). Four deaths and a funeral: from caspases to alternative mechanisms. Nat. Rev. Mol. Cell Biol. *2*, 589–598.

Levrero, M., De Laurenzi, V., Costanzo, A., Gong, J., Wang, J.Y., and Melino, G. (2000). The p53/p63/p73 family of transcription factors: overlapping and distinct functions. J. Cell. Sci. *113 (Pt 10)*, 1661–1670.

Li, J., Lee, B., and Lee, A.S. (2006). Endoplasmic reticulum stress-induced apoptosis: multiple pathways and activation of p53-up-regulated modulator of apoptosis (PUMA) and NOXA by p53. J. Biol. Chem. *281*, 7260–7270.

Lin, Y.S., and Green, M.R. (1988). Interaction of a common cellular transcription factor, ATF, with regulatory elements in both E1a- and cyclic AMP-inducible promoters. Proc. Natl. Acad. Sci. U.S.A. *85*, 3396–3400.

Loew, R., Heinz, N., Hampf, M., Bujard, H., and Gossen, M. (2010). Improved Tet-responsive promoters with minimized background expression. BMC Biotechnol. *10*, 81.

Lowe, S.W., and Sherr, C.J. (2003). Tumor suppression by Ink4a-Arf: progress and puzzles. Curr. Opin. Genet. Dev. *13*, 77–83.

Lu, L., Han, A.P., and Chen, J.J. (2001). Translation initiation control by heme-regulated eukaryotic initiation factor 2alpha kinase in erythroid cells under cytoplasmic stresses. Mol. Cell. Biol. *21*, 7971–7980.

Lunghi, P., Costanzo, A., Mazzera, L., Rizzoli, V., Levrero, M., and Bonati, A. (2009). The p53 family protein p73 provides new insights into cancer chemosensitivity and targeting. Clin. Cancer Res. *15*, 6495–6502.

Magnelli, L., Cinelli, M., Turchetti, A., and Chiarugi, V.P. (1994). Bcl-2 overexpression abolishes early calcium waving preceding apoptosis in NIH-3T3 murine fibroblasts. Biochem. Biophys. Res. Commun. *204*, 84–90.

Maran, A., and Mathews, M.B. (1988). Characterization of the double-stranded RNA implicated in the inhibition of protein synthesis in cells infected with a mutant adenovirus defective for VA RNA. Virology *164*, 106–113.

Mathai, J.P., Germain, M., Marcellus, R.C., and Shore, G.C. (2002). Induction and endoplasmic reticulum location of BIK/NBK in response to apoptotic signaling by E1A and p53. Oncogene *21*, 2534–2544.

Matsumoto, M., Minami, M., Takeda, K., Sakao, Y., and Akira, S. (1996). Ectopic expression of CHOP (GADD153) induces apoptosis in M1 myeloblastic leukemia cells. FEBS Lett. *395*, 143–147.

Ma, Y., Brewer, J.W., Diehl, J.A., and Hendershot, L.M. (2002). Two distinct stress signaling pathways converge upon the CHOP promoter during the mammalian unfolded protein response. J. Mol. Biol. *318*, 1351–1365.

Ma, Y., Shimizu, Y., Mann, M.J., Jin, Y., and Hendershot, L.M. (2010). Plasma cell differentiation initiates a limited ER stress response by specifically suppressing the PERK-dependent branch of the unfolded protein response. Cell Stress Chaperones *15*, 281–293.

Maytin, E.V., Ubeda, M., Lin, J.C., and Habener, J.F. (2001). Stress-inducible transcription factor CHOP/gadd153 induces apoptosis in mammalian cells via p38 kinase-dependent and -independent mechanisms. Exp. Cell Res. *267*, 193–204.

Melino, G., Lu, X., Gasco, M., Crook, T., and Knight, R.A. (2003). Functional regulation of p73 and p63: development and cancer. Trends Biochem. Sci. *28*, 663–670.

Micheau, O., and Tschopp, J. (2003). Induction of TNF receptor I-mediated apoptosis via two sequential signaling complexes. Cell *114*, 181–190.

Moll, U.M., and Slade, N. (2004). p63 and p73: roles in development and tumor formation. Mol. Cancer Res. *2*, 371–386.

Morales, A.A., Olsson, A., Celsing, F., Osterborg, A., Jondal, M., and Osorio, L.M. (2004). Expression and transcriptional regulation of functionally distinct Bmf isoforms in B-chronic lymphocytic leukemia cells. Leukemia *18*, 41–47.

Morishima, N., Nakanishi, K., Tsuchiya, K., Shibata, T., and Seiwa, E. (2004). Translocation of Bim to the endoplasmic reticulum (ER) mediates ER stress signaling for activation of caspase-12 during ER stress-induced apoptosis. J. Biol. Chem. *279*, 50375–50381.

Nakano, K., and Vousden, K.H. (2001). PUMA, a novel proapoptotic gene, is induced by p53. Mol. Cell *7*, 683–694.

Nicholson, D.W. (1999). Caspase structure, proteolytic substrates, and function during apoptotic cell death. Cell Death Differ. *6*, 1028–1042.

Nicholson, S.A., Okby, N.T., Khan, M.A., Welsh, J.A., McMenamin, M.G., Travis, W.D., Jett, J.R., Tazelaar, H.D., Trastek, V., Pairolero, P.C., et al. (2001). Alterations of p14ARF, p53, and p73 genes involved in the E2F-1-mediated apoptotic pathways in non-small cell lung carcinoma. Cancer Res. *61*, 5636–5643.

Nishitoh, H., Saitoh, M., Mochida, Y., Takeda, K., Nakano, H., Rothe, M., Miyazono, K., and Ichijo, H. (1998). ASK1 is essential for JNK/SAPK activation by TRAF2. Mol. Cell *2*, 389–395.

Normand, G., Hemmati, P.G., Verdoodt, B., von Haefen, C., Wendt, J., Güner, D., May, E., Dörken, B., and Daniel, P.T. (2005). p14ARF induces G2 cell cycle arrest in p53- and p21-deficient cells by down-regulating p34cdc2 kinase activity. J. Biol. Chem. *280*, 7118–7130.

Oda, E., Ohki, R., Murasawa, H., Nemoto, J., Shibue, T., Yamashita, T., Tokino, T., Taniguchi, T., and Tanaka, N. (2000). Noxa, a BH3-only member of the Bcl-2 family and candidate mediator of p53-induced apoptosis. Science *288*, 1053–1058.

Ozenne, P., Eymin, B., Brambilla, E., and Gazzeri, S. (2010). The ARF tumor suppressor: structure, functions and status in cancer. Int. J. Cancer *127*, 2239–2247.

Paliwal, S., Pande, S., Kovi, R.C., Sharpless, N.E., Bardeesy, N., and Grossman, S.R. (2006). Targeting of C-terminal binding protein (CtBP) by ARF results in p53-independent apoptosis. Mol. Cell. Biol. *26*, 2360–2372.

Perez, C.A., and Pietenpol, J.A. (2007). Transcriptional programs regulated by p63 in normal epithelium and tumors. Cell Cycle *6*, 246–254.

Perkins, C., Kim, C.N., Fang, G., and Bhalla, K.N. (1998). Overexpression of Apaf-1 promotes apoptosis of untreated and paclitaxel- or etoposide-treated HL-60 cells. Cancer Res. *58*, 4561–4566.

Petitjean, A., Cavard, C., Shi, H., Tribollet, V., Hainaut, P., and Caron de Fromentel, C. (2005). The expression of TA and DeltaNp63 are regulated by different mechanisms in liver cells. Oncogene *24*, 512–519.

Pimkina, J., and Murphy, M.E. (2009). ARF, autophagy and tumor suppression. Autophagy *5*, 397–399.

Pollice, A., Vivo, M., and La Mantia, G. (2008). The promiscuity of ARF interactions with the proteasome. FEBS Lett. *582*, 3257–3262.

Puthalakath, H., and Strasser, A. (2002). Keeping killers on a tight leash: transcriptional and post-translational control of the pro-apoptotic activity of BH3-only proteins. Cell Death Differ. *9*, 505–512.

Puthalakath, H., O'Reilly, L.A., Gunn, P., Lee, L., Kelly, P.N., Huntington, N.D., Hughes, P.D., Michalak, E.M., McKimm-Breschkin, J., Motoyama, N., et al. (2007). ER stress triggers apoptosis by activating BH3-only protein Bim. Cell *129*, 1337–1349.

Puthalakath, H., Villunger, A., O'Reilly, L.A., Beaumont, J.G., Coultas, L., Cheney, R.E., Huang, D.C., and Strasser, A. (2001). Bmf: a proapoptotic BH3-only protein regulated by interaction with the myosin V actin motor complex, activated by anoikis. Science *293*, 1829–1832.

Qu, L., Huang, S., Baltzis, D., Rivas-Estilla, A.-M., Pluquet, O., Hatzoglou, M., Koumenis, C., Taya, Y., Yoshimura, A., and Koromilas, A.E. (2004). Endoplasmic reticulum stress induces p53 cytoplasmic localization and prevents p53-dependent apoptosis by a pathway involving glycogen synthase kinase-3beta. Genes Dev. *18*, 261–277.

Rathmell, J.C., and Thompson, C.B. (2002). Pathways of apoptosis in lymphocyte development, homeostasis, and disease. Cell *109 Suppl*, S97–S107.

Reef, S., Zalckvar, E., Shifman, O., Bialik, S., Sabanay, H., Oren, M., and Kimchi, A. (2006). A short mitochondrial form of p19ARF induces autophagy and caspase-independent cell death. Mol. Cell *22*, 463–475.

Reimertz, C., Kögel, D., Rami, A., Chittenden, T., and Prehn, J.H.M. (2003). Gene expression during ER stress-induced apoptosis in neurons: induction of the BH3-only protein Bbc3/PUMA and activation of the mitochondrial apoptosis pathway. J. Cell Biol. *162*, 587–597.

Rizos, H., Darmanian, A.P., Mann, G.J., and Kefford, R.F. (2000). Two arginine rich domains in the p14ARF tumour suppressor mediate nucleolar localization. Oncogene *19*, 2978–2985.

Rocher, C., Faucheu, C., Blanchet, A.M., Claudon, M., Hervé, F., Durand, L., Harnois, M., Diu-Hercend, A., and Lalanne, J.L. (1997). Identification of five new genes, closely related to the interleukin-1beta converting enzyme gene, that do not encode functional proteases. Eur. J. Biochem. *246*, 394–400.

Rogers, T.B., Inesi, G., Wade, R., and Lederer, W.J. (1995). Use of thapsigargin to study Ca2+ homeostasis in cardiac cells. Biosci. Rep. *15*, 341–349.

Ron, D. (2002). Translational control in the endoplasmic reticulum stress response. J. Clin. Invest. *110*, 1383–1388.

Rong, Y., and Distelhorst, C.W. (2008). Bcl-2 protein family members: versatile regulators of calcium signaling in cell survival and apoptosis. Annu. Rev. Physiol. *70*, 73–91.

Rong, Y.-P., Aromolaran, A.S., Bultynck, G., Zhong, F., Li, X., McColl, K., Matsuyama, S., Herlitze, S., Roderick, H.L., Bootman, M.D., et al. (2008). Targeting Bcl-2-IP3 receptor interaction to reverse Bcl-2's inhibition of apoptotic calcium signals. Mol. Cell *31*, 255–265.

Rudner, J., Lepple-Wienhues, A., Budach, W., Berschauer, J., Friedrich, B., Wesselborg, S., Schulze-Osthoff, K., and Belka, C. (2001). Wild-type, mitochondrial and ER-restricted Bcl-2 inhibit DNA damage-induced apoptosis but do not affect death receptor-induced apoptosis. J. Cell. Sci. *114*, 4161–4172.

Rutkowski, D.T., and Kaufman, R.J. (2003). All roads lead to ATF4. Dev. Cell *4*, 442–444.

Rzymski, T., Milani, M., Singleton, D.C., and Harris, A.L. (2009). Role of ATF4 in regulation of autophagy and resistance to drugs and hypoxia. Cell Cycle *8*, 3838–3847.

Sanger, F., Nicklen, S., and Coulson, A.R. (1977). DNA sequencing with chain-terminating inhibitors. Proc. Natl. Acad. Sci. U.S.A. *74*, 5463–5467.

Sauane, M., Su, Z.-Z., Gupta, P., Lebedeva, I.V., Dent, P., Sarkar, D., and Fisher, P.B. (2008). Autocrine regulation of mda-7/IL-24 mediates cancer-specific apoptosis. Proc. Natl. Acad. Sci. U.S.A. *105*, 9763–9768.

Scaffidi, C., Fulda, S., Srinivasan, A., Friesen, C., Li, F., Tomaselli, K.J., Debatin, K.M., Krammer, P.H., and Peter, M.E. (1998). Two CD95 (APO-1/Fas) signaling pathways. Embo J. *17*, 1675–1687.

Scheuner, D., Patel, R., Wang, F., Lee, K., Kumar, K., Wu, J., Nilsson, A., Karin, M., and Kaufman, R.J. (2006). Double-stranded RNA-dependent protein kinase phosphorylation of the alpha-subunit of eukaryotic translation initiation factor 2 mediates apoptosis. J. Biol. Chem. *281*, 21458–21468.

Schmelzle, T., Mailleux, A.A., Overholtzer, M., Carroll, J.S., Solimini, N.L., Lightcap, E.S., Veiby, O.P., and Brugge, J.S. (2007). Functional role and oncogene-regulated expression of the BH3-only factor Bmf in mammary epithelial anoikis and morphogenesis. Proc. Natl. Acad. Sci. U.S.A. *104*, 3787–3792.

Schmutte, C., Tombline, G., Rhiem, K., Sadoff, M.M., Schmutzler, R., von Deimling, A., and Fishel, R. (1999). Characterization of the human Rad51 genomic locus and examination of tumors with 15q14-15 loss of heterozygosity (LOH). Cancer Res. *59*, 4564–4569.

Schröder, M., and Kaufman, R.J. (2005). The mammalian unfolded protein response. Annu. Rev. Biochem. *74*, 739–789.

Schwann, T. (1839). Mikroskopische Untersuchungen Über die Uebereinstimmung in der Struktur und dem Wachsthum der Thiere und Pflanzen (Berlin: Oswalds).

Sharpe, J.C., Arnoult, D., and Youle, R.J. (2004). Control of mitochondrial permeability by Bcl-2 family members. Biochim. Biophys. Acta *1644*, 107–113.

Sharpless, N.E. (2005). INK4a/ARF: a multifunctional tumor suppressor locus. Mutat. Res. *576*, 22–38.

Sharpless, N.E., and DePinho, R.A. (1999). The INK4A/ARF locus and its two gene products. Curr. Opin. Genet. Dev. *9*, 22–30.

Shaulian, E., Zauberman, A., Ginsberg, D., and Oren, M. (1992). Identification of a minimal transforming domain of p53: negative dominance through abrogation of sequence-specific DNA binding. Mol. Cell. Biol. *12*, 5581–5592.

Sherr, C.J. (2006). Divorcing ARF and p53: an unsettled case. Nat. Rev. Cancer *6*, 663–673.

Shibue, T., and Taniguchi, T. (2006). BH3-only proteins: integrated control point of apoptosis. Int. J. Cancer *119*, 2036–2043.

Shimizu, S., and Tsujimoto, Y. (2000). Proapoptotic BH3-only Bcl-2 family members induce cytochrome c release, but not mitochondrial membrane potential loss, and do not directly modulate voltage-dependent anion channel activity. Proc. Natl. Acad. Sci. U.S.A. *97*, 577–582.

Slade, N., and Horvat, A. (2011). Targeting p73--a potential approach in cancer treatment. Curr. Pharm. Des. *17*, 591–602.

Slee, E.A., Adrain, C., and Martin, S.J. (2001). Executioner caspase-3, -6, and -7 perform distinct, non-redundant roles during the demolition phase of apoptosis. J. Biol. Chem. *276*, 7320–7326.

Spriggs, K.A., Bushell, M., Mitchell, S.A., and Willis, A.E. (2005). Internal ribosome entry segment-mediated translation during apoptosis: the role of IRES-trans-acting factors. Cell Death Differ. *12*, 585–591.

Stewart, Z.A., and Pietenpol, J.A. (2001). p53 Signaling and cell cycle checkpoints. Chem. Res. Toxicol. *14*, 243–263.

Stiewe, T., and Pützer, B.M. (2000). Role of the p53-homologue p73 in E2F1-induced apoptosis. Nat. Genet. *26*, 464–469.

Stone, K.R., Mickey, D.D., Wunderli, H., Mickey, G.H., and Paulson, D.F. (1978). Isolation of a human prostate carcinoma cell line (DU 145). Int. J. Cancer *21*, 274–281.

Sugimoto, M., Kuo, M.-L., Roussel, M.F., and Sherr, C.J. (2003). Nucleolar Arf tumor suppressor inhibits ribosomal RNA processing. Mol. Cell *11*, 415–424.

Su, N., and Kilberg, M.S. (2008). C/EBP homology protein (CHOP) interacts with activating transcription factor 4 (ATF4) and negatively regulates the stress-dependent induction of the asparagine synthetase gene. J. Biol. Chem. *283*, 35106–35117.

Szegezdi, E., Fitzgerald, U., and Samali, A. (2003). Caspase-12 and ER-stress-mediated apoptosis: the story so far. Ann. N. Y. Acad. Sci. *1010*, 186–194.

Szegezdi, E., Macdonald, D.C., Ní Chonghaile, T., Gupta, S., and Samali, A. (2009). Bcl-2 family on guard at the ER. Am. J. Physiol., Cell Physiol. *296*, C941–C953.

Tanaka, S., Saito, K., and Reed, J.C. (1993). Structure-function analysis of the Bcl-2 oncoprotein. Addition of a heterologous transmembrane domain to portions of the Bcl-2 beta protein restores function as a regulator of cell survival. J. Biol. Chem. *268*, 10920–10926.

Tanaka, T., Tsujimura, T., Takeda, K., Sugihara, A., Maekawa, A., Terada, N., Yoshida, N., and Akira, S. (1998). Targeted disruption of ATF4 discloses its essential role in the formation of eye lens fibres. Genes Cells *3*, 801–810.

di Tommaso, A., Hagen, J., Tompkins, V., Muniz, V., Dudakovic, A., Kitzis, A., Ladeveze, V., and Quelle, D.E. (2009). Residues in the alternative reading frame tumor suppressor that influence its stability and p53-independent activities. Exp. Cell Res. *315*, 1326–1335.

Tsujimoto, Y., and Croce, C.M. (1986). Analysis of the structure, transcripts, and protein products of bcl-2, the gene involved in human follicular lymphoma. Proc. Natl. Acad. Sci. U.S.A. *83*, 5214–5218.

Tsukada, J., Yoshida, Y., Kominato, Y., and Auron, P.E. (2011). The CCAAT/enhancer (C/EBP) family of basic-leucine zipper (bZIP) transcription factors is a multifaceted highly-regulated system for gene regulation. Cytokine *54*, 6–19.

Ubeda, M., Wang, X.Z., Zinszner, H., Wu, I., Habener, J.F., and Ron, D. (1996). Stress-induced binding of the transcriptional factor CHOP to a novel DNA control element. Mol. Cell. Biol. *16*, 1479–1489.

Vattem, K.M., and Wek, R.C. (2004). Reinitiation involving upstream ORFs regulates ATF4 mRNA translation in mammalian cells. Proc. Natl. Acad. Sci. U.S.A. *101*, 11269–11274.

Vaux, D.L., and Korsmeyer, S.J. (1999). Cell death in development. Cell *96*, 245–254.

Vaux, D.L., Cory, S., and Adams, J.M. (1988). Bcl-2 gene promotes haemopoietic cell survival and cooperates with c-myc to immortalize pre-B cells. Nature *335*, 440–442.

Verhaak, R.G.W., Goudswaard, C.S., van Putten, W., Bijl, M.A., Sanders, M.A., Hugens, W., Uitterlinden, A.G., Erpelinck, C.A.J., Delwel, R., Löwenberg, B., et al. (2005). Mutations in nucleophosmin (NPM1) in acute myeloid leukemia (AML): association with other gene abnormalities and previously established gene expression signatures and their favorable prognostic significance. Blood *106*, 3747–3754.

Vogt, C. (1842). Untersuchungen über die Entwicklungsgeschichte der Geburtshelferkröte (Alytes obstetricans).

Weber, J.D., Jeffers, J.R., Rehg, J.E., Randle, D.H., Lozano, G., Roussel, M.F., Sherr, C.J., and Zambetti, G.P. (2000). p53-independent functions of the p19(ARF) tumor suppressor. Genes Dev. *14*, 2358–2365.

Wei, M.C., Zong, W.X., Cheng, E.H., Lindsten, T., Panoutsakopoulou, V., Ross, A.J., Roth, K.A., MacGregor, G.R., Thompson, C.B., and Korsmeyer, S.J. (2001). Proapoptotic BAX and BAK: a requisite gateway to mitochondrial dysfunction and death. Science *292*, 727–730.

Westfall, M.D., and Pietenpol, J.A. (2004). p63: Molecular complexity in development and cancer. Carcinogenesis *25*, 857–864.

Wick, W., Petersen, I., Schmutzler, R.K., Wolfarth, B., Lenartz, D., Bierhoff, E., Hümmerich, J., Müller, D.J., Stangl, A.P., Schramm, J., et al. (1996). Evidence for a novel tumor suppressor gene on chromosome 15 associated with progression to a metastatic stage in breast cancer. Oncogene *12*, 973–978.

Williams, B.R. (1999). PKR; a sentinel kinase for cellular stress. Oncogene *18*, 6112–6120.

Willis, A., Jung, E.J., Wakefield, T., and Chen, X. (2004). Mutant p53 exerts a dominant negative effect by preventing wild-type p53 from binding to the promoter of its target genes. Oncogene *23*, 2330–2338.

Willis, S.N., Fletcher, J.I., Kaufmann, T., van Delft, M.F., Chen, L., Czabotar, P.E., Ierino, H., Lee, E.F., Fairlie, W.D., Bouillet, P., et al. (2007). Apoptosis initiated when BH3 ligands engage multiple Bcl-2 homologs, not Bax or Bak. Science *315*, 856–859.

Xirodimas, D.P., Chisholm, J., Desterro, J.M.S., Lane, D.P., and Hay, R.T. (2002). P14ARF promotes accumulation of SUMO-1 conjugated (H)Mdm2. FEBS Lett. *528*, 207–211.

Yang, A., Kaghad, M., Wang, Y., Gillett, E., Fleming, M.D., Dötsch, V., Andrews, N.C., Caput, D., and McKeon, F. (1998). p63, a p53 homolog at 3q27-29, encodes multiple products with transactivating, death-inducing, and dominant-negative activities. Mol. Cell *2*, 305–316.

Yao, J.-Y., and Chen, J.-K. (2010). TAp63 plays compensatory roles in p53-deficient cancer cells under genotoxic stress. Biochem. Biophys. Res. Commun. *403*, 310–315.

Yoshida, H. (2007). ER stress and diseases. Febs J. *274*, 630–658.

Yoshida, H., Matsui, T., Yamamoto, A., Okada, T., and Mori, K. (2001). XBP1 mRNA is induced by ATF6 and spliced by IRE1 in response to ER stress to produce a highly active transcription factor. Cell *107*, 881–891.

Youle, R.J., and Strasser, A. (2008). The BCL-2 protein family: opposing activities that mediate cell death. Nat. Rev. Mol. Cell Biol. *9*, 47–59.

Yuan, J., and Yankner, B.A. (2000). Apoptosis in the nervous system. Nature *407*, 802–809.

Yun, J.-P., Chew, E.C., Liew, C.-T., Chan, J.Y.H., Jin, M.-L., Ding, M.-X., Fai, Y.H., Li, H.K.R., Liang, X.-M., and Wu, Q.-L. (2003). Nucleophosmin/B23 is a proliferate shuttle protein associated with nuclear matrix. J. Cell. Biochem. *90*, 1140–1148.

Zaika, A.I., and El-Rifai, W. (2006). The role of p53 protein family in gastrointestinal malignancies. Cell Death Differ. *13*, 935–940.

Zhang, D., and Armstrong, J.S. (2007). Bax and the mitochondrial permeability transition cooperate in the release of cytochrome c during endoplasmic reticulum-stress-induced apoptosis. Cell Death Differ. *14*, 703–715.

Zhang, P., McGrath, B.C., Reinert, J., Olsen, D.S., Lei, L., Gill, S., Wek, S.A., Vattem, K.M., Wek, R.C., Kimball, S.R., et al. (2002). The GCN2 eIF2alpha kinase is required for adaptation to amino acid deprivation in mice. Mol. Cell. Biol. *22*, 6681–6688.

Zhang, Y., Xiong, Y., and Yarbrough, W.G. (1998). ARF promotes MDM2 degradation and stabilizes p53: ARF-INK4a locus deletion impairs both the Rb and p53 tumor suppression pathways. Cell *92*, 725–734.

Zhou, J., Liu, C.Y., Back, S.H., Clark, R.L., Peisach, D., Xu, Z., and Kaufman, R.J. (2006). The crystal structure of human IRE1 luminal domain reveals a conserved dimerization interface required for activation of the unfolded protein response. Proc. Natl. Acad. Sci. U.S.A. *103*, 14343–14348.

Zhu, W., Cowie, A., Wasfy, G.W., Penn, L.Z., Leber, B., and Andrews, D.W. (1996). Bcl-2 mutants with restricted subcellular location reveal spatially distinct pathways for apoptosis in different cell types. Embo J. *15*, 4130–4141.

Zindy, F., Eischen, C.M., Randle, D.H., Kamijo, T., Cleveland, J.L., Sherr, C.J., and Roussel, M.F. (1998). Myc signaling via the ARF tumor suppressor regulates p53-dependent apoptosis and immortalization. Genes Dev. *12*, 2424–2433.

Zuker, M. (2003). Mfold web server for nucleic acid folding and hybridization prediction. Nucleic Acids Res. *31*, 3406–3415.

Zuzarte-Luís, V., and Hurlé, J.M. (2002). Programmed cell death in the developing limb. Int. J. Dev. Biol. *46*, 871–876.

7. Appendix

7.1 Abbreviations

°C	degrees celsius
A	Ampere
Ad	adenovirus
AIF	apoptosis inducing factor
APAF-1	apoptotic protease activating factor 1
Ask1	apoptosis-signal-regulating kinase 1
ATF	activating transcription factor
ATP	adenosine triphosphate
Bad	Bcl-2 antagonist of cell death
Bak	Bcl-2 antagonist/killer
Bax	Bcl-2 associated X protein
Bcl-2	B-cell lymphoma-2
Bcl-B	Bcl-2-like 10
Bcl-w	Bcl-2-like 2
Bcl-x_L	B-cell lymphoma-extra large
BH	Bcl-2 homology
Bid	BH3-interacting domain death agonist
bidest	double destilled
Bim	Bcl-2 interacting mediator of cell death
Bmf	Bcl-2 modifying factor
Bok	Bcl-2-related ovarian killer
bp	base pairs
BSA	bovine serum albumin
bZip	basic Leucine Zipper
C/EBP	cAMP response element-binding protein
cAMP	cyclic adenosinmonophosphate
cDNA	complementary DNA
CHOP	C/EBP homologous protein
CMV	cytomegalovirus
Da	Dalton

DD	death domain
DDIT3	DNA damage inducible transcript 3
DED	death-effector domain
DIABLO	direct IAP-binding protein with low pI
DISC	death-induced signalling complex
DMEM	Dulbecco's Modified Eagle Medium
DMSO	dimethylsulfoxid
DNA	desoxyribonucleinacid
DOX	doxycyclin
EDTA	ethylendiamintetraaceticacid
EGTA	ethylenglykoltetraaceticacid
eIF2α	α-subunit of eucaryotic translation initiation factor 2
ER	endoplasmic reticulum
ERSE	ER stress response element
EtBr	ethidiumbromid
F	Farad
FACS	fluorescence activated cell sorting
FADD	Fas associated death domain
FCS	fetal calf serum
g	gram
g	gravity (9,81 m/s^2)
G418	geneticin
GADD	growth arrest and DNA damage inducible gene
h	hour
Hdm-2	human double minute 2
Hrk	Harakiri
IAP	inhibitor of apoptosis
IRE1	inositol-requiring enzyme 1
IRES	internal ribosomal entry site
ITR	inverted terminal repeats
JNK	c-Jun N-terminal kinase
l	Liter
m	meter

M	molar
MAPK	mitogen-activated protein kinase
Mcl-1	myeloid cell leukaemia sequence-1
MCS	multiple cloning site
min	minute
MOI	multiplicity of infection
Nbk/Bik	Natural born killer/Bcl-2-interacting killer
NGF	nerve growth factor
nt	nucleotide
OD	optical density
ORF	open reading frame
PBS	phosphate buffered saline
PCR	polymerase chain reaction
PERK	pancreatic ER kinase-like ER kinase
pH	potential of hydrogen (potentia Hydrogenii)
Puma	p53 upregulated modulator of apoptosis
Q-VD-OPh	Quinolyl-Valyl-O-methylaspartyl-(2,6-difluorophenoxy)-methyl ketone
RNA	ribonucleinacid
rpm	rounds per minute
RT	room temperature
S1/2P	site-1/2 protease
SDS	sodiumdodecylsulfat
sec	second
SMAC	second mitochondria-derived activator of caspase
SPIKE	small protein with inherit killing effects
tBid	truncated Bid
TEMED	N,N,N',N'-Tetramethylethylendiamin
TNF	tumour necrosis factor
TRADD	TNF-receptor associated death domain
TRAF2	TNF-receptor associated factor 2
TRAIL	TNF related apoptosis inducing ligand
tTA	tetracycline-responsive transcriptional activator
U	unit

UPR	unfolded protein response
V	Volt
v/v	volume/volume
Vol.	volume
W	Watt
w/v	weight/volumen
w/w	weight/weight
wt	wildtype

7.2 Bcl-2 modifying factor (Bmf) promoter region

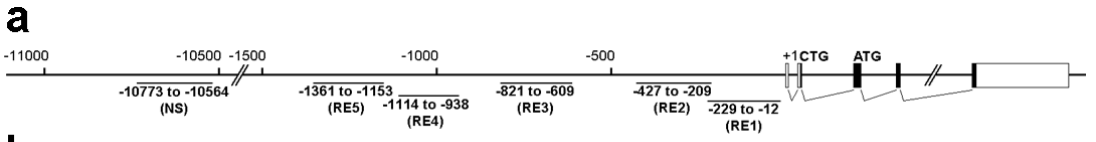

b

```
-1500  AATACAGATTCTTCAGTCTGGCATTCCAGGGACACCTCTGTAGTCTGACCTGAACCCACC  -1441
-1440  TGCCCATGCCTACCGTTCGTAAATCTCAGTGTGCACCCAATGATCCAGTCACCAAGCCTC  -1381
-1380  CCTCTGCTCCCTGCACAGGTAAGCTCTCCAGCTCAGCACTTCAGTCTGCTACCCTTAGGC  -1321
-1320  CTGGGCTATTCTTTTTTATTTTATTTTATTTTTATTTTTTTGAGACGGAGTCTCATTGTC  -1261
-1260  GCCCAGGCTGGAGTGCGGTGGCGCTATCTCCGCCCACTGCAACCTTCACCTCCTAGGTTC  -1201
-1200  AAGCAATTCTCCTACCTCAGCCTCCCAAGTAGCTGGGATTACAGGCATGCGCCACCACGC  -1141
-1140  CCGCCTGATTTTTGTATTTTTAGTAGAGACAGGGTTTCCCGTGTTGGCCAGGCTGGTCTC  -1081
-1080  CAACCACTGAGCTCAAGTGAACCACCCGCCTCGGCCTCCCAAAGTGTTGGGATTACAGGC  -1021
-1020  GTGAGACATGTGCATCTGGTTTTCCTTATTGAAAAATATTTCCCATTCAATTTAAAAGCT  -961
 -960  GTCTCCCTGAGGCCTTCTCCAGCCTTTGTATTCTGAATTTTTCTGCATTCCTCAATAGTC  -901
 -900  ATTATCCTTGGAATGAATACAATTCCAATAACTTTTCACTATTTTCAGGGCTACCTCTCC  -841
 -840  TAGTAGACTGTAAGCTCCTTGAGGGCAGACGCCAGGTTTCTGGCACTCAGCCCAATATCT  -781
 -780  GGCACAGAGTAGGTGCTCGGTAAATGCCTGTGAAGTAGCCCATAGACTCCCTTACGCGGT  -721
 -720  CTGCAGGACATGCTGCTCTCCTGGCAGCACCAGCACAGTCTCTAAATGCTGCCATATGCG  -661
 -660  AGATATGTGTCAACCGCTCAAGCAGCCCCGGCCTTCTTGAGCGCTCCGCTTCTCAGCCAG  -601
 -600  GTGCTTATTTTGCCAGTGCCCACGCCCAGTCAAGAAGAGGACCTAAGGGCTCCCCTGGAT  -541
 -540  GTGTTTGTTTCAAACACACCTTCAGCTTTGGAGCTGCAGTTTTCTTCCGACCTGCTCGGC  -481
 -480  AGGCGGGAGGGAGCTTTCCCCTGAGGCTGGGATCCCATAGGGACCCGCACCCTGCACCCT  -421
 -420  GCACCCACTGGACGCACCAGCCTCATAAAAAAAACTCCCCGCCTCCTTCCCCCCTCCCTTT  -361
 -360  GTGGACGCGCAGCAATTATTCTGCCCATTGCCGTGAAAAAGAAGACAAAAGTTACTTTGG  -301
 -300  CGCCCCCTCTCCCACACCTAATACAGAGGATTCAGGGACTCTCTGGCGCTTCCAGAGCCT  -241
 -240  GTGTTAGGGACAGAATCCGCACTGGCGACGGCGCTCCGACTGCGCTTCTGGCGACGGTCG  -181
 -180  GAATTTTGCTCGGCCCCTTGCAATGTTTCCATGGGAAGGTTCGTACATTCGTGACCGTCC  -121
 -120  CTGGCAGCGGCCCAGCCCGGGACTTGGCGCTTCACTCGCCATTGGTCAGTCCTCGGCGTG  -61
  -60  ACGCGCAGGGGGGCGGGGCCTCATCAGCTGTTTGCGGGATGCCCCGAGCAGGCGTATTTT  -1
   +1  GGAAACAATACCGCACCGTGCGGAGTGGCCTCCTCCCGCCCCGGCCTGTGCCCGCCGCCG  +60
  +61  CCGCCGCCCCTGCCTGCGCCTCCCGCCTCCTGCCGCAGCCCGGTGAGCGCCCGGGTGGCC  +120
 +121  GCCGGGGGCCGGGCGGAGTTGGATCGCAGCTCCTTGGGGAAGTGGGGAGCGGAGTCGCGC  +180
 +181  TGCGCACGGGGGCCCGGGAAGGGTTTGGGCTGCGGACGTCTGGGGTGACCATGAAGAACT  +240
 +241  GGGGCGCTGGGGTGAGGGAACGGGGTGCAGAACCCACAGTTGGGTGCGCTGCTCCAAGAG  +300
 +301  GGAACTTGGGGGTAGCATTTGGGACTCGAAGGAGTTGGGTCCAGGTAGGCAGGGGAACCT  +360
 +361  GGGGTGCACTGCTGAGCAGACCTGGGCGCCCGAGAACGGCCCAGCCTCTGGGTCTGACTT  +420
 +421  TGGGATAGGACAGGAGCTGTGGGGCATCCTGCCTCTCTGCGGAGTCTGAAGGCTCCTCTC  +480
 +481  CTTAACAGCTGGGCTTTTTCCCTCCTTCCCAATCGAGTCTGGGCGTCCAGCCCCCGAGTG  +540
 +541  CTCGTCACGCTGGACCCTGGCGCGGAGCCCTGGCATCACGACTCGGAGGCCGAGACTCTC  +600
 +601  TCCTGGAGTCACCCAGGTCTGGGGTGTGTGTGTGTGTGTGTGTGTGTGTGTTCCTA  +660
```

Figure 28. Promoter region of *bmf*. (**a**) Putative binding sites with corresponding ChIP PCR fragments (RE1 to RE5 and nonspecific; NS). BMF mRNA and exons (ENSG00000104081) in bigger boxes, coding region in black. (b) Promoter sequence from -1500 to +660 respective to transcription start site +1. Primer indicated as arrows above and below sequence. Putative CHOP and ATF4 binding sites in green and pink, respectively. Exons indicated with grey background. CTG start site and coding region starting in exon 2 in black letters.

Acknowledgements

I would like to thank Professor Dr. Peter Daniel for his guidance and for giving me the opportunity to work in his group, whose help and suggestions helped me during the time of this research. I am thankful to PD Dr. Philipp Hemmati for his helpful inputs and encouragement throughout the process of this work and for being a good friend and neighbour. I would also warmly acknowledge Dr. 'Commander' Bernd Gillissen for his very helpful advices, whose broad knowledge and long and stimulating discussions not only during lunchtime helped me a lot.

I am thankful to Professor Dr. Harald Saumweber and PD Dr. Jürgen Eberle for reviewing my thesis.

I would also like to thank all members of the Daniel research group, especially Antje and Anja Richter for their exceptional assistance. Many thanks to my colleagues and co-workers Sandy Adjemian, Dr. Cindrilla Chumduri, Kerstin Dietze, Dr. Gaby Forro, Dr. Nina Gebhardt, Dr. Clarissa von Haefen, Daniel Heinze, Christian Herrberger, Limin Liu, Anna Michalak, Dr. Ana Milojkovic, Annika Müer, Anja Müller, Thomas Pretzsch, Thomas Rathjen, Jana Roßius, Josefine Ruß, Nicolas Terliesner, and Dr. Jana Wendt.

Thanks to all friends who made my stay in Berlin very pleasant; you know who you are.

Last but not least, I am grateful to my family for encouraging me all these years.

Eidesstattliche Erklärung

Hiermit erkläre ich, dass ich die vorgelegte Dissertationsschrift mit dem Thema: „Bedeutung des p53-Signalwegs für Apoptoseaktivierung und Zellzyklusarrestregulation durch das $p14^{ARF}$ Tumorsuppressorgen“ selbst verfasst und keine anderen als die angegebenen Quellen und Hilfsmittel benutzt, ohne die Hilfe Dritter verfasst und auch in Teilen keine Kopien anderer Arbeiten dargestellt habe.

Außerdem erkläre ich hiermit, dass ich mich nicht anderweitig um einen entsprechenden Doktorgrad beworben habe.

Die Promotionsordnung der Mathematisch-Naturwissenschaftlichen Fakultät I der Humboldt-Universität zu Berlin habe ich gelesen und akzeptiert.

Tim Overkamp

Berlin, den 30. Januar 2012